Center for Cold-Formed Steel Structures Library

Wei-Wen Yu Center for Cold-Formed Steel Structures

01 Aug 1965

Torsional-flexural buckling of thin-walled open sections

Pen J. Fang

Recommended Citation

Fang, Pen J., "Torsional-flexural buckling of thin-walled open sections" (1965). *Center for Cold-Formed Steel Structures Library*. 159.
https://scholarsmine.mst.edu/ccfss-library/159

TORSIONAL-FLEXURAL BUCKLING
OF THIN-WALLED OPEN SECTIONS

by

Pen J. Fang
Research Assistant

George Winter
PROJECT DIRECTOR

Department of Structural Engineering

School of Civil Engineering

Cornell University

Report No. 320

TORSIONAL-FLEXURAL BUCKLING

OF THIN-WALLED OPEN SECTIONS

by

Pen J. Fang

Research Assistant

George Winter

Project Director

Ithaca, New York   August, 1965

CONTENTS

INTRODUCTION

Compression members with thin-walled open sections, because of their low torsional rigidities and because their cross-sectional configuration is such that the centroid and the shear center often do not coincide, can buckle at loads well below the Euler load by interaction of torsion and bending. Fast expanding applications of such sections in civil and architectural engineering call for an extensive investigation of torsional-flexural buckling.

Basic theory of torsional-flexural buckling is treated by a number of authors,[1,2] and simplifications of the basic theory in the elastic range for the design purposes together with some test results were reported previously.[3] Some investigation of inelastic torsional-flexural buckling of as-rolled, thick-walled I-beams by application of bi-axial moments has been reported.[6,7,8] However, there has not been sufficient investigation of axially loaded columns with thin-walled open sections in the inelastic range.

All inelastic buckling problems are inherently non-linear and non-static. In view of the even more complex nature of torsional-flexural buckling, simplifications of the basic theory for practical purposes are necessary. While the simplification may reduce the design procedure to an easier form, the computed values must also be reasonably accurate when compared to the actual buckling loads.

This investigation, primarily semi-empirical, was conducted for the following objectives:

1. To develop and verify an approximate inelastic torsional-flexural buckling theory based on certain simplifying assumptions.

2. To recommend a practical design procedure and a formulation of code provisions against torsional-flexural buckling covering both the elastic and inelastic ranges.

A series of tests on specimens of various cross-sectional shapes and dimensions were made to verify the basic theory. The test results agree with the predicted values within reasonable limits.

BASIC THEORY

Axially compressed members with thin-walled open sections, because of their low torsional rigidities, can buckle by twisting at loads well below the Euler load. Also, because of their cross-sectional configuration, the centroid and the shear center frequently do not coincide and, therefore, torsion and flexure interact.

Members having singly symmetrical cross-sections may buckle in pure flexure or in the torsional-flexural mode. Based on linear theory,[1,2,3] the critical torsional-flexural stress in the elastic range is given by the following quadratic interaction equation:

$$(\sigma_{cr})_E = \frac{1}{2K} [(\sigma_x + \sigma_\phi) - \sqrt{(\sigma_x + \sigma_\phi)^2 - 4k\,\sigma_x\,\sigma_\phi} \,] \quad (1a)$$

in which

$(\sigma_{cr})_E$ = the elastic torsional-flexural buckling stress;

$$K = 1 - (\frac{x_o}{r_o})^2 \qquad (1b)$$

$$\sigma_x = \frac{\pi^2 E}{(L/r_x)^2} \qquad (1c)$$

$$\sigma_\phi = \frac{1}{I_p} [GJ + \frac{E C_w \pi^2}{L^2}] \qquad (1d)$$

x_o = the coordinate of the shear center with regard to the centroid;

r_o = the polar radius of gyration about the shear center

$$= \sqrt{\frac{I_x + I_y}{A} + x_o^2} \quad ;$$

r_x = the radius of gyration about the x-axis;

A = the cross-sectional area;

I_p = the polar moment of inertia about the shear center.

For thin-walled open sections comprising plate elements which do not significantly restrain each other rotationally, Eq. (1a) gives rather accurate account of the interaction of the two fundamental modes.

For members of small or moderate slenderness with walls of greater thicknesses, the average compressive stress prior to buckling may exceed the proportional limit of the material. In this case failure occurs at an inelastic torsional-flexural stress which is less than the computed elastic buckling stress.

According to the tangent modulus theory, the flexural buckling stress in the inelastic range (buckling about the

x-axis) is given by the well-known Engesser-Shanley equation:

$$(\sigma_x)_t = \frac{\pi^2 E_t}{(L/r_x)^2} \qquad (2)$$

In the analysis and derivation of the equations governing torsional-flexural buckling in the elastic range, the so-called Euler method is used.[1,3] Many practical column problems including torsional-flexural buckling in the elastic range can be treated as static buckling problems for perfect mathematical models. A static stability criterion may not be useful, however, for nonlinear problems. Shanley pointed out that the time factor and behavior of loading must be taken into account in the inelastic column buckling, which leads to the tangent modulus concept, in contrast to the double modulus theory of v. Karman which is the result of a mere extension of the Euler method.

The critical average compression stress of the purely torsional mode in the inelastic range is then

$$(\sigma_\phi)_t = \frac{1}{I_p} [G_t J + \frac{E_t C_w \pi^2}{L^2}] \qquad (3)$$

in which E_t is the tangent modulus defined by $\frac{d\sigma}{d\epsilon}$, and G_t = the tangent modulus of shear defined by $\frac{d\tau}{d\sigma}$. Eq. (3) comes directly from Eq. (1d) because during buckling in the inelastic range, infinitesimal shear stresses $d\tau$ are superimposed on axial compressive stresses, the ratio τ/λ between excess shear stresses and excess shear strain being G_t. The second term in the bracket of Eq. (1d) represents the component of internal resisting torque due to warping of column

as it twists, E refers to the axial stress thus caused; hence in the inelastic range, it becomes E_t by applying the Shanley inelastic buckling concept.

Thus the critical torsional-flexural buckling stress in the inelastic domain can be given by

$$(\sigma_{cr})_t = \frac{1}{2k} \left[(\sigma_x)_t + (\sigma_\phi)_t - \sqrt{\left\{(\sigma_x)_t + (\sigma_\phi)_t\right\}^2 - 4k(\sigma_x)_t \, (\sigma_\phi)_t} \right] \quad (4)$$

There are several theories and suggestions for computing the inelastic moduli in Eq. (4). However, most of the theories and methods lead to quite complicated and inconvenient procedures. For example, P. P. Bijlaard[10] derived the following expression for G_t:

$$G_t = E/(2 + 2\nu + 3e) \quad (5)$$

in which

ν = Poisson's ratio;

$e = (E/E_s) - 1$;

E_s = the secant modulus.

F. Bleich[2] suggested the relationship

$$G_t = G \sqrt{\frac{E_t}{E}} \quad (6)$$

If these expressions are substituted in Eqs. (3) and (4) and combined with an appropriate expression for the stress-strain relationship of the material, the resulting equation needs laborious and time-consuming solution. (See Appendix D.)

We shall assume now that the ratio of tangent modulus of shear to elastic modulus is equal to that of tangent

modulus to Young's modulus, namely, E_t/E, so that

$$G_t = G \frac{E_t}{E} = \frac{E_t}{2(1 + \nu)} \qquad (7)$$

This is equivalent to saying that the ratio of the two moduli remains constant. This assumption is in accordance with that made by K. Roik[9] and F. Bleich.[2] It cannot be proved rigorously but may be justified practically because for most cases of torsional buckling, the shearing stresses play only a minor role (although the case of the equal legged angle seems to deviate somewhat from this reasoning). Hence, even relatively crude approximations in the shear terms have comparatively little effect on computed critical loads.

The relation (7) leads to somewhat smaller value of G_t than other expressions, and therefore, to a more conservative buckling stress. The computation is greatly simplified, however, by this approximation. Eq. (3) can then be written as

$$(\sigma_\phi)_t = \frac{1}{I_p} [G_t J + \frac{E_t C_w \pi^2}{L^2}]$$
$$= \frac{1}{I_p} [\frac{E_t}{2(1+\nu)} J + \frac{E_t C_w \pi^2}{L^2}] \qquad (8)$$

Thus, if one has an expression for E_t as a function of stress, for given E, proportional limit and yield strength of the material, the inelastic torsional-flexural buckling can be easily calculated.

In order to determine stress-strain curves of the columns, stub column tests were made. Typical effective over-all stress-strain relationship of the specimens are shown in Figs. 2, 3, 4 and 5.

All stress-strain curves reflected the well-known effects of cold forming.[5] They were practically linear up to at least half of the yield strength determined as the stress corresponding to 0.2% residual strain. Above the proportional limit, they gradually deviate from linearity and rapidly curve as the stress approaches yielding. In the present case, the non-linearity above the proportional limit is due to the effect of cold forming which produces zones of higher yield strength at corners.

To obtain the stress-strain relationship, we assume that the E_t/E ratio follows a parabolic law; thus, the expression for E_t can be written as

$$E_t = CE \left[\frac{\sigma}{\sigma_y} - \left(\frac{\sigma}{\sigma_y} \right)^2 \right] \qquad (9)$$

where

$$C = f(\sigma, \sigma_p, \sigma_y)$$

Hence, C is a numerical parameter, dependent on the full section proportional limit which in turn is dependent on the properties of virgin material, amount of cold forming and on the cross-sectional dimensions.

From the stress-strain curves of the stub column tests, E_t was measured using a "tangentiometer." A tangentiometer is a semi-transparent mirror fixed perpendicularly to a straight base. Holding the mirror perpendicular to the paper on which the stress-strain curve is drawn, one can adjust the position of the mirror until the reflected image of the curve coincides with the image transmitted through

the mirror; the surface of the mirror is then normal to the curve at that point. The slope of the curve at the point can be read at the base. The E_t/E ratios are plotted against $\frac{\sigma}{\sigma_y}$ as shown in Fig. 6. If a curve is drawn through the center of the scatter band, C is seen to be 4.5. For comparison, a curve based on C = 4 is also plotted, and seen to represent the lower limit of the scatter band. This value, C = 4, is the one currently used for steel column design for flexural buckling, taking the proportional limit as one-half of the yield strength.

For most practical cases, the majority of buckling stresses fall under 90% of the yielding strength. It is seen from Fig. 6 that the curve corresponding to C = 4 is the lower bound of the group of the experimental data. For a more gradually yielding stress-strain curve, C tends to be lower, as is the cases of hat and lipped angle sections, Figs. (4) and (5). Conversely, C tends to be higher for angle section, Fig. (2), while for channel section it is about the intermediate, Fig. (4). This effect can be observed later from the buckling test results plotted in Fig. (14). The points for hat and lipped angle sections generally fell somewhat below the theoretical curved based on C = 4.5 and those for angle section are generally above the curve, with those for channel section being in best agreement with the theoretical curve.

The tangent modulus can then be expressed as

$$E_t = 4.5 \; E \; [\frac{\sigma}{\sigma_y} (1 - \frac{\sigma}{\sigma_y})]$$

(10)

To derive a stress-strain curve from this equation, one notes that

$$E_t = \frac{d\sigma}{d\varepsilon}$$

and substitutes this differential into Eq. (10) to get

$$\varepsilon = \frac{1}{4.5E} \int \frac{d\sigma}{\frac{\sigma}{\sigma_y}(1 - \frac{\sigma}{\sigma_y})} + C_1$$

carrying out the integration

$$\varepsilon = C_1 + \frac{1}{4.5E} \ln \left| \frac{\sigma/\sigma_y}{1 - \sigma/\sigma_y} \right|$$

The constant of integration, C_1, can be determined by the condition of the proportional limit, i.e.,

$$\frac{E_t}{E}\Big|_{\sigma_p} = 1$$

whence, Eq. (10) becomes

$$1 = 4.5 \left[\frac{\sigma_p}{\sigma_y} - \left(\frac{\sigma_p}{\sigma_y} \right)^2 \right]$$

Solving for $\frac{\sigma_p}{\sigma_y}$, one obtains

$$\frac{\sigma_p}{\sigma_y} = \frac{2}{3}$$

from which the proportional σ_p above which Eq. (10) applies, is

$$\sigma_p = \frac{2}{3} \sigma_y.$$

Noting that $\varepsilon \Big|_{\sigma_p = \frac{2}{3}\sigma_y} = \frac{2}{3}\frac{\sigma_y}{E}$,

$$C_1 = 0.513 \frac{\sigma_y}{E}$$

one finally obtains

$$\varepsilon = \frac{\sigma_y}{4.5E} \left[2.306 + \ln \left| \frac{\sigma/\sigma_y}{1 - \sigma/\sigma_y} \right| \right] \qquad (11)$$

Eq. (11) depicts the stress-strain curve above the proportional limit up to the yield strength, corresponding to Eq. (10). Stress-strain curves based on this equation are plotted as dashed curves in Figs. (2) to (5), for comparison with measured curves. Agreement is seen to be reasonable.

At incipient buckling, σ becomes $(\sigma_{cr})_t$ in Eq. (10), i.e.,

$$E_t = 4.5 \ E \ [\ \frac{(\sigma_{cr})_t}{\sigma_y} \left\{ 1 - \frac{(\sigma_{cr})_t}{\sigma_y} \right\} \ ] \qquad (12)$$

Substituting Eq. (12) into Eqs. (2) and (8),

$$(\sigma_x)_t = 4.5 \ \frac{(\sigma_{cr})_t}{\sigma_y} \ [\ 1 - \frac{(\sigma_{cr})_t}{\sigma_y} \ ] \ \sigma_x \qquad (13)$$

$$(\sigma_\phi)_t = 4.5 \ \frac{(\sigma_{cr})_t}{\sigma_y} \ [\ 1 - \frac{(\sigma_{cr})_t}{\sigma_y} \ ] \ \sigma_\phi \qquad (14)$$

Eq. (4) together with Eqs. (13) and (14) becomes

$$(\sigma_{cr})_t = 4.5 \ \frac{(\sigma_{cr})_t}{\sigma_y} \ [\ 1 - \frac{(\sigma_{cr})_t}{\sigma_y} \ ] \ (\sigma_{cr})_E$$

and finally the torsional-flexural buckling stress in the inelastic domain becomes

$$(\sigma_{cr})_t = \sigma_y \ [1 - \frac{\sigma_y}{4.5 \ (\sigma_{cr})_E}] \qquad (15)$$

where $(\sigma_{cr})_E$ is the elastic critical torsional-flexural buckling stress computed by Eq. (1a).

One obtains the same result by defining an effective slenderness ratio as follows.

In flexural buckling, if one knows the slenderness ratio, L/r, one can compute the buckling stress

in which $(\sigma_x)_E$ is the computed elastic Euler stress, which is higher than the actual buckling stress in the inelastic range.

If one equates $(\sigma_{cr})_t$ of torsional-flexural buckling to the above flexural buckling stress and solves the resulting equation for (λ/r), one gets the effective slenderness ratio; or conversely, one can compute the torsional-flexural buckling stress if one knows the effective slenderness ratio, $(\lambda/r)_{eff}$.

$$(\sigma_{cr})_t = \frac{\pi^2 E_t}{(\lambda/r)^2_{eff}} \tag{16}$$

Rewriting Eq. (16) analogously to the flexural case, one obtains

$$(\sigma_{cr})_t = \frac{E_t}{E} \frac{\pi^2 E}{(\lambda/r)^2_{eff}} \tag{17}$$

Then

$$\frac{\pi^2 E}{(\lambda/r)^2_{eff}} = (\sigma_{cr})_E \tag{18}$$

which is the computed elastic torsional-flexural buckling stress given by Eq. (1a). Therefore $(L/r)_{eff}$ can be computed by

$$(\frac{\lambda}{r})^2_{eff} = \frac{\pi^2 E}{(\sigma_{cr})_E} \tag{19}$$

In the elastic domain, i.e., below the proportional limit, Eq. (19) gives the actual elastic torsional-flexural buckling stress.

Substituting Eq. (10) into Eq. (17),

$$(\sigma_{cr})_t = 4.5 \frac{(\sigma_{cr})_t}{\sigma_y} [1 - \frac{(\sigma_{cr})_t}{\sigma_y}] (\sigma_{cr})_E$$

and finally

$$(\sigma_{cr})_t = \sigma_y [1 - \frac{\sigma_y}{4.5 (\sigma_{cr})_E}] \tag{15}$$

as before.

Both approaches are based on the assumption expressed
in Eq. (5). However, the physical meaning is better vis-
ualized in the first derivation.

It is now possible to extend the calculation pro-
cedures of the elastic case into the inelastic range and by
applying Eq. (15) to obtain the critical torsional-flexural
buckling stress in the inelastic range. The computed values
in Table II are based on Eq. (15).

EXPERIMENTAL INVESTIGATION

The purpose of the experimental investigation was to
verify the basic theory in the foregoing. Altogether, 30
tests were conducted on specimens having various sectional
shapes and dimensions.

The main parameters which must be considered in choosing
specimens are as follows:

1. w/t ratio of the plate elements of specimens.

As this ratio increases, there may be local buckling
premature to the over-all column buckling under axial com-
pression. For the present investigation, the w/t ratios
were chosen such that premature local buckling was avoided.
Within such range of w/t ratios, a variety of cross-sectional
dimensions were designed.

2. Wall-thickness.

If wall thickness is sufficiently small, the torsional
rigidity of the cross-section is correspondingly reduced and
the buckling load is so low that the average compressive
stress cannot reach the inelastic domain. Therefore, steel

sheet thicknesses of 10 to 13 gages were selected.

3. Yield strength of material.

As discussed in the basic theory, the basic yield strength of the material is of great consequence to the column buckling stress and also to the local buckling. Hence, materials having relatively low yield strength were used.

4. Shape of specimen.

Tests were confined to shapes having singly symmetrical sections, to which most of the commonly used shapes belong.

5. End conditions.

Fully fixed end conditions were chosen. This was to eliminate the complex end fittings necessary for testing column with other end conditions. Moreover, the simpler the arrangement of the end restraints, the less error would be involved in aligning the specimen.

Specimens and Test Procedure

Specimens are grouped into four categories: plain equal legged angles, lipped angles, plain channels and hat sections. The cross-sectional configuration is shown in Fig. 1. A summary of specimen shapes and their dimensions is given in Table 1.

All tests were conducted on columns with length less than 70 in. The fixed end conditions were achieved by welding steel plates of 3/8 to 1/2 in. thickness to both ends of the specimen, which were then set in hydrostone placed on the base and head of the test machine.

The materials used for the specimens were 10 gage hot rolled sheets and 12 and 13 gage cold reduced sheets. Column specimens were made by press braking at a local shop (Champion Sheet Metal Co., Cortland, N.Y.) to specified dimensions.

Stub column compression tests were made to evaluate the effective over-all stress-strain relationship of the specimens. A stub column is a short piece cut from the specimen to be tested. While details of the stub column test procedure are fully described elsewhere,[5] a brief explanation will be given below.

A schematical setup of a stub column test is depicted in Fig. 7. The specimen was surrounded by hydrostone cast in a steel pipe to limit plate local buckling. SR-4 strain gages were attached to the plate elements of the stub column and were then coated with wax in order to secure waterproof. Each strain gage was then covered with a half section of metal tube approximately 7 1/2 in. long split longitudinally. Water-proofing wax was again coated along the tubing. The specimens were then greased and wrapped in aluminum foil to minimize friction between the surface of the specimen and hydrostone. The entire assemblage was cast in hydrostone contained in a 4 in. steel pipe or 6 in. square tube of 7 1/2 in. length, depending on the size of the specimen. Before the stub column was placed in hydrostone, the ends were cut so that the end surfaces were perpendicular to the longitudinal axis; both ends were milled to smooth surfaces

after the specimen was cast in hydrostone. After the hydrostone had hardened completely and heat generated was dissipated, the specimen was brought to test.

In testing, the specimen was placed on a milled plate of 1-1 1/2 in. thickness which was fixed by hydrostone on the base of the testing machine. The plate was checked to be horizontal by means of a bubble tube. Under the head of the machine, the same arrangement was made.

The stub column cross-sectional area was determined accurately by measuring the weight and length of the specimen. The average stresses were computed and plotted against the average strain readings of the strain gages. Typical stress-strain curves are shown in Figs. 2, 3, 4 and 5. (Others are included in Appendix A.)

Basic instrumentation of the column tests consists of two needles attached to the column walls at mid-height and a circular ring with scale increments of 0.01 inch to measure the rotation of the column as indicated by the movement of the needles; dial gages to measure the column deflection at mid-height; and electrical resistance strain gages at certain points on the column walls mainly to check the column alignment. The vertical alignment was first checked by a plumb-bob and also by a bubble tube.

The column specimens were loaded in a hydraulic test machine with load increment of 500 to 2000 lbs., depending on the specimen and the predicted buckling load. As the buckling load was approached, the load increment was reduced. Typical test setup and testing are shown in Figs. 8 and 9.

The applied average stresses, P/A, were plotted against the measured rotations at mid-height and against the deflections in the direction perpendicular to the axis of symmetry.

Discussion of Results

Typical stress-deformation curves are shown in Figs. 10, 11, 12 and 13. (The curves for all other specimens are given in Appendix B.) It is seen that the behavior of the specimens is similar to that of an axially loaded column with imperfections. The stress-deformation curves show gradually increasing rotations and simultaneous lateral deflections in the intermediate range, with rapidly increasing deformations as the buckling stress was approached.

The stress-deformation curves show that failure occurred at the stresses in the inelastic domain. They also show that there was no apparent post-buckling strength. This confirms again that post-buckling strength depends on $\frac{\sigma_y}{\sigma_{cr}}$ ratio, i.e., the greater the ratio, the smaller will be the difference between the buckling load and the failure load, as reported before. Since the inelastic buckling stress is close to the yielding strength, post-buckling strength cannot be expected.

An interesting discussion was presented by N. J. Hoff[4] concerning the definition of buckling load of an inelastic column. He observed that there is no definition of experimental buckling load in a manner acceptable to all research men. The maximum load has the most clear-cut physical significance and is also easily observed experimentally. So-called critical load is based on the classical concept of

stability and is obtained as the Eigenvalue of the load
at which neighboring, slightly deflected equilibrium con-
figuration exist simultaneously with the initial config-
uration of deflections. The extension of this concept
leads to the double modulus load which gives a value higher
than the maximum inelastic column load. The tangent modulus
load has the merit that it can be easily calculated as soon
as the stress-strain curve is known. It also agrees, on
the average, with the maximum load observed with actual,
somewhat imperfect columns.

In view of this, the maximum observed stresses (i.e.,
the P/A at maximum load) are given in Table II for compar-
ison with the computed values. A quick over-all comparison
is presented in Fig. 14. A non-dimensional curve is plotted
taking $\lambda = \frac{1}{\pi} \sqrt{\frac{\sigma_y}{E}} (L/r)_{eff}$ vs. $\frac{\sigma_{cr}}{\sigma_y}$ as shown. The scat-
tering of the experimental data is not large in general, and
the agreement with the theoretical curve is close.

It is seen that the only significant unconservative
deviations from the C = 4.5 curve (up to 15%) occurred for
three hat sections. Hat sections had the largest number of
corners of all sections tested and therefore, probably the
largest imperfections. This is confirmed by the over-all
shape of the load-deformation curves at the hat section
columns.

For comparison, $(\sigma_{cr})_t$ based on C = 4.5 are computed
and are listed in Table II. Two additional curves based
on C = 5 and C = 4 are also plotted in Fig. 14, the latter
corresponding to CRC column curve except (L/r) is $(L/r)_{eff}$

in this case. The buckling stresses of angle sections are
closer to the values computed by using C = 5, while those
of lipped angle and hat sections are closer to the values
by C = 4. This is to be expected since the stress-strain
curve for angle section is more of the sharp yielding type,
while for lipped angle and hat sections it is more of a
gradually yielding pattern.

It is seen from Fig. 14 that, if desired for simplicity,
one may get more conservative, yet reasonable, torsional-
flexural buckling stresses for all tested shapes by replacing
4.5 by 4.0 in Eq. (15).

SUMMARY AND CONCLUSIONS

1. The most difficult factor in the analysis of in-
elastic torsional-flexural buckling is the determination
of the appropriate tangent modulus of shear. In order to
simplify the computations and yet obtain reasonably accurate
value of computed buckling stress, an assumption was made
in Eq. (7). This makes possible the simple extension of
the computation procedure of the elastic case into the
inelastic range.

2. As the best fit to stub column test results, the
tangent modulus, E_t, was expressed in the parabolic form:

$$E_t = 4.5 \; E \; \frac{\sigma}{\sigma_y} \; (1 - \frac{\sigma}{\sigma_y})$$

to represent the over-all stress-strain relationship of
the columns.

3. The torsional-flexural buckling stress in the inelastic range (i.e., for $(\sigma_{cr})_t \geq \sigma_p = \frac{2}{3}\sigma_y$) can be computed by the following formula:

$$(\sigma_{cr})_t = \sigma_y \left[1 - \frac{\sigma_y}{4.5(\sigma_{cr})_E}\right]\qquad(15)$$

in which

$$(\sigma_{cr})_E = \frac{1}{2[1-(\frac{x_o}{r_o})^2]}\left[\sigma_x + \sigma_\phi - \sqrt{(\sigma_x + \sigma_\phi)^2 - 4[1-(\frac{x_o}{r_o})^2]\sigma_x \cdot \sigma_\phi}\right]$$

4. Thirty tests on full size columns were made. The experimental results agreed with the computed values within a close range.

5. More conservative values of buckling stress may be obtained by replacing the numerical factor 4.5 in Eq. (15) by 4. In this case, if $(L/r)_{eff}$ is used in place of (L/r), the CRC parabolic column curve for flexural buckling can also be employed for thin-walled members which buckle in a torsional-flexural mode.

REFERENCES

1. Timoshenko, S. P., and J. M. Gere. Theory of Elastic Stability, McGraw-Hill, 1961.

2. Bleich, F. Buckling Strength of Metal Structures, McGraw-Hill, 1952.

3. First Progress Report on Torsional-Flexural Buckling of Thin-Walled Open Sections (by A. Chajes and G.Winter, 1963).

4. Hoff, N. J. Buckling and Stability, Journal of Royal Aeronautical Society, v. 58, p. 1, January, 1954.

5. Karren, K. Effects of Cold-Forming on Light-gage Steel Members, Sixth Progress Report, Dept. of Structural Eng., Cornell University.

6. Galambos, T. V. and Y. Fukumoto. Inelastic Lateral-torsional Buckling of Beam-Columns, Fritz Engineering Lab. Report No. 205A.34.

7. Galambos, T. V., and P. F. Adams and Y. Fukumoto. Further Studies on the Lateral-Torsional Buckling of Steel Beam-Columns, Fritz Eng. Lab Report No. 205A.36.

8. Bernstiel, C., and Michalos, J. Ultimate Load of H-Columns under Biaxial Bending, J. Struc. Division, Trans. ASCE, April, 1963.

9. Roik, K. Biegedrillknicken mittig gedrückter Stäbe mit offenem Profil im unelastischen Bereich, Der Stahlbau, 1956, p. 10.

10. Bijlaard, P. P., Fisher, G. P. Interaction of Column and Local Buckling, NACA TN 2640, 1952.

TABLE 1. SUMMARY OF SPECIMENS

| Section | Specimen | Dimensions (in) | | | | L | σ_y(ksi) |
		a	b	c	t		
Plain Angle	A-1	1.93			0.135	56.0	44.7
	A-2	1.83			0.135	40.0	44.7
	A-3	2.35			0.135	55.0	41.4
	A-4	2.39			0.135	55.0	41.4
	A-5	2.60			0.135	30.0	41.4
	A-6	1.438			0.103	39.98	30.0
Lipped Angle	LA-1	2.135	0.568		0.1365	40.0	47.0
	LA-2	2.635	0.8175		0.135	50.0	45.6
	LA-3	2.135	0.568		0.1365	65.02	41.0
	LA-4	2.635	0.8175		0.135	65.04	45.6
	LA-5	1.847	.8086		0.1028	59.97	31.7
	LA-6	2.007	.9166		0.103	49.98	31.7
	LA-7	1.584	0.780		0.0908	49.97	32.2
	LA-8	1.582	0.8125		0.103	50.4	34.25
	LA-9	1.675	0.825		0.090	49.97	32.2
Channel	CH-1	2.135	1.568		0.135	55.03	45.25
	CH-2	1.603	1.552		0.103	34.0	31.0
	CH-3	1.603	1.552		0.103	40.03	31.0
	CH-4	1.5468	1.5684		0.1032	60.05	31.0
	CH-5	2.057	2.069		0.103	60.0	30.4
	CH-6	2.068	1.829		0.1023	54.97	30.4
	CH-7	1.546	1.568		0.1045	50.03	31.0
	CH-8	2.047	1.819		0.1028	55.0	30.4
	CH-9	1.584	1.534		0.0866	45.0	31.0
Hat	HA-1	2.135	2.135	1.068	0.135	45.0	46.9
	HA-2	2.635	2.135	1.318	0.135	49.94	46.9
	HA-3	2.135	2.135	1.068	0.135	60.0	46.9
	HA-4	1.587	1.857	0.8085	0.103	50.03	36.5
	HA-5	1.581	1.811	0.775	0.090	50.0	36.5
	HA-6	2.098	2.058	1.059	0.1019	60.0	30.7

Note: Cross-sectional dimensions a, b and c denote inside middle-line dimensions.

TABLE 2   TEST RESULTS

Specimen		Buckling Stress (ksi)				
		Tested	Computed			
			C=4	% Diff.	C=4.5	% Diff.
Angle	A-1	38.31	35.6	− 7.07	36.65	− 4.53
	A-2	38.26	36.6	− 4.34	37.50	− 2.02
	A-3	33.20	28.5	−14.1	29.89	−11.10
	A-4	33.18	29.1	−12.3	30.43	− 9.04
	A-5	32.2	27.4	−14.9	28.90	−11.4
	A-6	22.49	23.8	+ 5.82	24.57	+ 8.25
Lipped Angle	LA-1	36.6	36.0	− 1.64	37.22	+ 2.31
	LA-2	34.6	37.9	+ 9.53	38.76	+10.8
	LA-3	30.3	30.9	+ 0.99	32.71	+ 8.0
	LA-4	30.23	29.6	− 2.08	31.28	+ 3.45
	LA-5	26.46	24.3	− 8.16	25.10	− 5.3
	LA-6	23.90	23.8	− 0.42	24.73	+ 7.0
	LA-7	24.96	25.7	+ 2.96	26.40	+ 5.45
	LA-8	27.17	28.0	+ 3.05	28.70	+ 5.23
	LA-9	27.05	25.5	− 5.74	26.21	− 0.34
Channel	CH-1	38.79	39.8	+ 0.05	40.82	+ 4.95
	CH-2	29.46	28.2	− 4.28	28.49	− 3.4
	CH-3	27.95	27.5	− 1.61	27.93	− 0.71
	CH-4	24.98	25.4	+ 1.68	25.98	− 3.85
	CH-5	25.24	25.8	+ 2.22	26.27	− 4.18
	CH-6	27.28	26.4	− 3.22	26.90	− 1.41
	CH-7	27.05	26.4	− 2.40	26.94	− 0.41
	CH-8	26.40	26.5	− 0.38	26.96	+ 2.1
	CH-9	26.73	26.6	− 0.487	27.13	+ 1.48
Hat	HA-1	38.19	38.7	+ 1.33	39.58	+ 3.52
	HA-2	38.94	38.9	− 0.10	39.72	+ 1.96
	HA-3	31.60	34.1	+ 7.91	34.95	+ 8.27
	HA-4	23.75	26.9	+13.7	28.00	+15.20
	HA-5	22.57	25.6	+13.4	26.83	+15.60
	HA-6	23.32	23.9	+ 2.42	24.68	+ 5.50
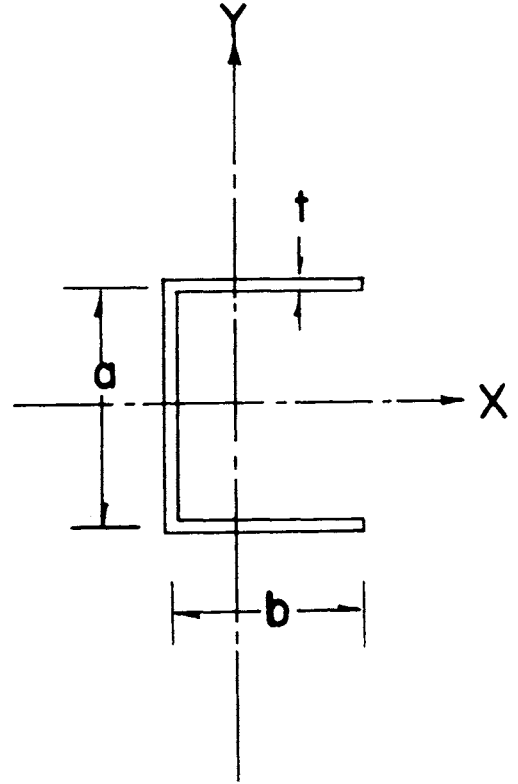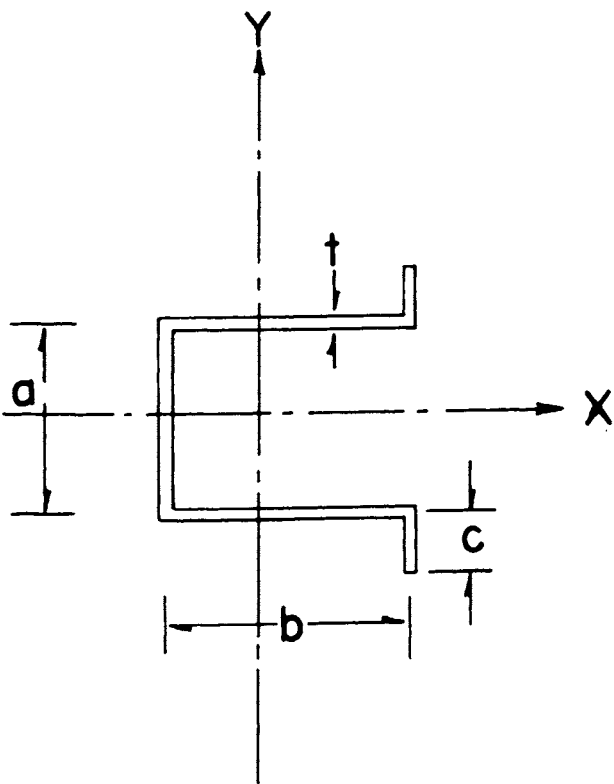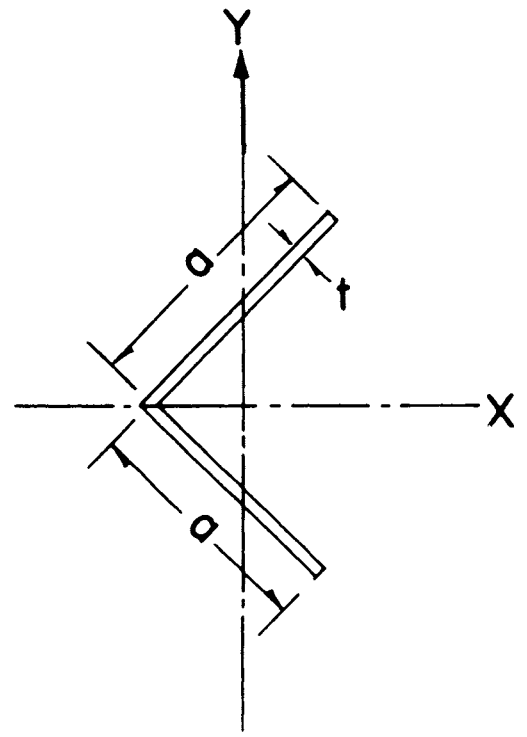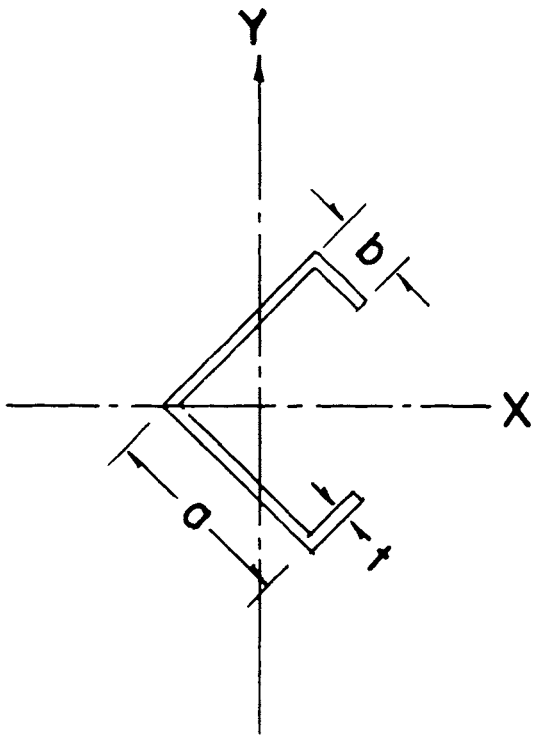
FIG.1. SINGLY SYMMETRICAL SECTIONS
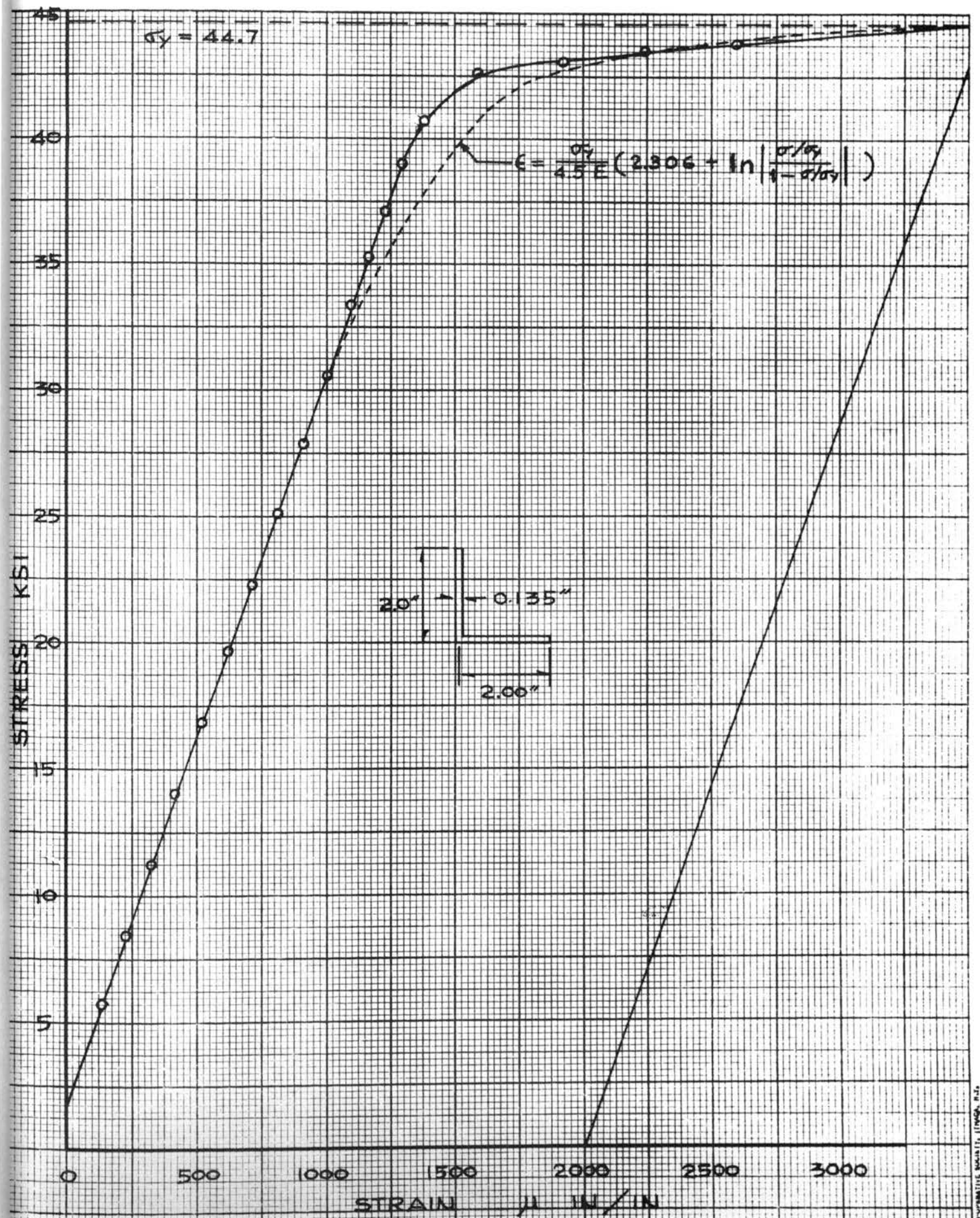
$$\epsilon = \frac{\sigma_y}{4.5\,E}\left(2.306 + \ln\left|\frac{\sigma/\sigma_y}{1-\sigma/\sigma_y}\right|\right)$$

$\sigma_y = 44.7$

STRESS KSI

STRAIN μ IN/IN

2.0"   ⊢ 0.135"

2.00"

FIG - 2   STUB COL. STRESS - STRAIN CURVE

FIG - 3 STUB COL. STRESS - STRAIN CURVE

$\sigma_y = 32.4$ KSI

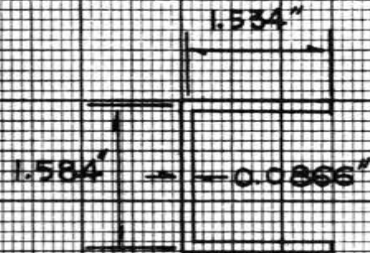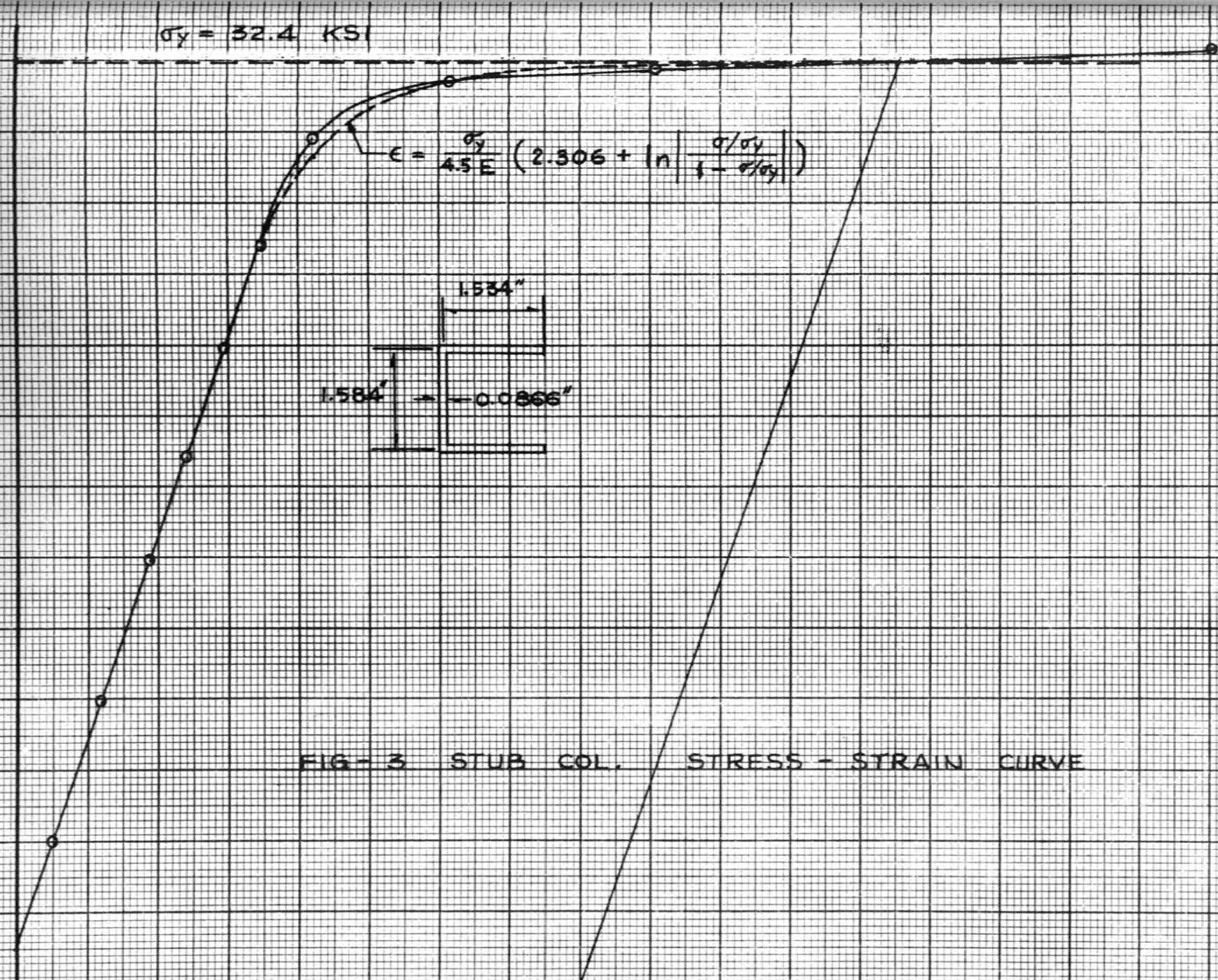$$\epsilon = \frac{\sigma_y}{4.5 E}\left(2.306 + \ln\left|\frac{\sigma/\sigma_y}{1 - \sigma/\sigma_y}\right|\right)$$

STRESS, KSI

STRAIN μ IN / IN

$\sigma_y = 34.25 \text{ KSI}$

$$\epsilon = \frac{\sigma_y}{4.5E}\left(2.306 + \ln\left|\frac{\sigma/\sigma_y}{1-\sigma/\sigma_y}\right|\right)$$

1.582"

0.103"

0.81"

1.582"

STRESS KSI

35

30

25

20

815

10

5

0   500   1000   1500   2000   2500   3000

STRAIN   μ IN/IN

FIG - 4   STUB COL. STRESS - STRAIN CURVE

$$\epsilon = \frac{\sigma_y}{45E}\left(2.306 + \ln\left|\frac{\sigma/\sigma_y}{1 - \sigma/\sigma_y}\right|\right)$$

$\sigma_y = 56.5$ KSI

STRESS KSI

1.81"

0.775"

1.58"   0.09"

0.775"

1.8"

STRAIN μ IN / IN
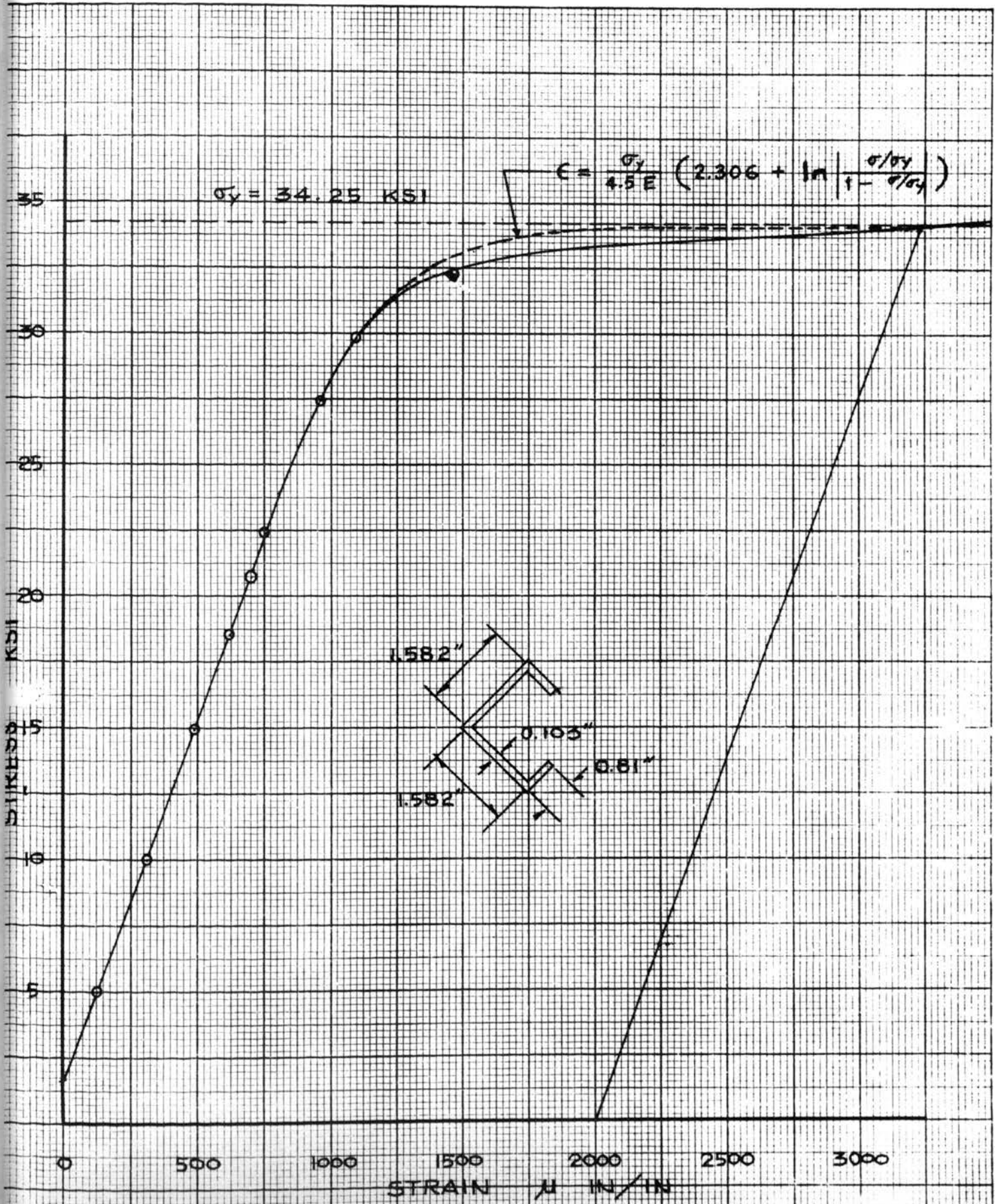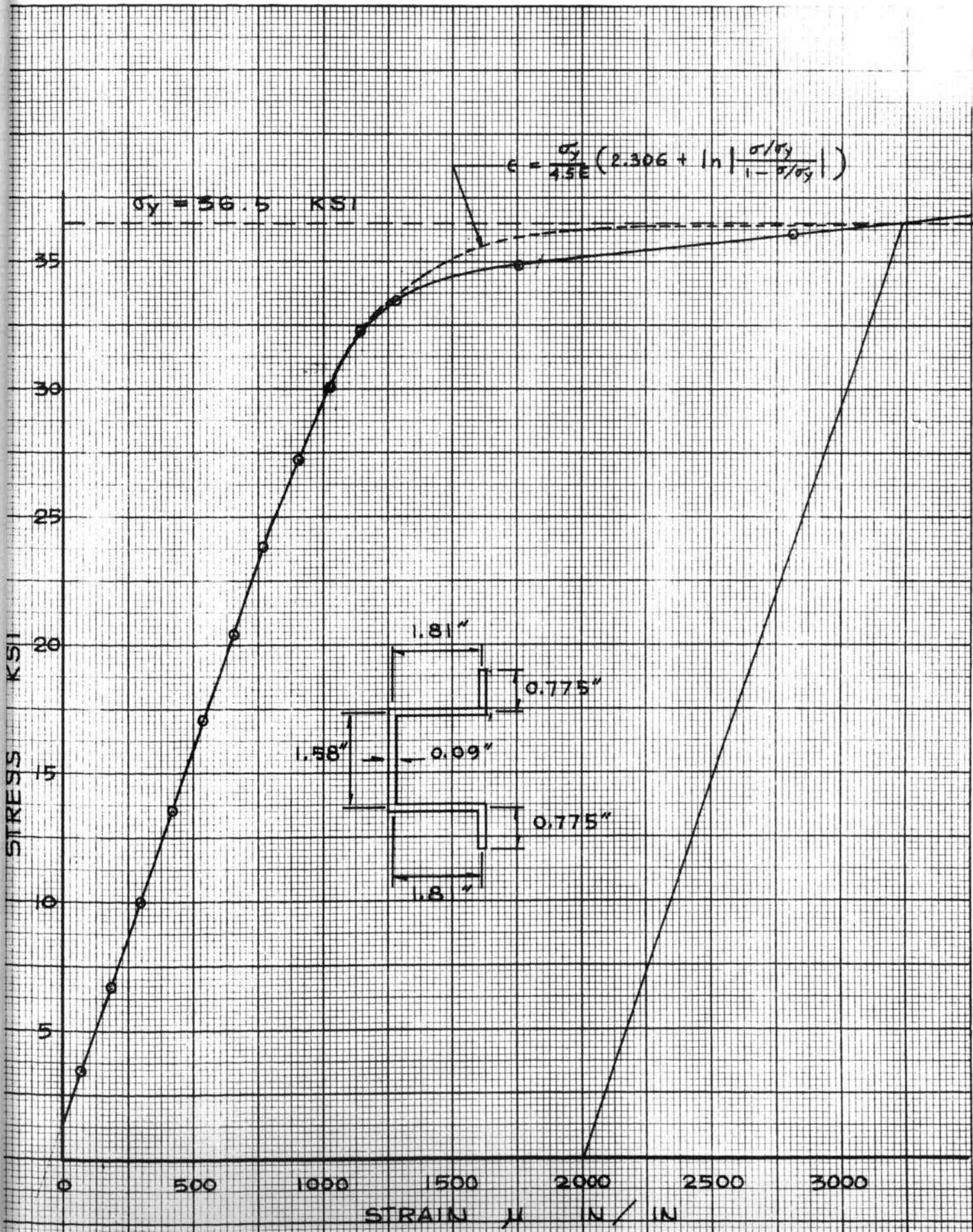
FIG - 5   STUB COL. STRESS - STRAIN CURVE

$$\frac{E_t}{E} = 4.5 \frac{\sigma}{\sigma_y}\left(1 - \frac{\sigma}{\sigma_y}\right)$$

$$\frac{E_t}{E} = 4 \frac{\sigma}{\sigma_y}\left(1 - \frac{\sigma}{\sigma_y}\right)$$
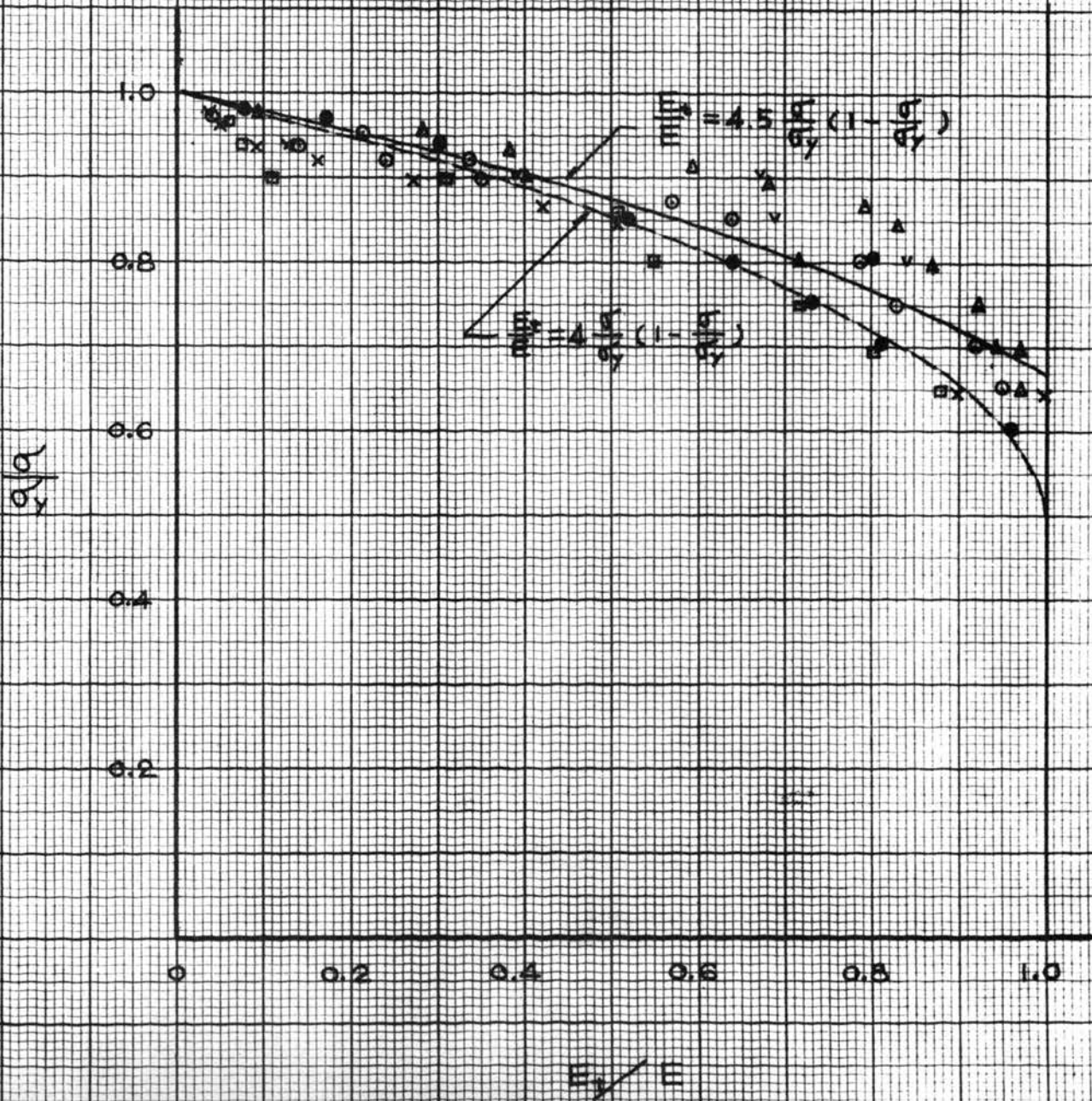
FIG - 6 TANGENT MODULI FROM STUB COLUMN TESTS

MACHINE HEAD

HYDROSTONE

MILLED STEEL ℞

SPECIMEN

STEELPIPE CASING

MILLED STEEL ℞

HYDROSTONE

MACHINE BASE

8"

7 3/4"

A

A

SR-4 STRAIN GAGE

METAL TUBING

HYDROSTONE

STEEL PIPE CASING

A – A
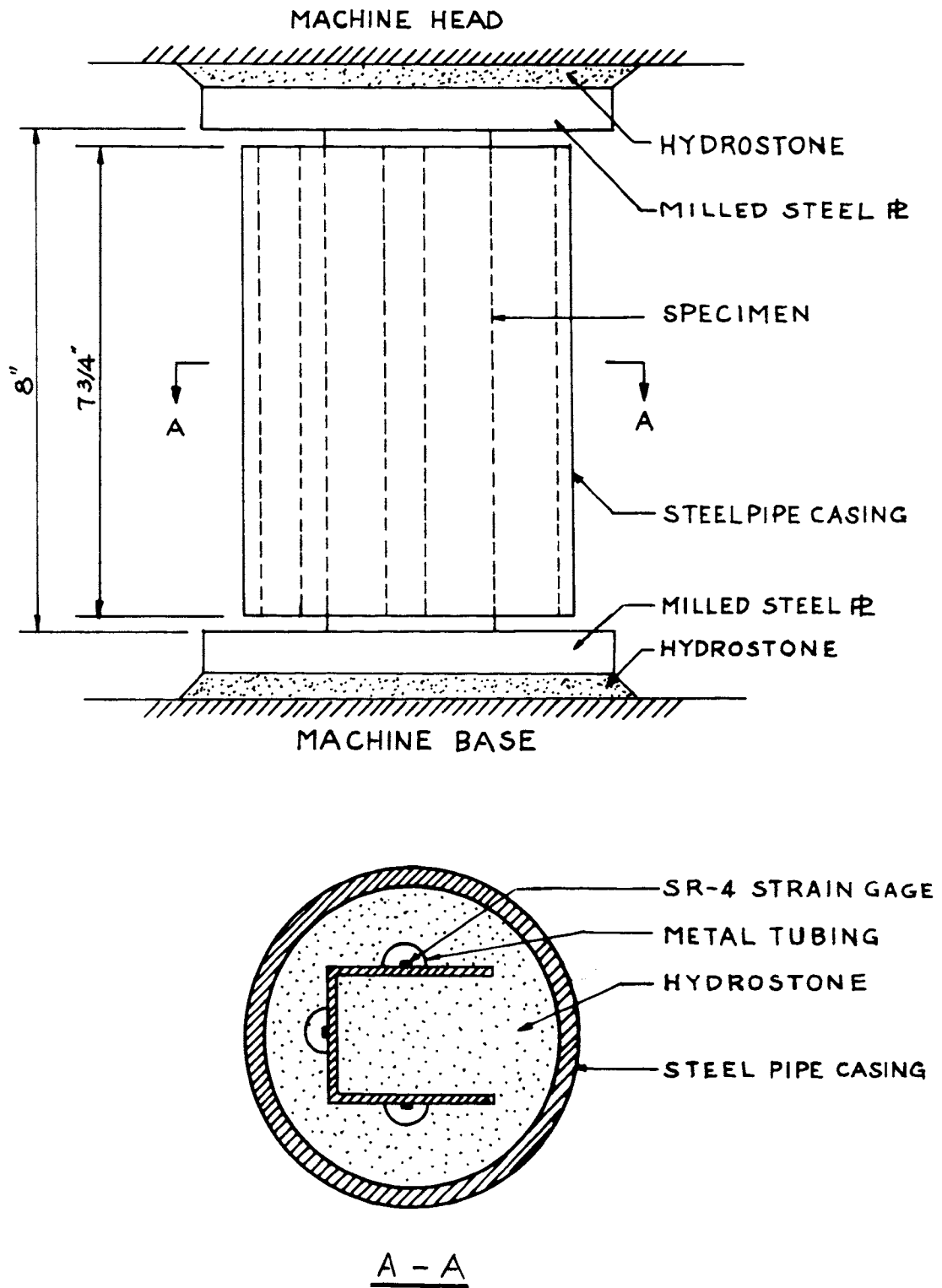
FIG. 7 STUB COLUMN TEST SET-UP
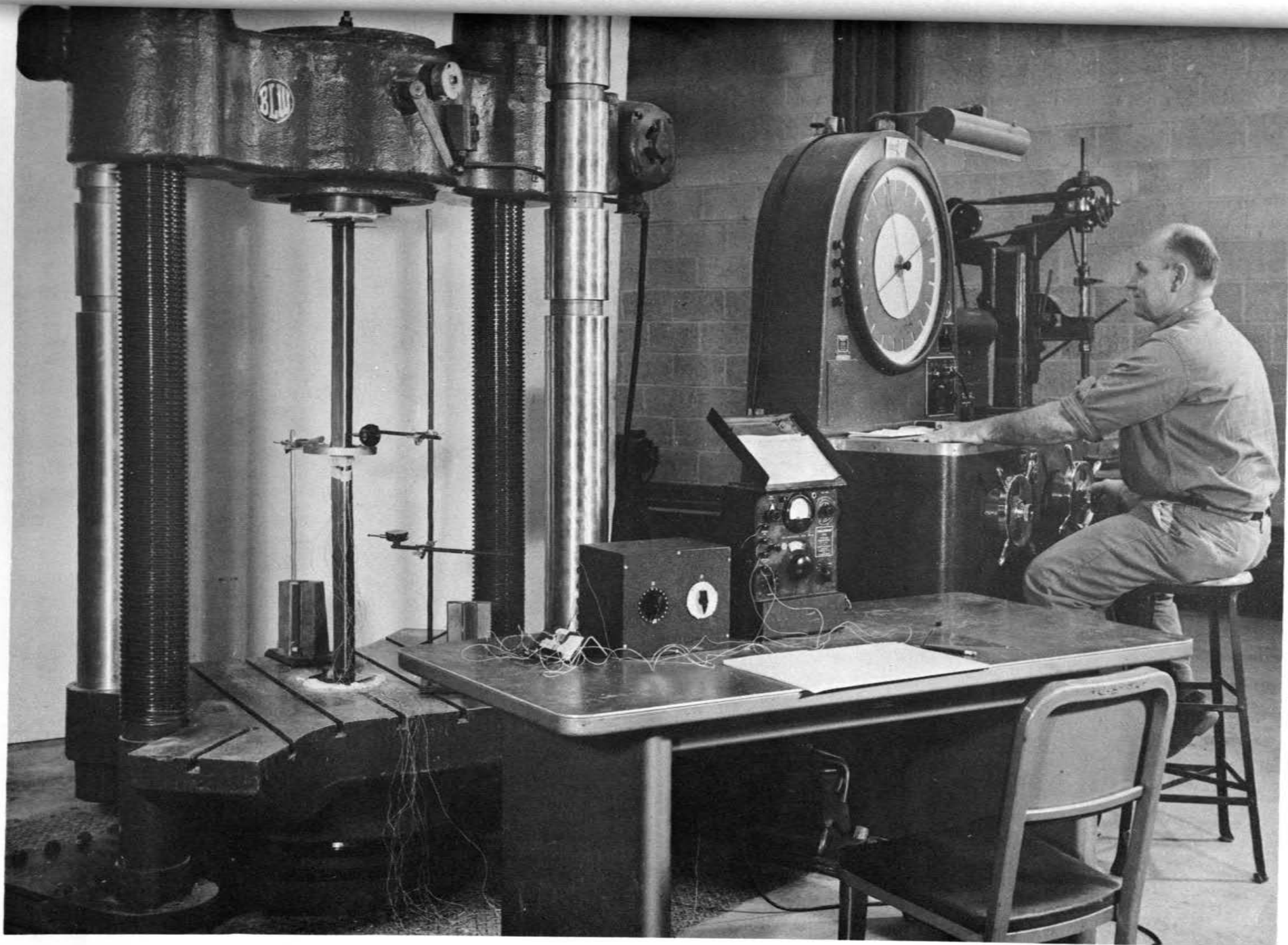
FIG. 8   COLUMN TEST SET-UP
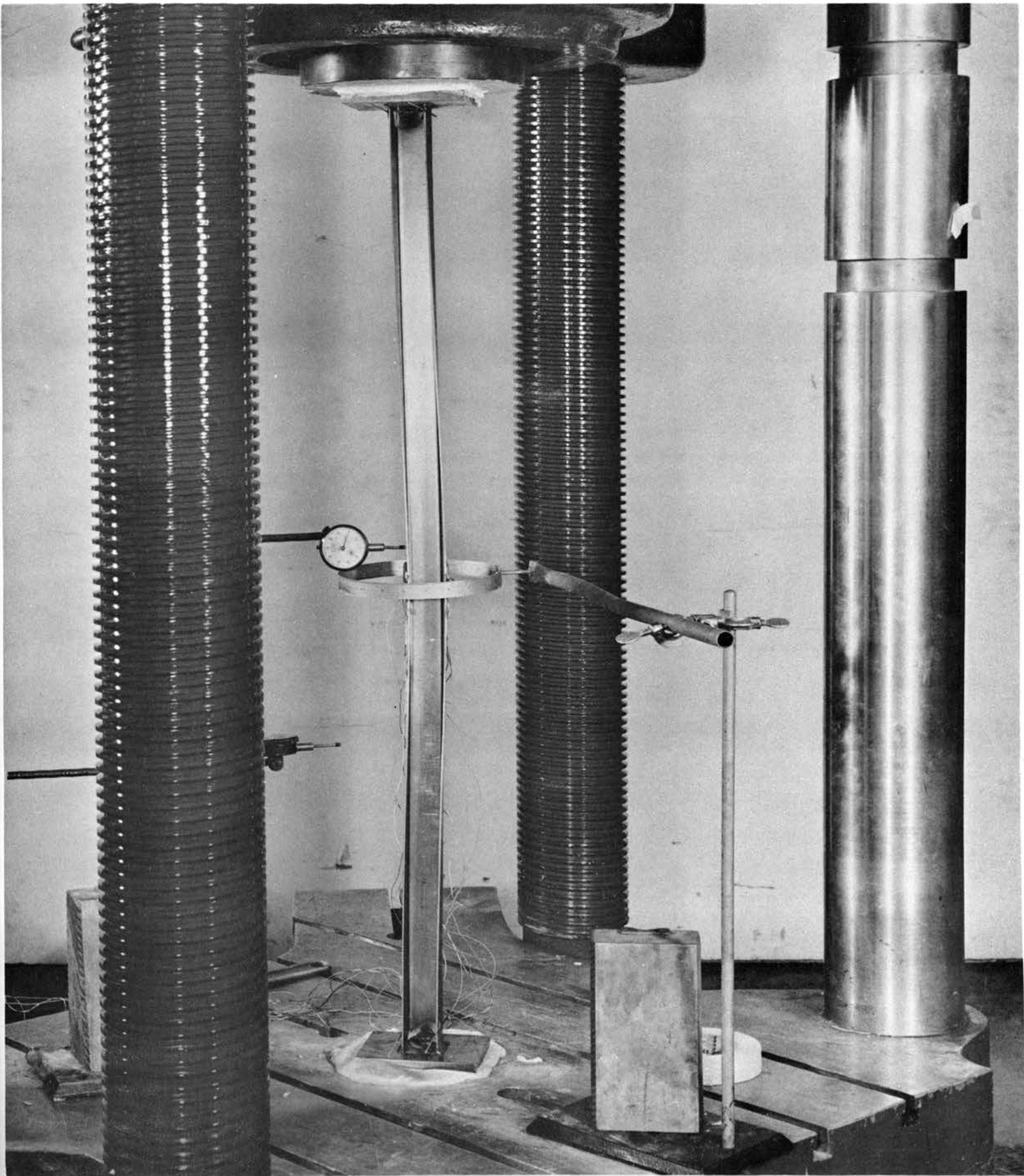
FIG. 9. COLUMN TEST (CHANNEL SECTION)

FIG — 10 STRESS — DEFORMATION CURVE

TEST A-4

$(\sigma_{cr})_t = 30.43$ KSI

$(\sigma_{cr})_t = 30.43$ KSI

STRESS KSI

MID HEIGHT ROTATION — RADIANS
$(\times 10^{-3})$

MID HEIGHT DEFLECTION
N $(\times 10^{-3})$
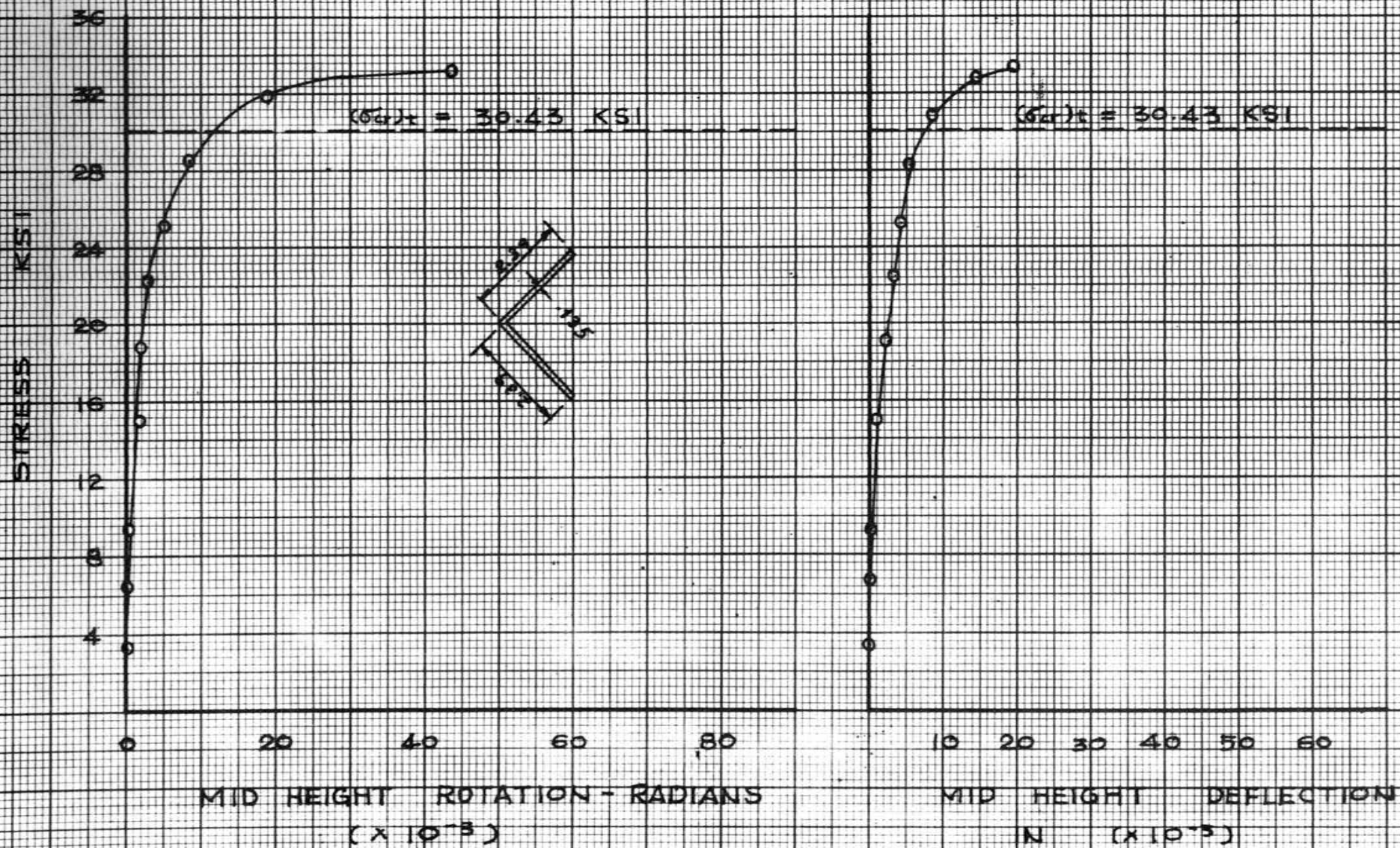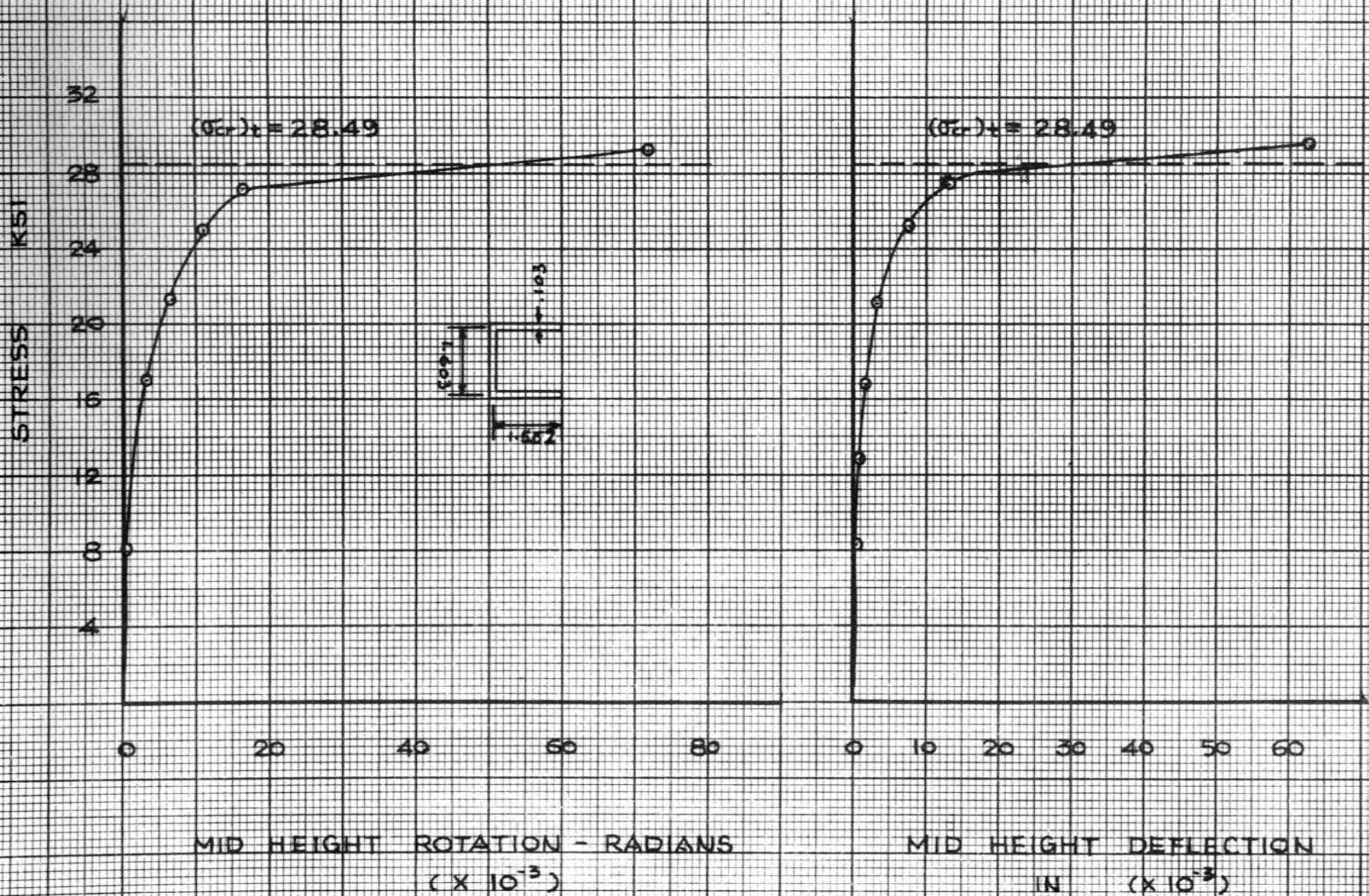
FIG - 11   STRESS - DEFORMATION   CURVE
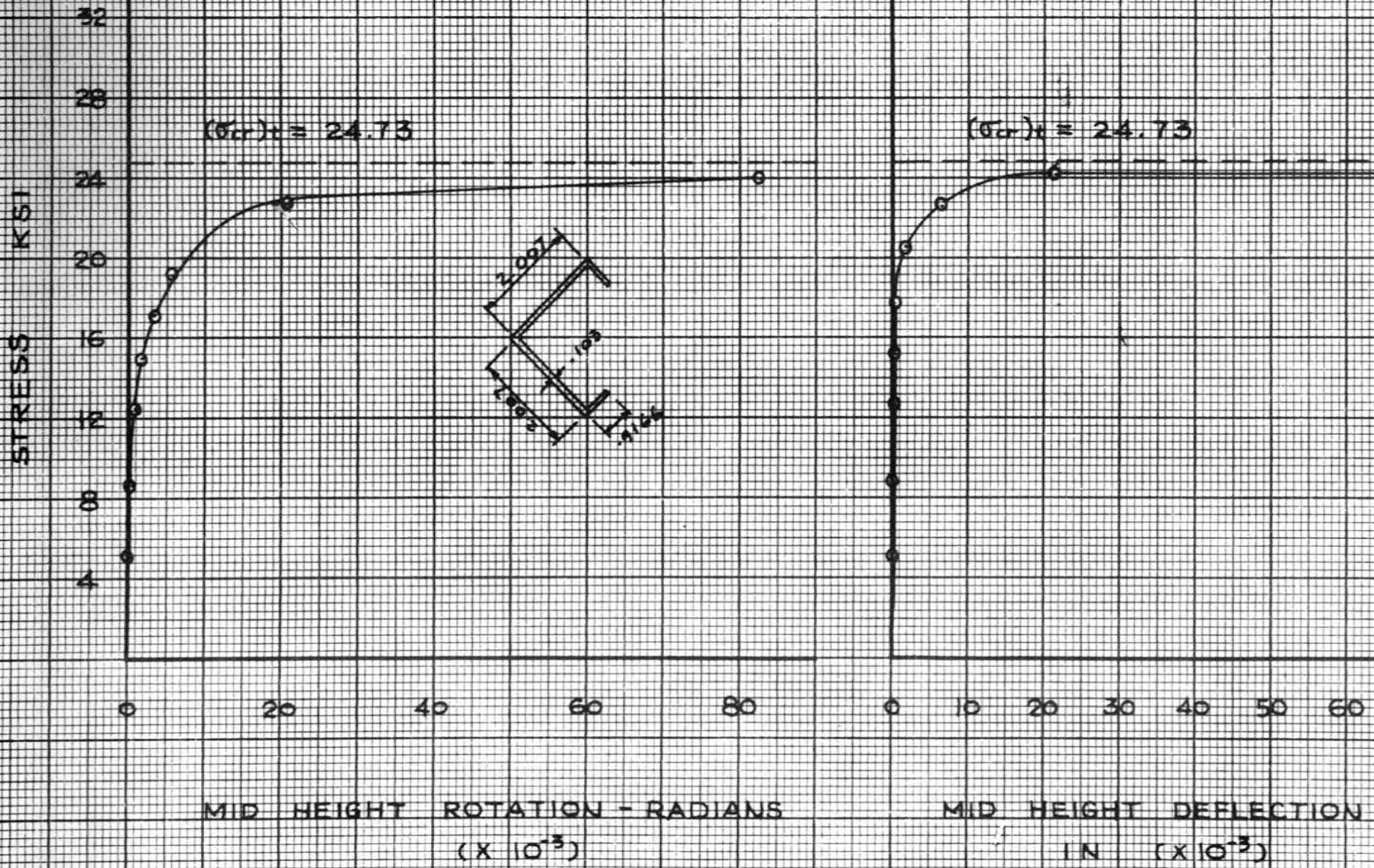
FIG - 12 STRESS - DEFORMATION CURVE

TEST HA-16

FIG. 13 STRESS - DEFORMATION CURVE

$(\sigma_{cr})_t = 24.68$

$(\sigma_{cr})_t = 24.68$

STRESS KSI

MID HEIGHT ROTATION - RADIANS
$(\times 10^{-3})$

MID HEIGHT DEFLECTION
IN $(\times 10^{-3})$

2.16"
1.11"
2.2"
0.1018"
1.11"
2.16"
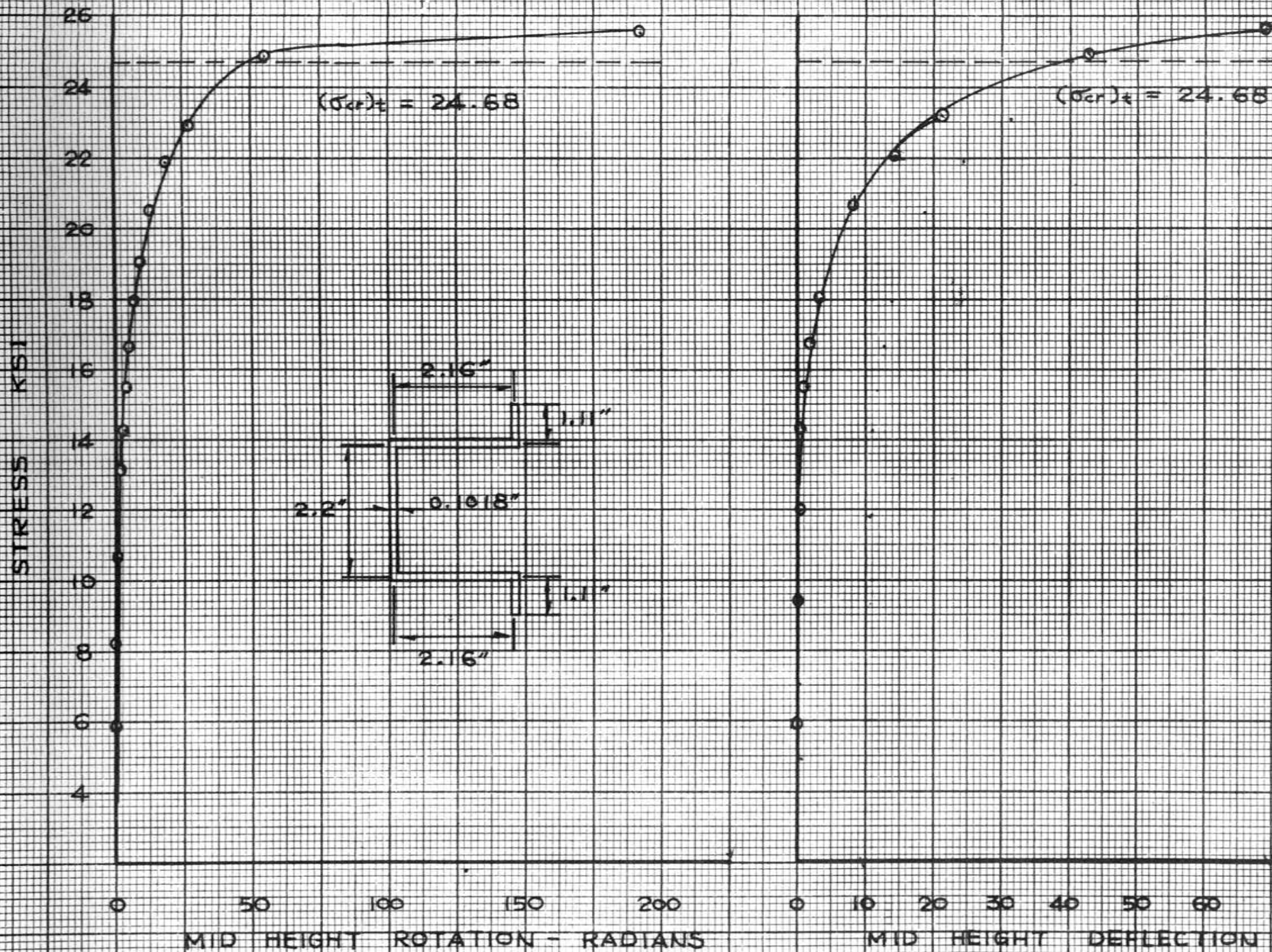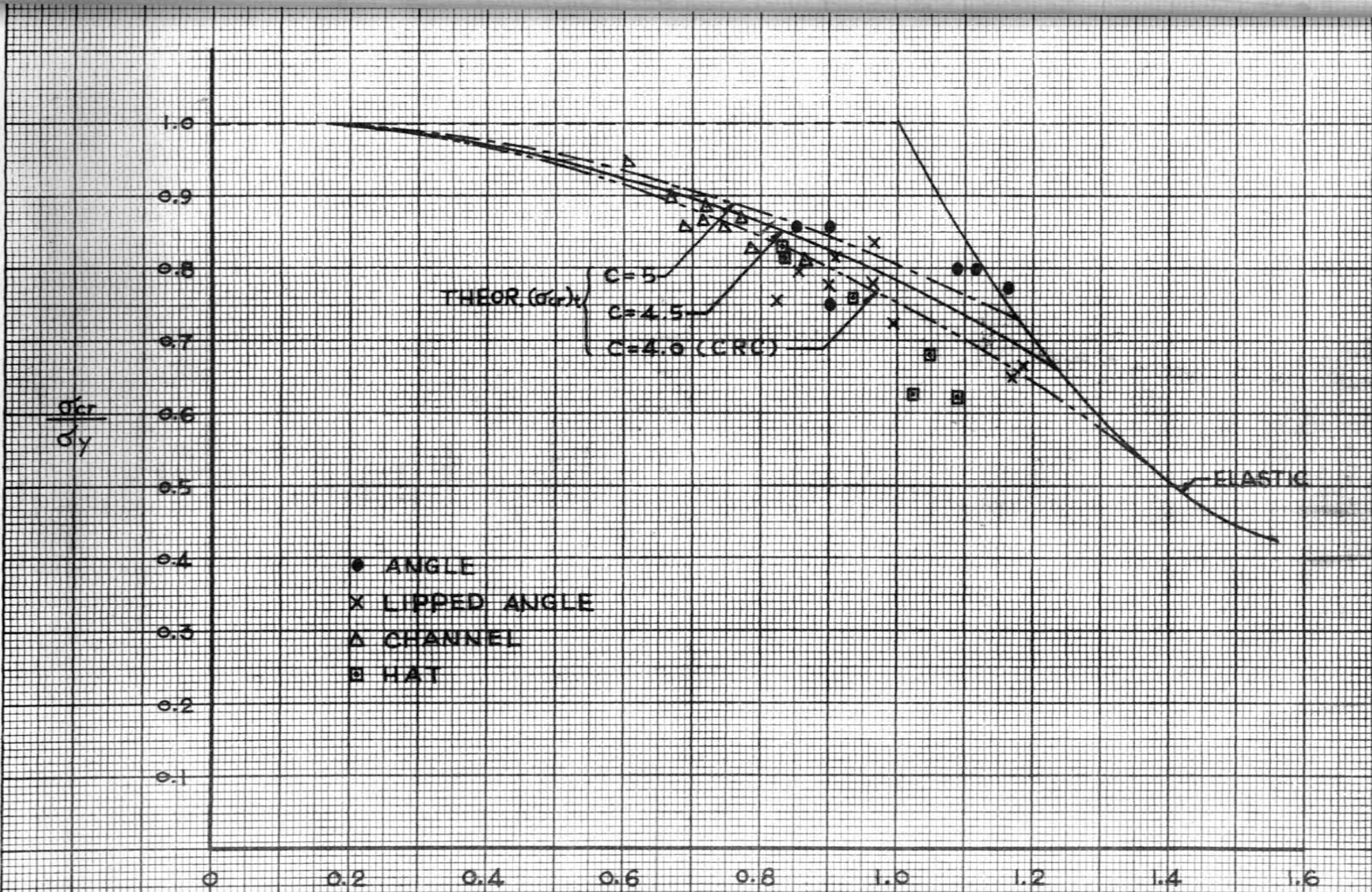
FIG - 14 COLUMN TEST RESULTS

APPENDIX A

Stub Column Stress-Strain Curves
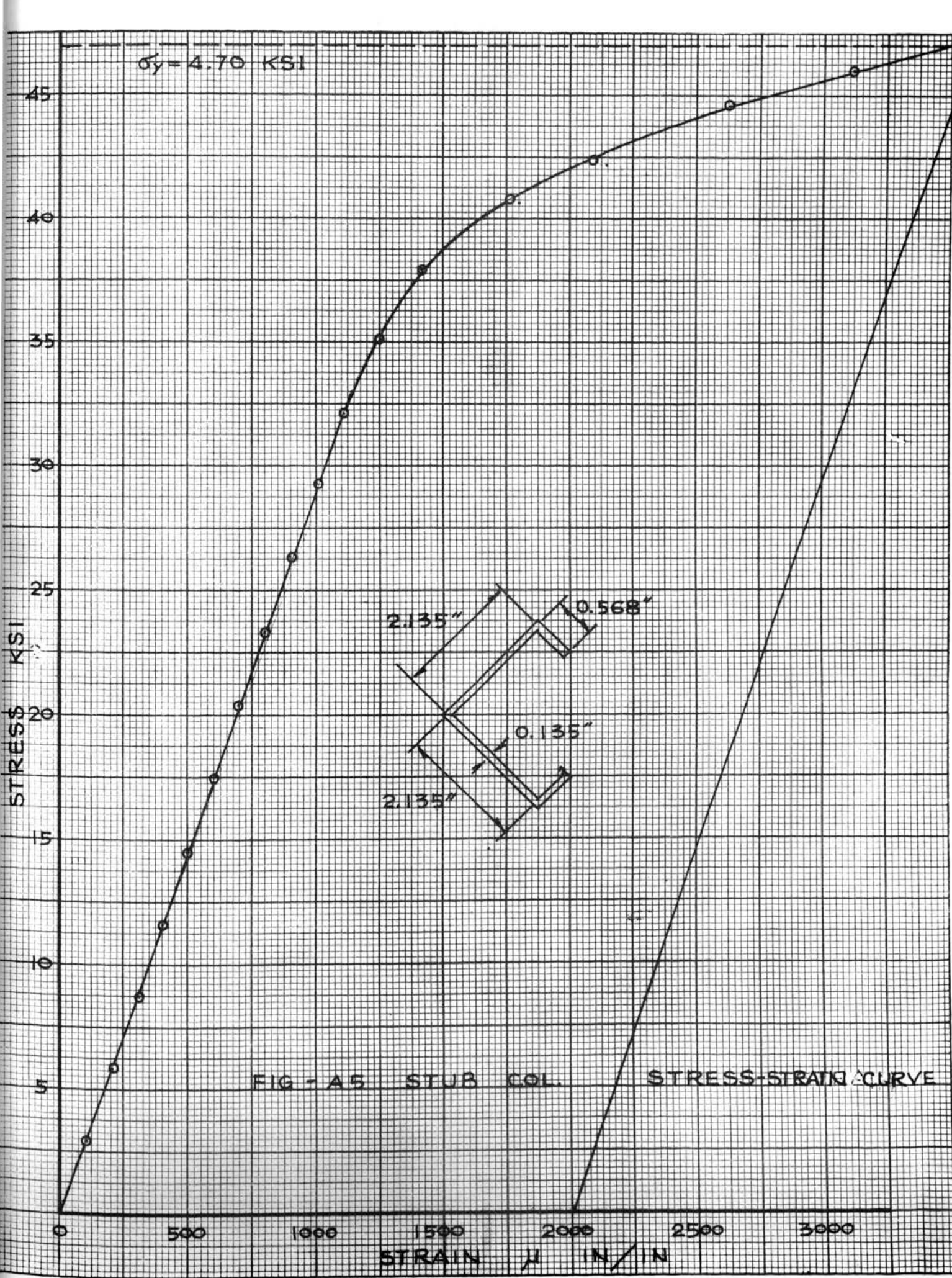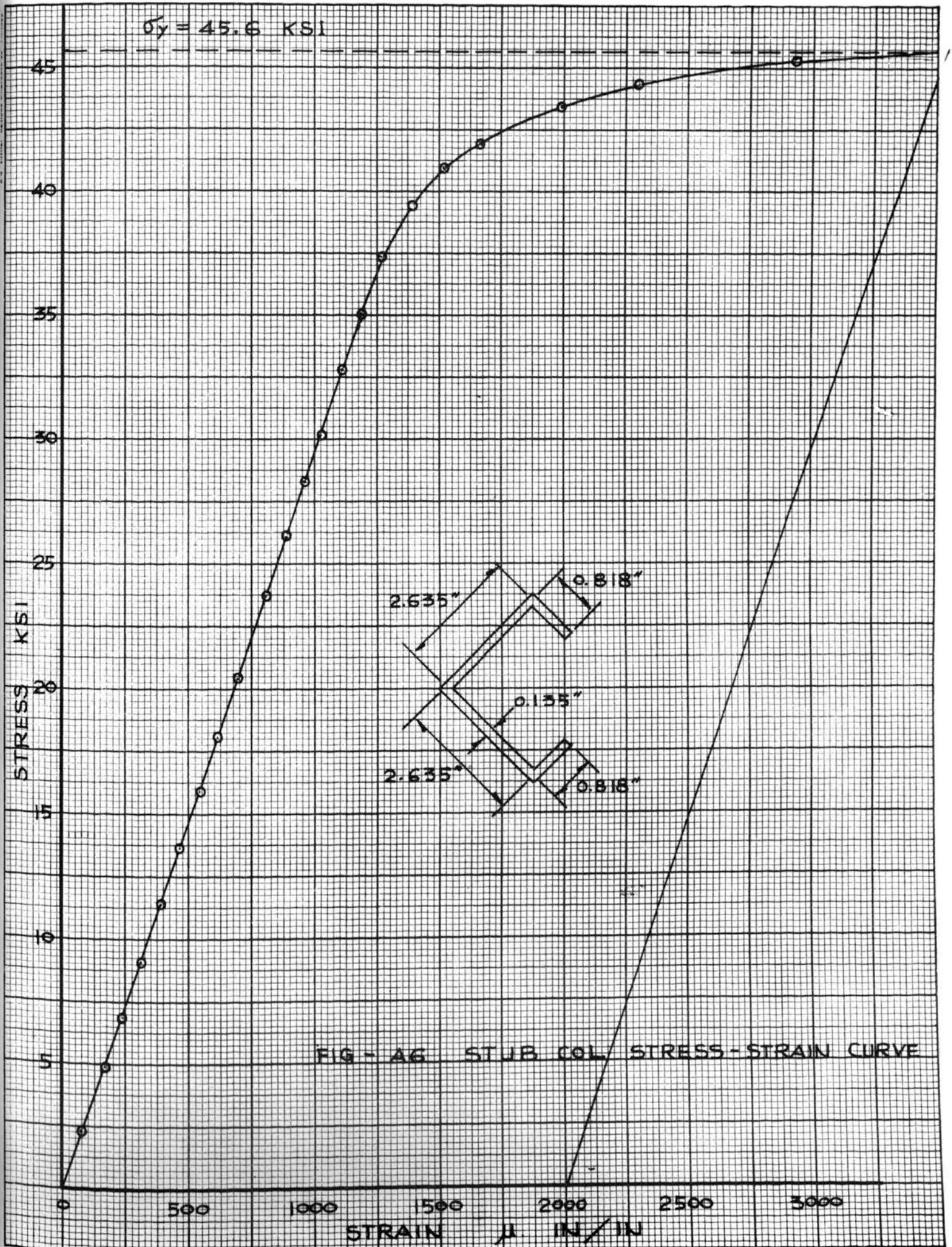
FIG - A1   STUB COL.   STRESS - STRAIN   CURVE

$\sigma_y = 30.0$ KSI

STRESS KSI

STRAIN μ IN / IN

1.45"

0.135"

1.45"
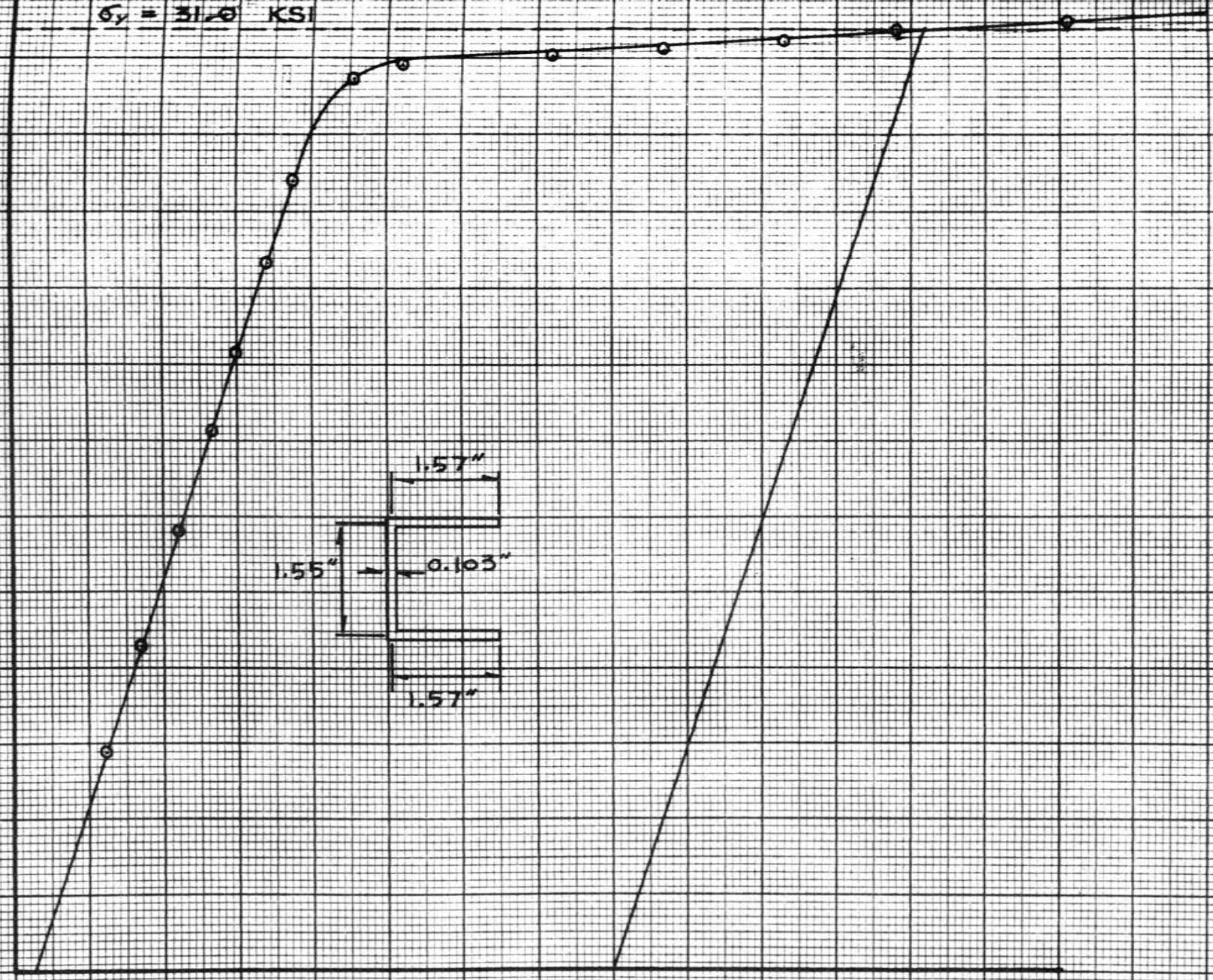
$\sigma_y = 41.4$ KSI

2.57"

0.135"

2.57"
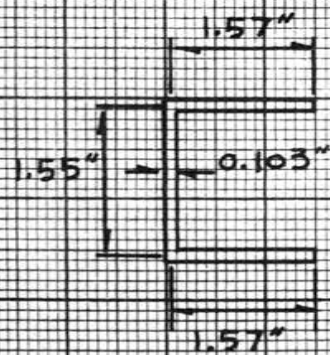
STRAIN μ IN/IN
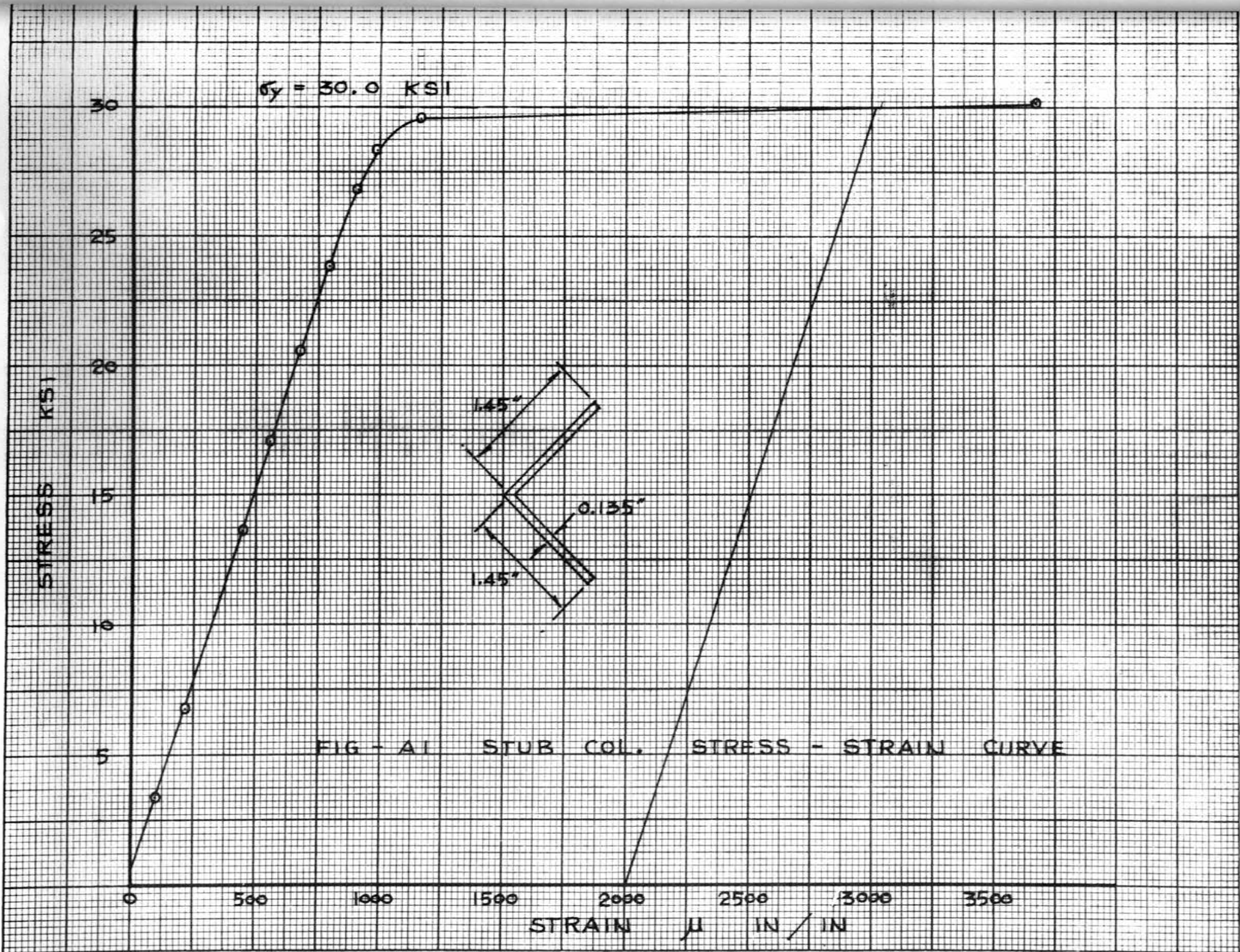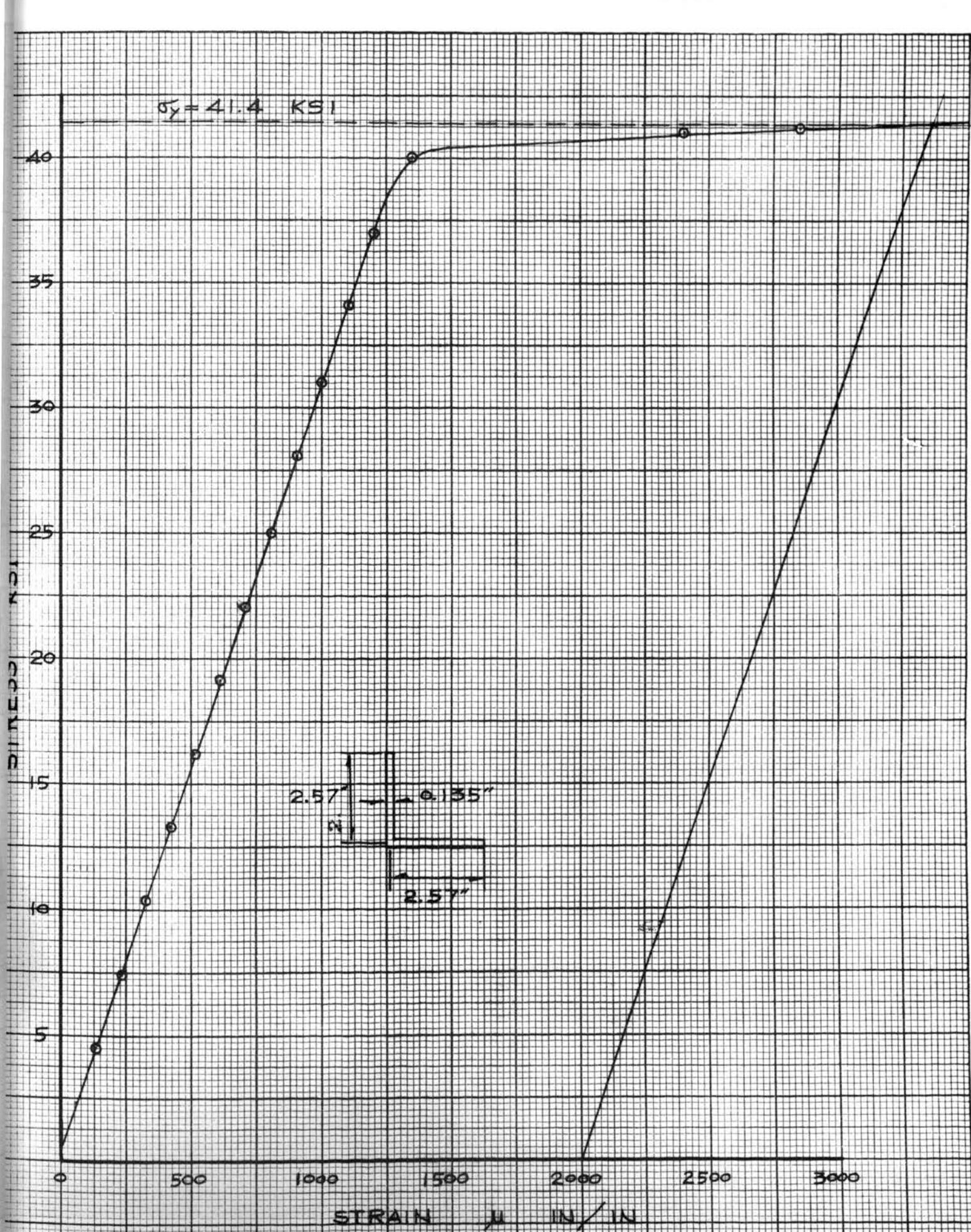
FIG - A2   STUB   COL   STRESS - STRAIN CURVE
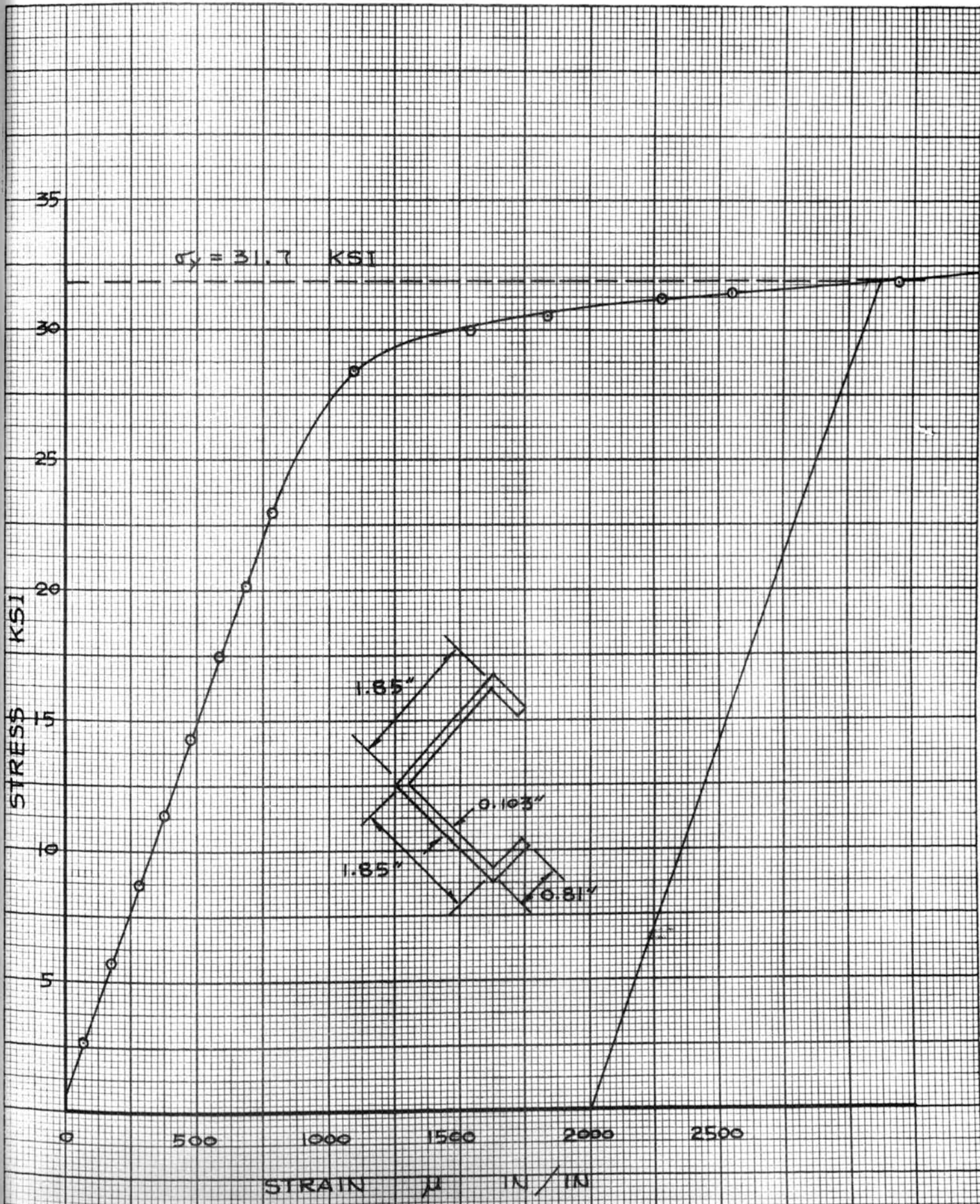
FIG - A3   STUB   COL   STRESS - STRAIN   CURVE
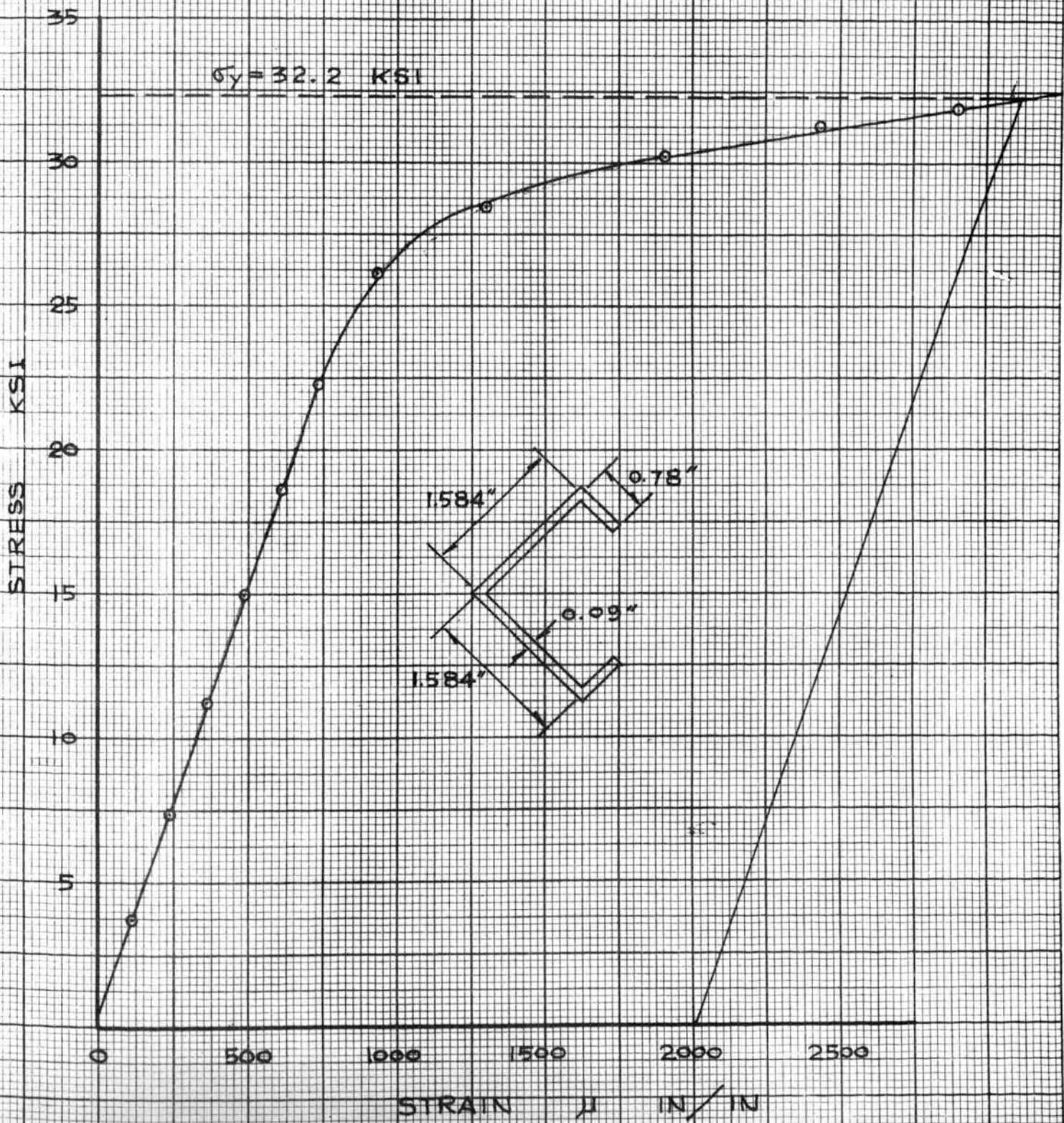
FIG - A4 STUB COL. STRESS - STRAIN CURVE

FIG - A5   STUB COL.   STRESS-STRAIN CURVE

$\sigma_y = 4.70$ KSI

STRESS   KSI

STRAIN μ IN/IN

2.135"   0.568"
0.135"
2.135"

FIG - A6 STUB COL STRESS-STRAIN CURVE

FIG - A7 STUB COL. STRESS - STRAIN CURVE

$\sigma_y = 31.0$ KSI

STRESS KSI

STRAIN μ IN/IN

1.53"
1.58"
0.09"
1.53"

FIG - A8 STUB COL. STRESS - STRAIN CURVE
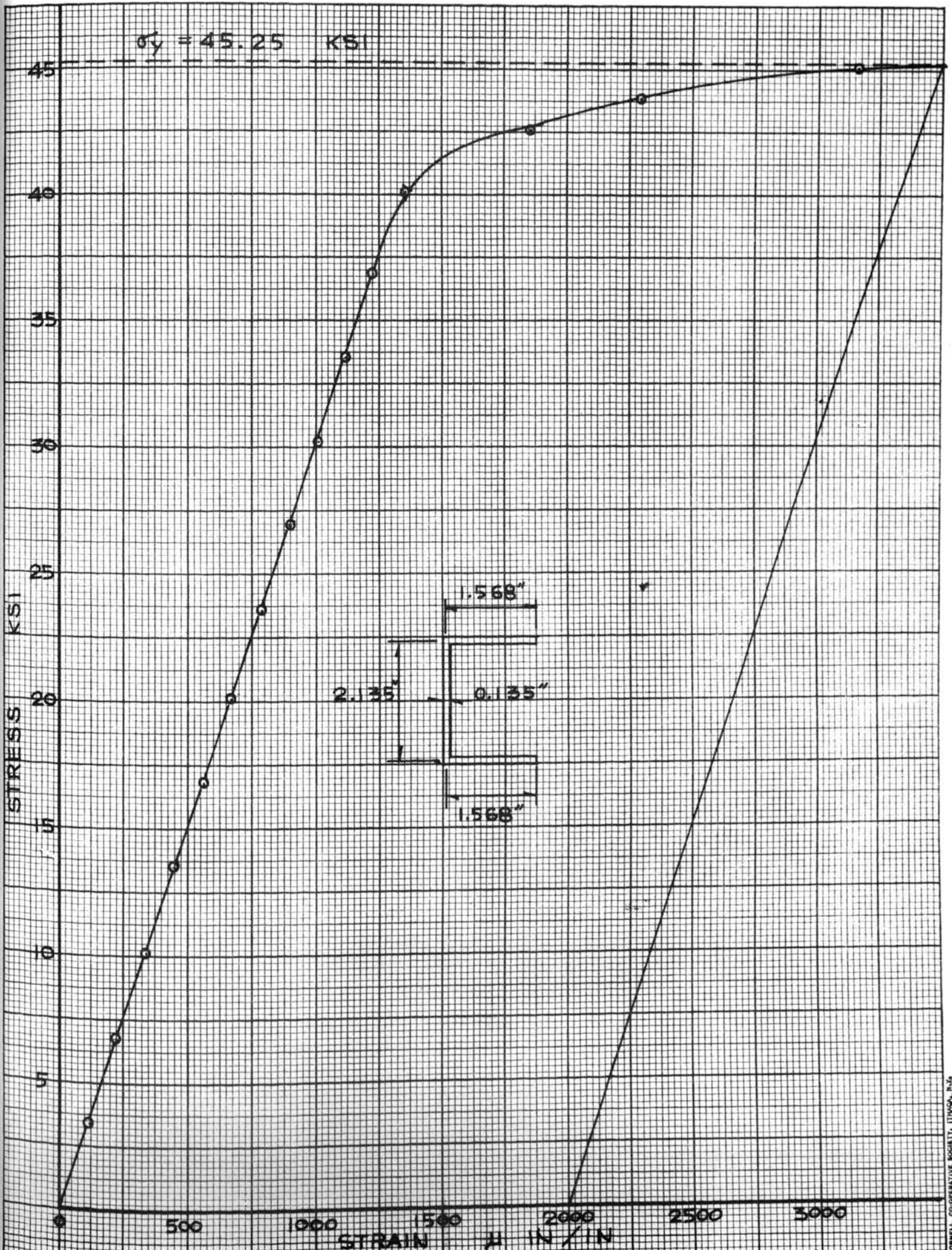
FIG - A9 STUB COL STRESS - STRAIN CURVE

FIG - A9 STUB COL STRESS - STRAIN CURVE

FIG - A10 STUB COL. STRESS - DEFORMATION CURVE
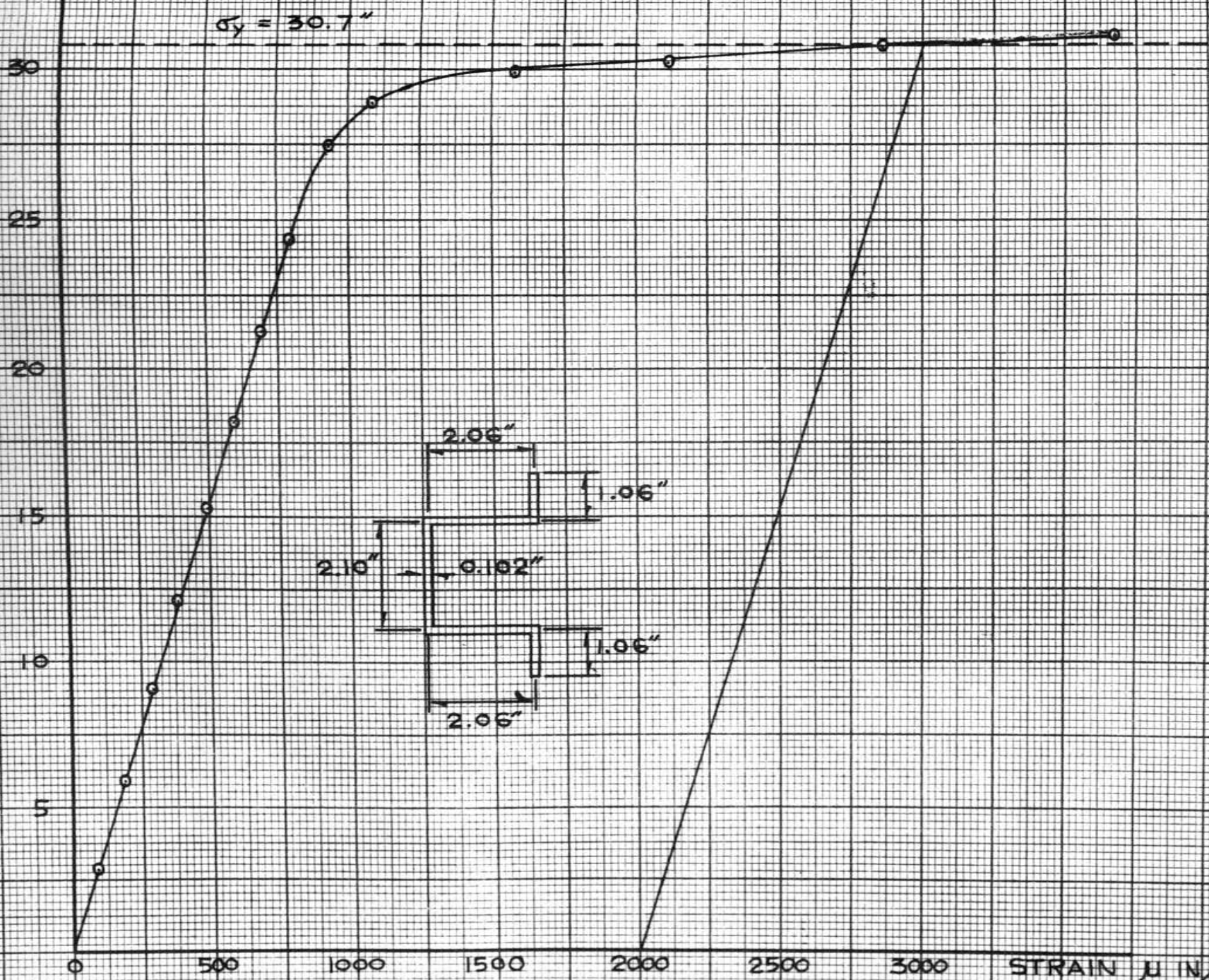
$\sigma_y = 30.4$ KSI

STRESS KSI

STRAIN μ IN / IN

2.069"
2.057" — 0.103"
2.069"

FIG - A 1   STUB COL. STRESS - STRAIN CURVE

$\sigma_y = 30.7''$

STRESS KSI

STRAIN μ IN/IN
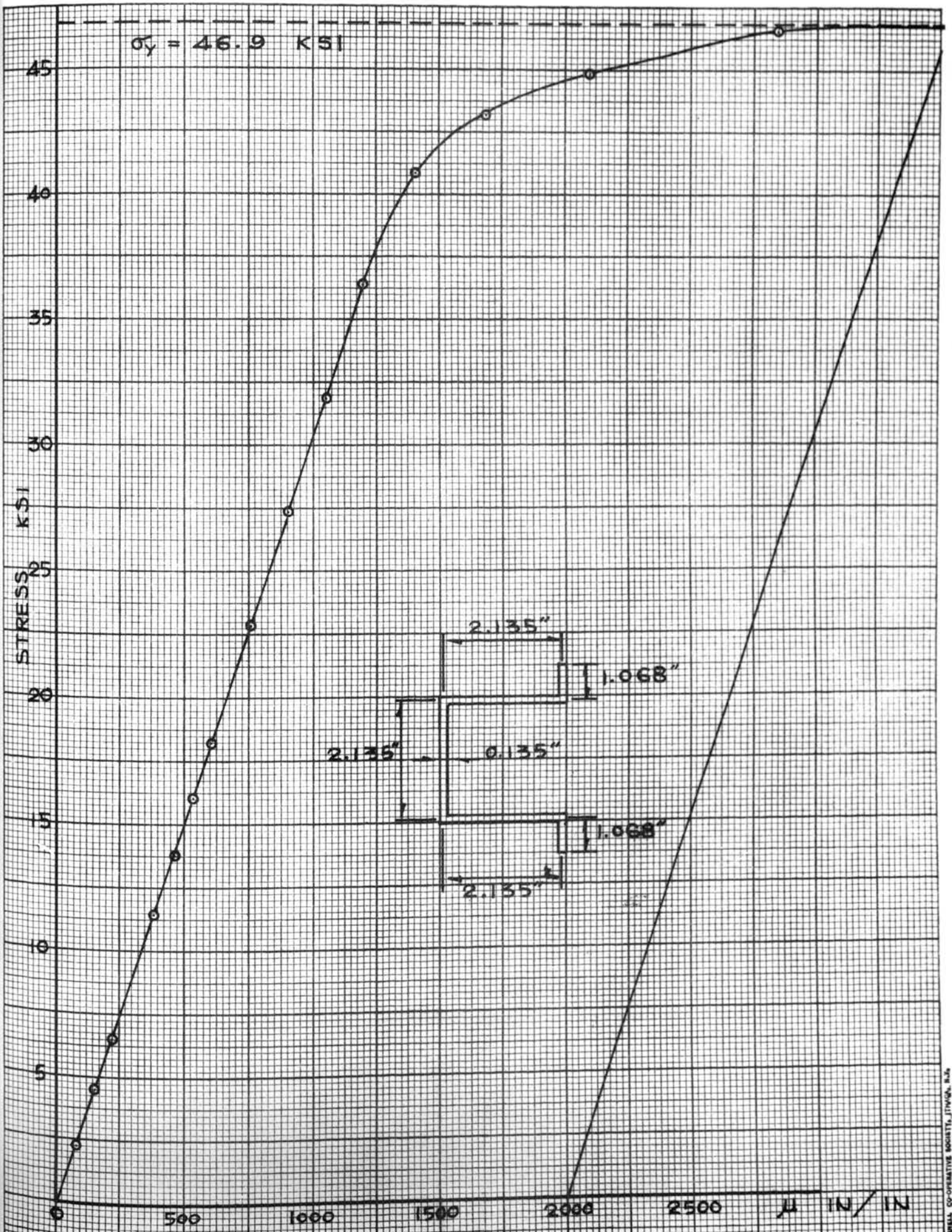
2.06"

1.06"

2.10"   0.102"

1.06"

2.06"
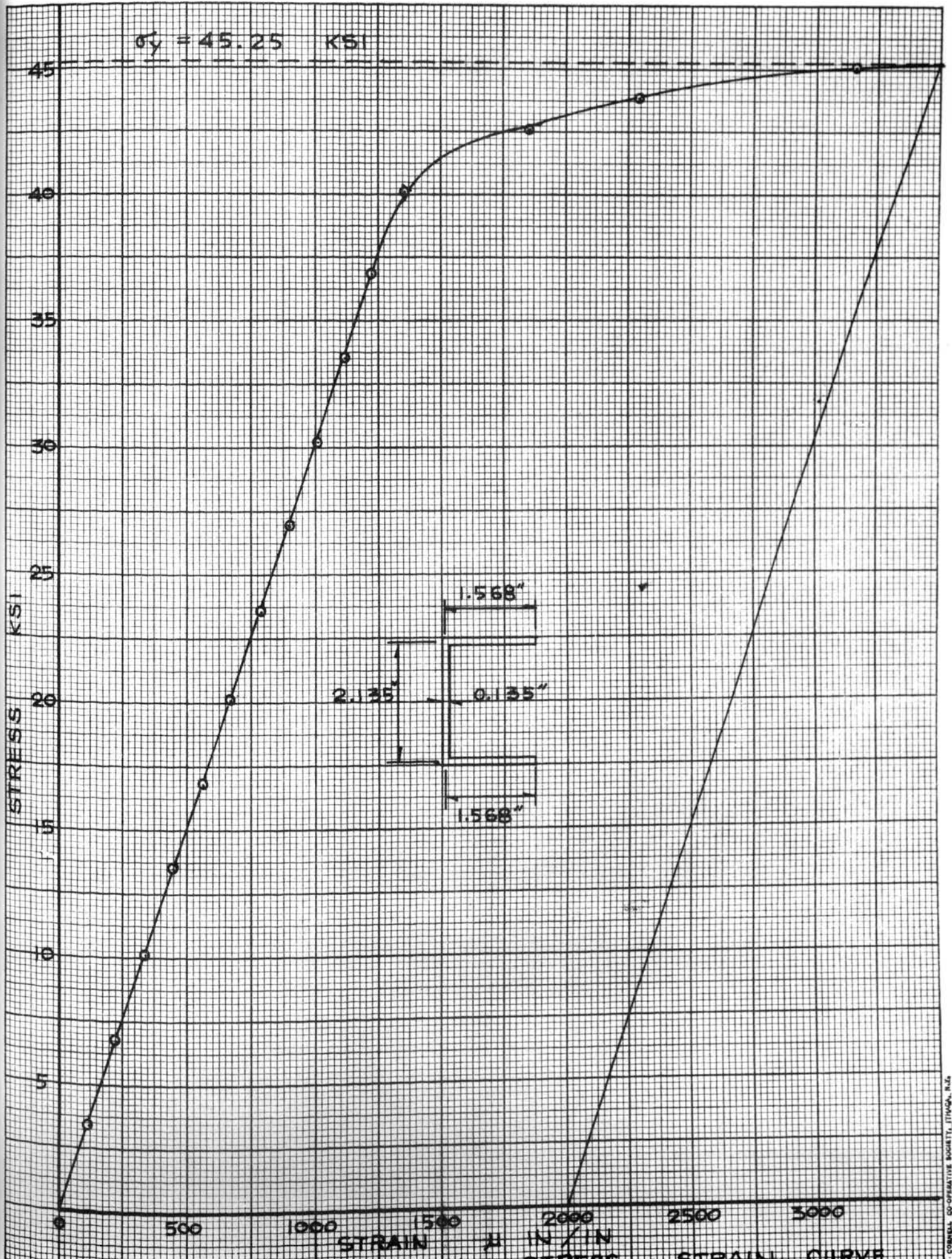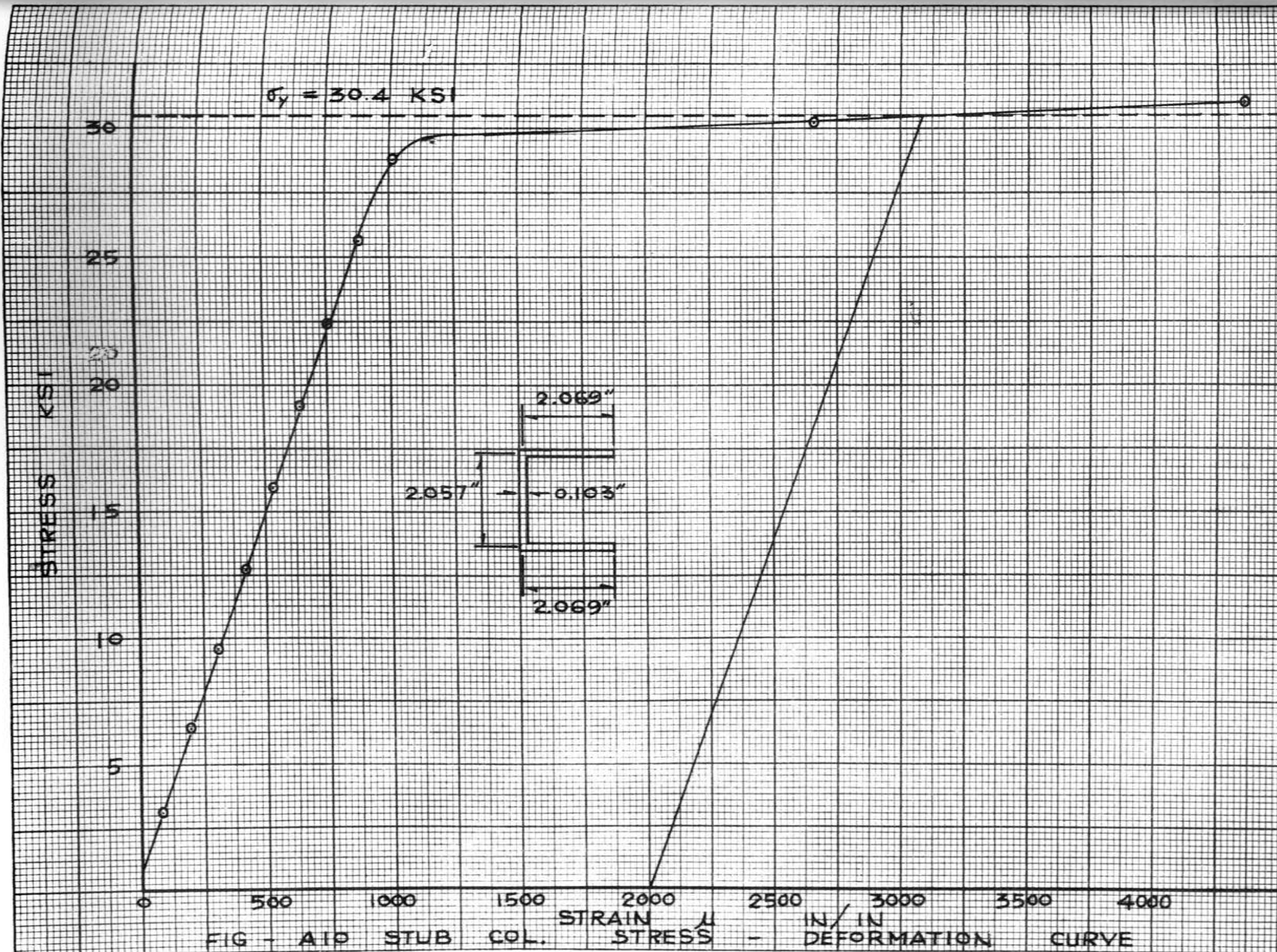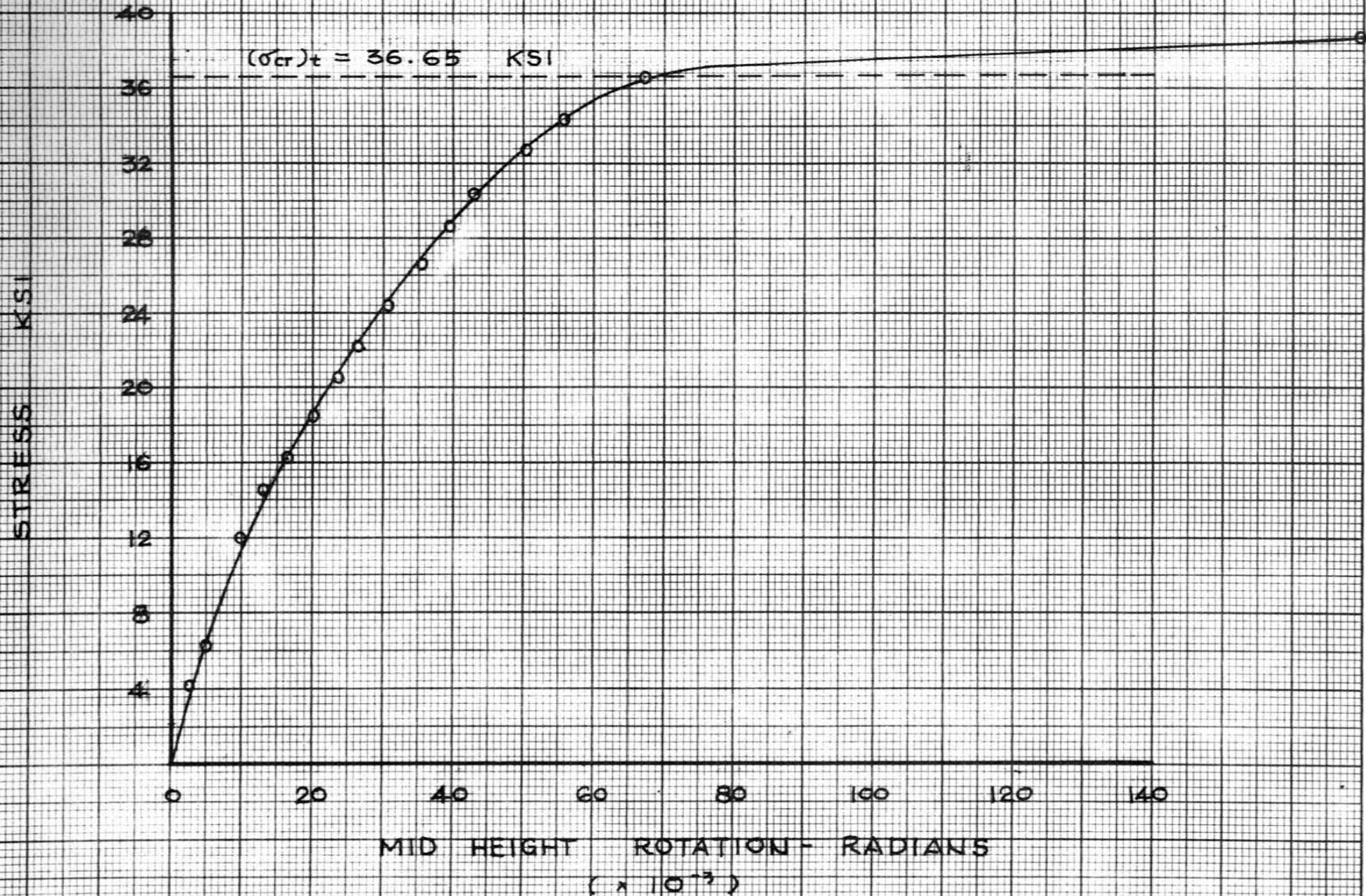
FIG - A12 STUB COL. STRESS - STRAIN CURVE

APPENDIX B

Stress-Deformation Curves of Column Specimens

FIG - BAI   STRESS - DEFORMATION CURVE
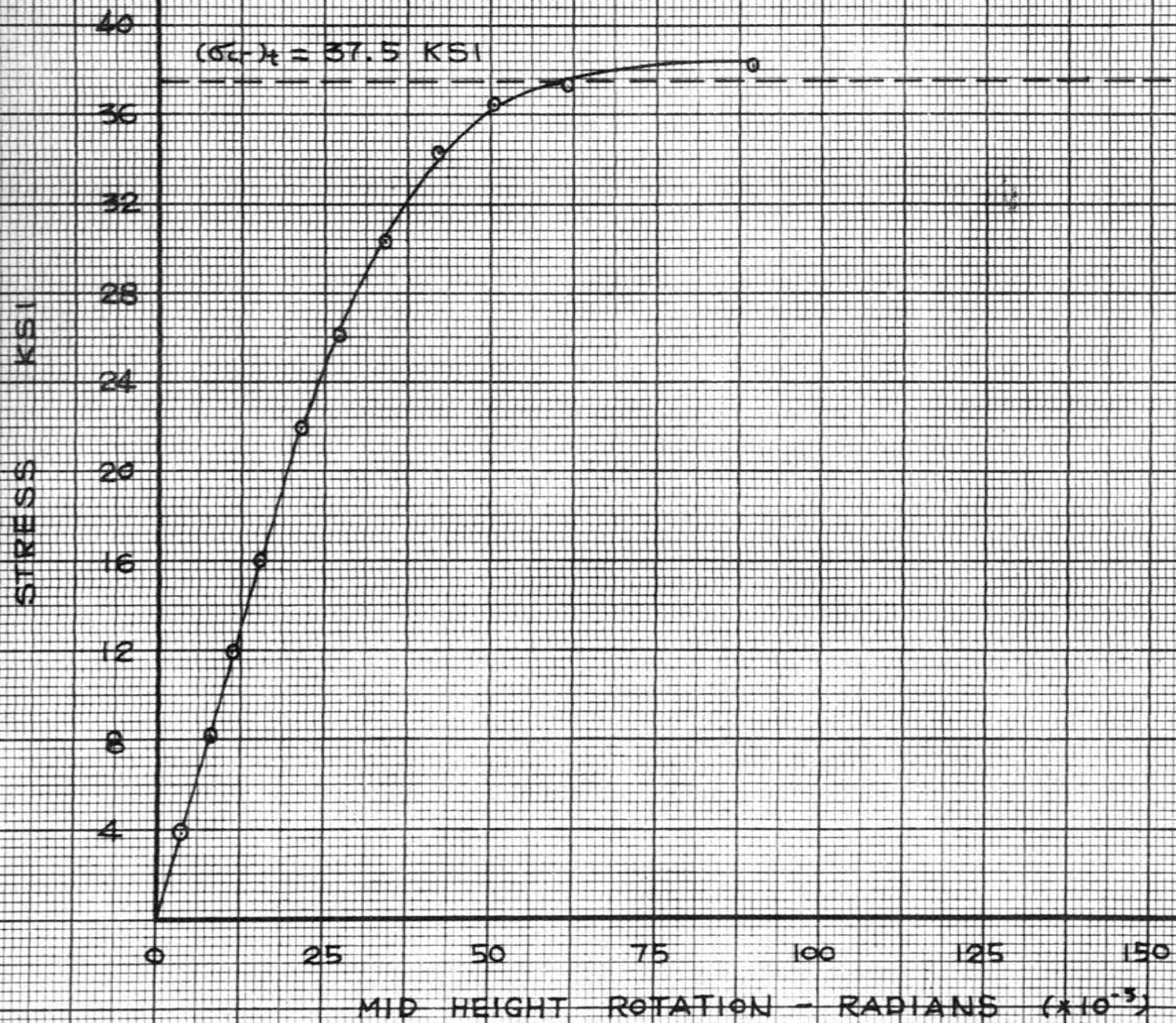
TEST   A - I

$(\sigma_{cr})_t = 36.65$ KSI

STRESS KSI

MID HEIGHT ROTATION - RADIANS

$(\times 10^{-3})$

TEST A-2

$(\sigma_{cr})_t = 37.5$ KSI

STRESS KSI

MID HEIGHT ROTATION - RADIANS $(\times 10^{-3})$

FIG - BA2 STRESS - DEFORMATION CURVE

FIG - BA6 STRESS DEFORMATION CURVE

TEST LA- 1

$(\sigma_{cr})t = 37.22$ KSI $(\sigma_{cr})t = 37.22$ KSI

STRESS KSI

36
32
28
24
20
16
12
8
4

0   20   40   60   80   10   20   30 40   50   60   70

MID HEIGHT ROTATION - RADIANS $(\times 10^{-3})$ MID HEIGHT DEFLECTION

FIG - BLAI STRESS - DEFORMATION CURVE   IN $(\times 10^{-3})$

$(\sigma_{cr})_t = 38.76$ KSI $(\sigma_{cr})_t = 38.76$ KSI

STRESS KSI

MID HEIGHT ROTATION - RADIANS (×10⁻³)   MID HEIGHT DEFLECTION IN (×10⁻³)

FIG - BLA 2   STRESS - DEFORMATION CURVE

TEST 1A-3

$(\sigma_{cr})_t = 32.71$ KSI $(\sigma_{cr})_t = 32.71$ KSI

STRESS KSI

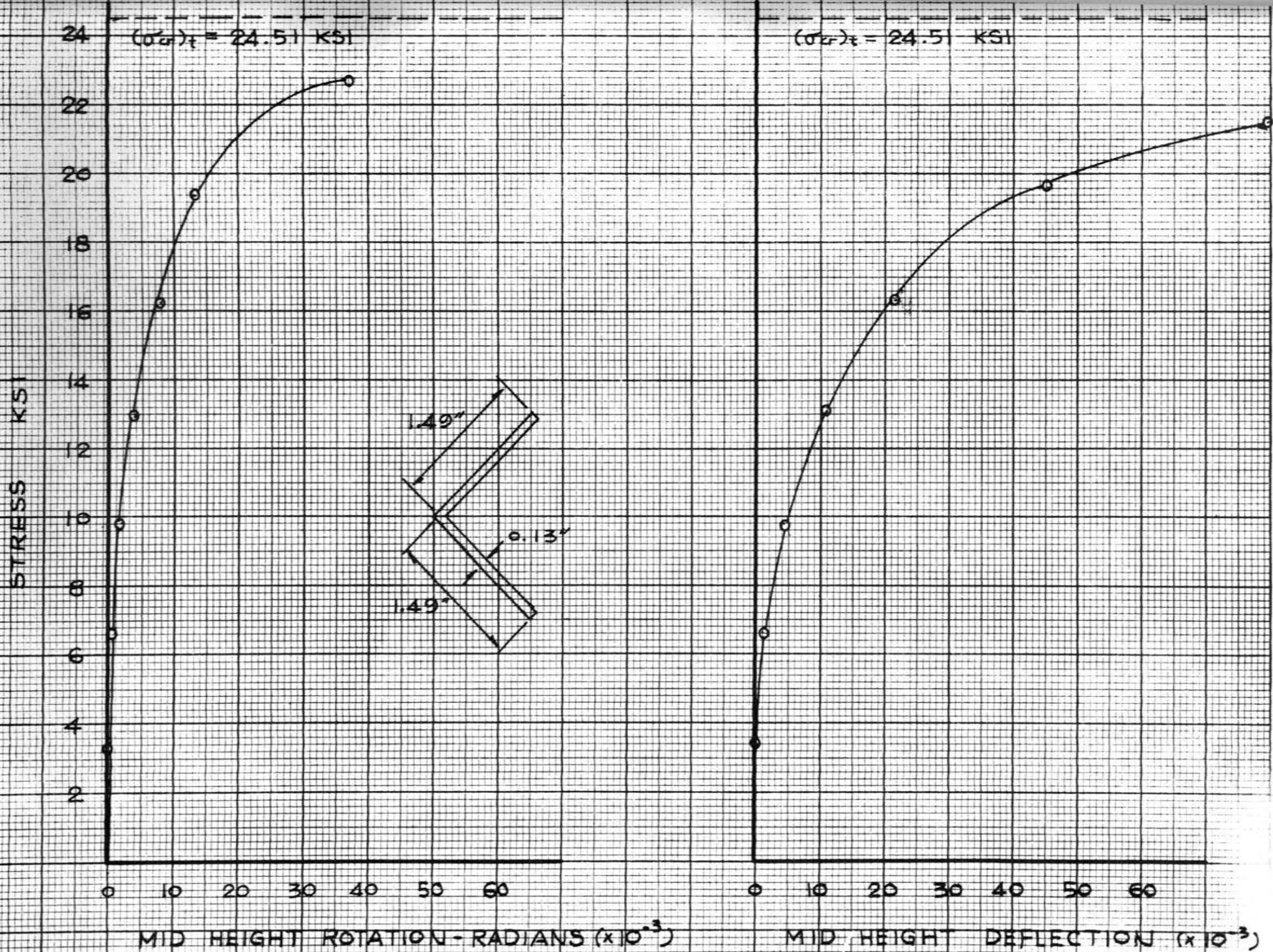MID HEIGHT ROTATION - RADIANS $(\times 10^{-3})$ MID HEIGHT DEFLECTION IN $(\times 10^{3})$
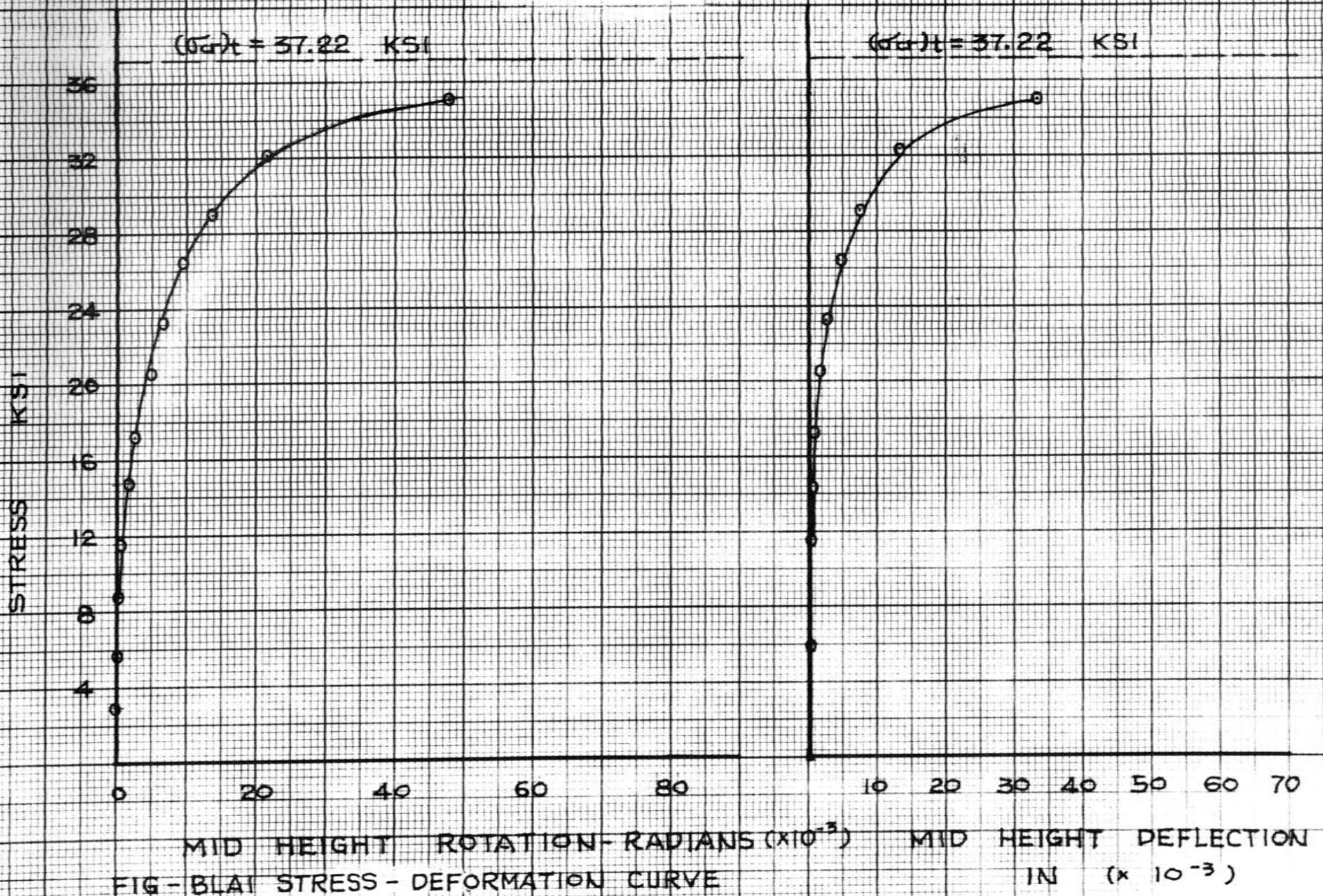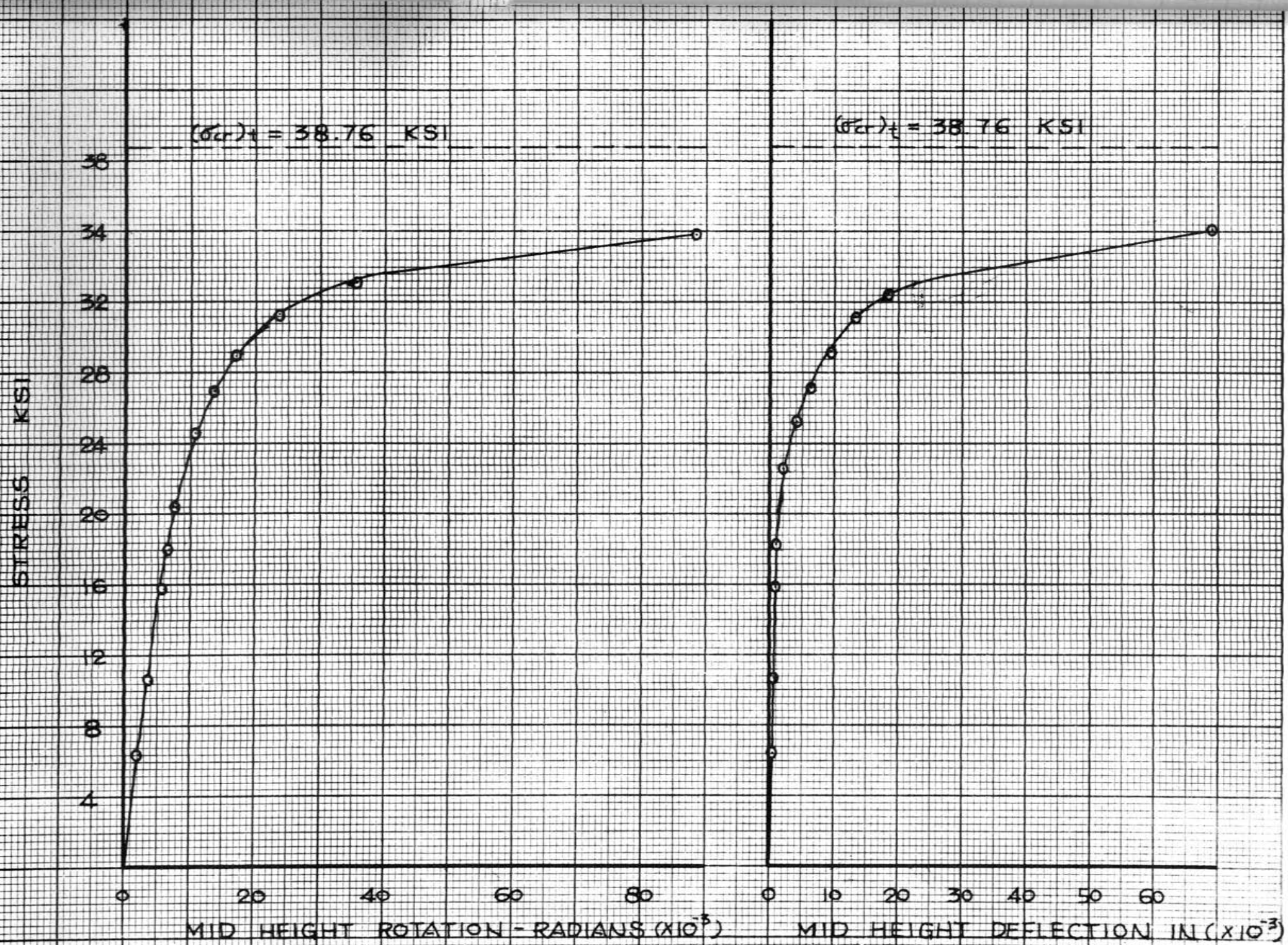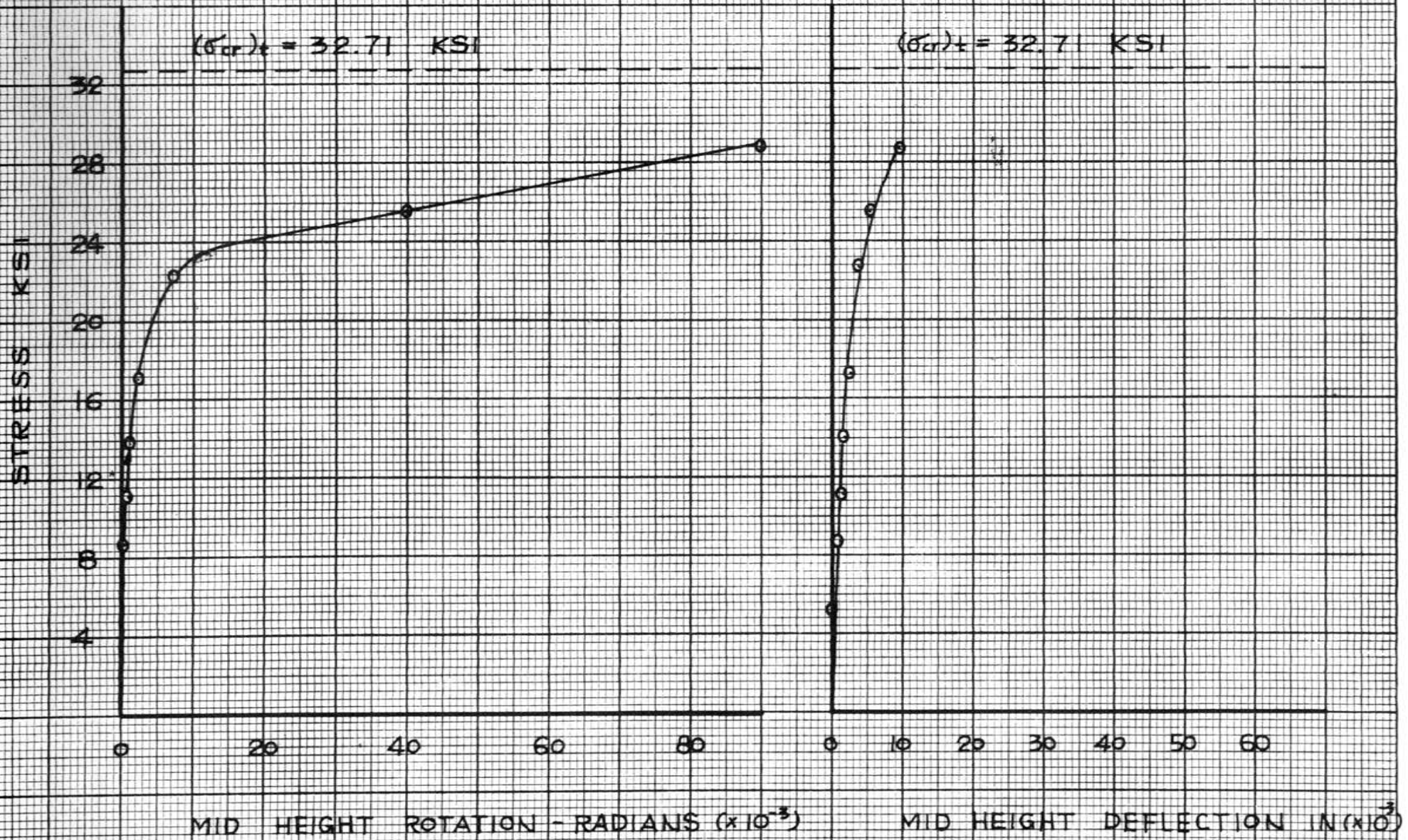
FIG - BLA 3   STRESS - DEFORMATION CURVE

TEST   LA-4
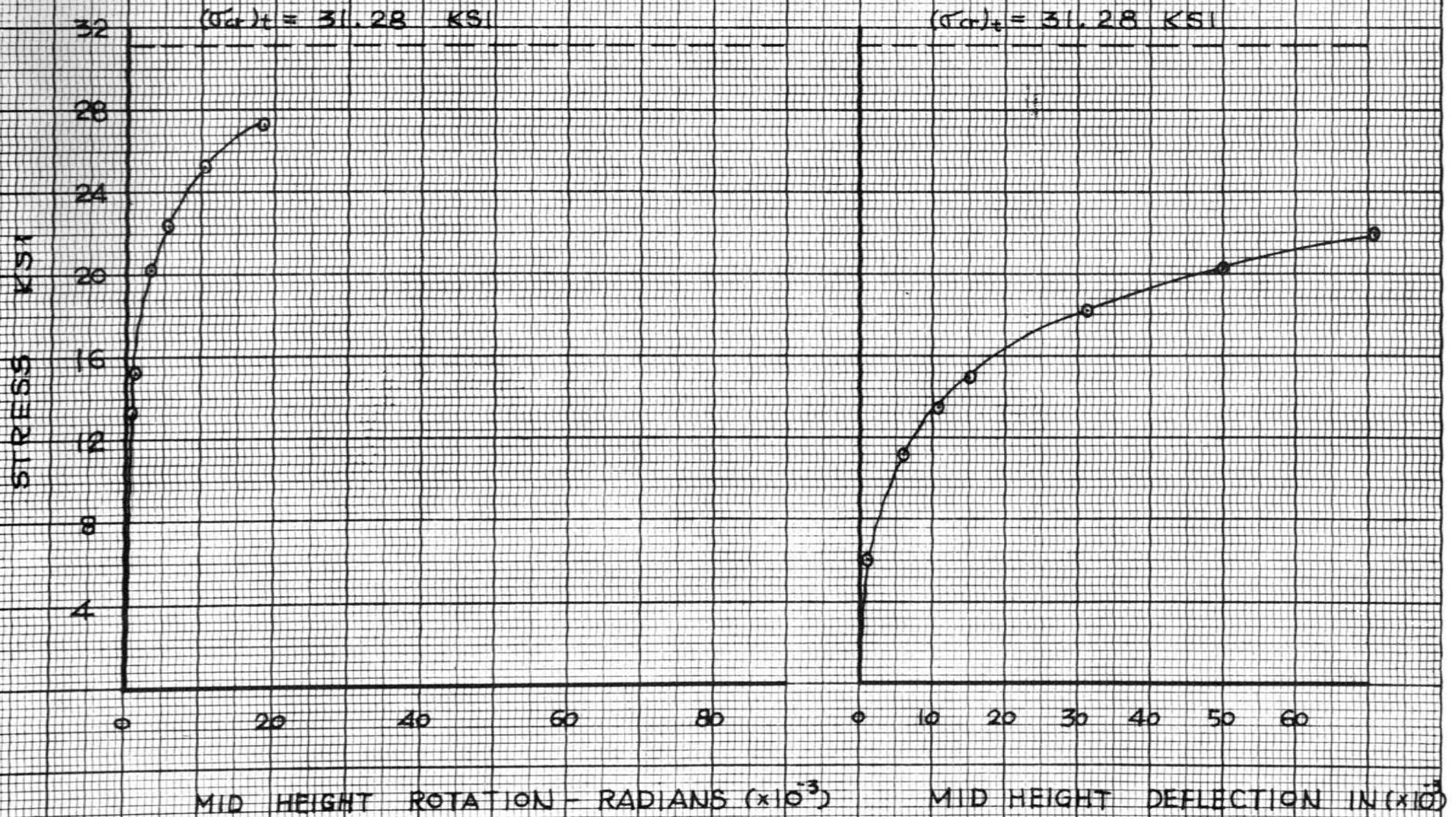
FIG - BLA4   STRESS - DEFORMATION   CURVE
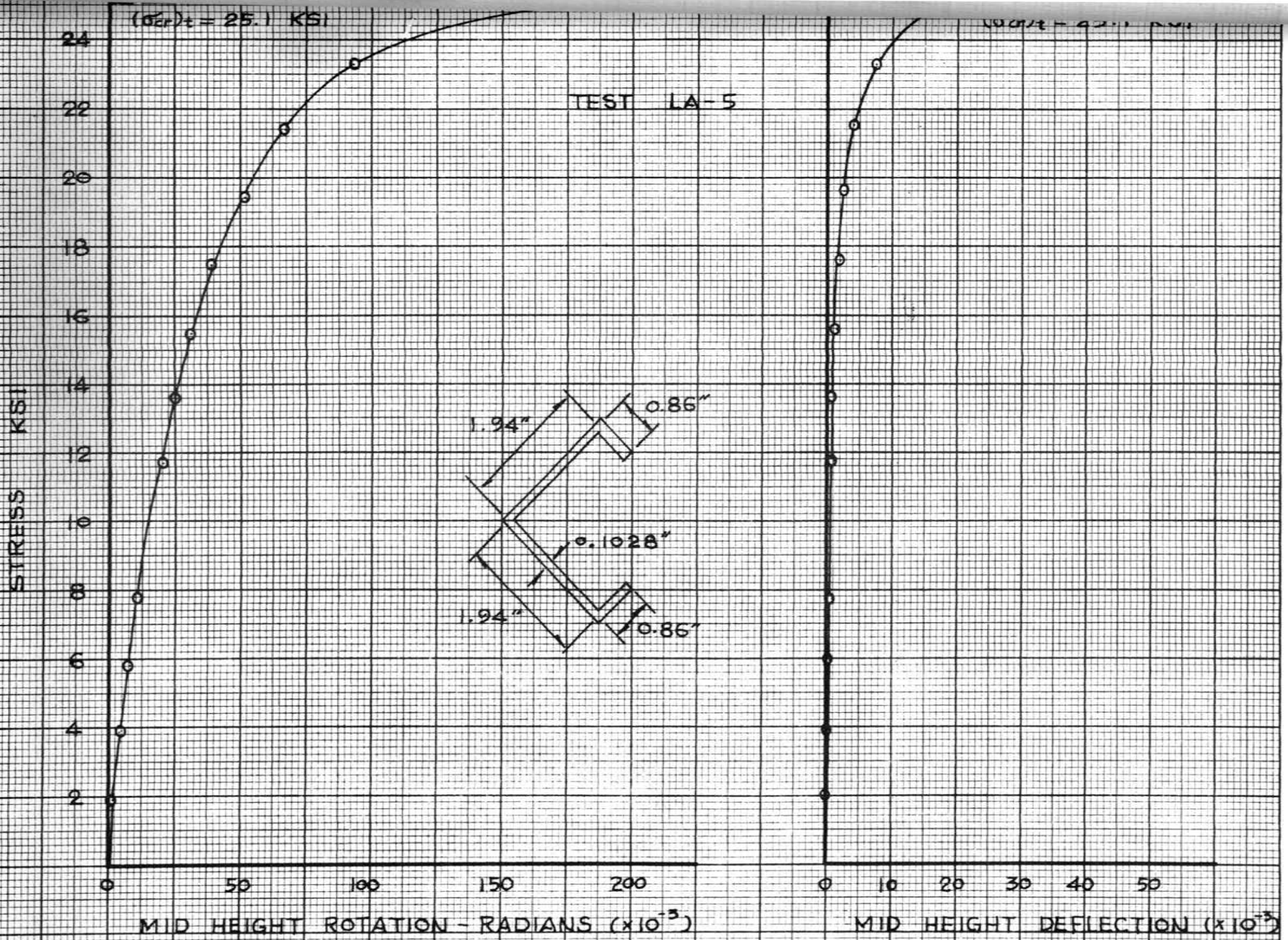
FIG-8LA5 STRESS DEFLECTION CURVE

FIG - B1A8   STRESS - DEFORMATION   CURVE

TEST   1A - 8

$(\sigma_{cr})_t = 28.70$ KSI

$(\sigma_{cr})_t = 28.70$ KSI

STRESS   KSI

MID HEIGHT ROTATION - RADIANS
($\times 10^{-3}$)

MID HEIGHT DEFLECTION
IN   ($\times 10^{-3}$)

TEST   CH - 1

FIG - BCH I   STRESS - DEFORMATION CURVE

TEST   CH - 3

$(\sigma_{cr})_t = 27.95$ KSI

$(\sigma_u)_t = 27.95$ KSI

STRESS KSI
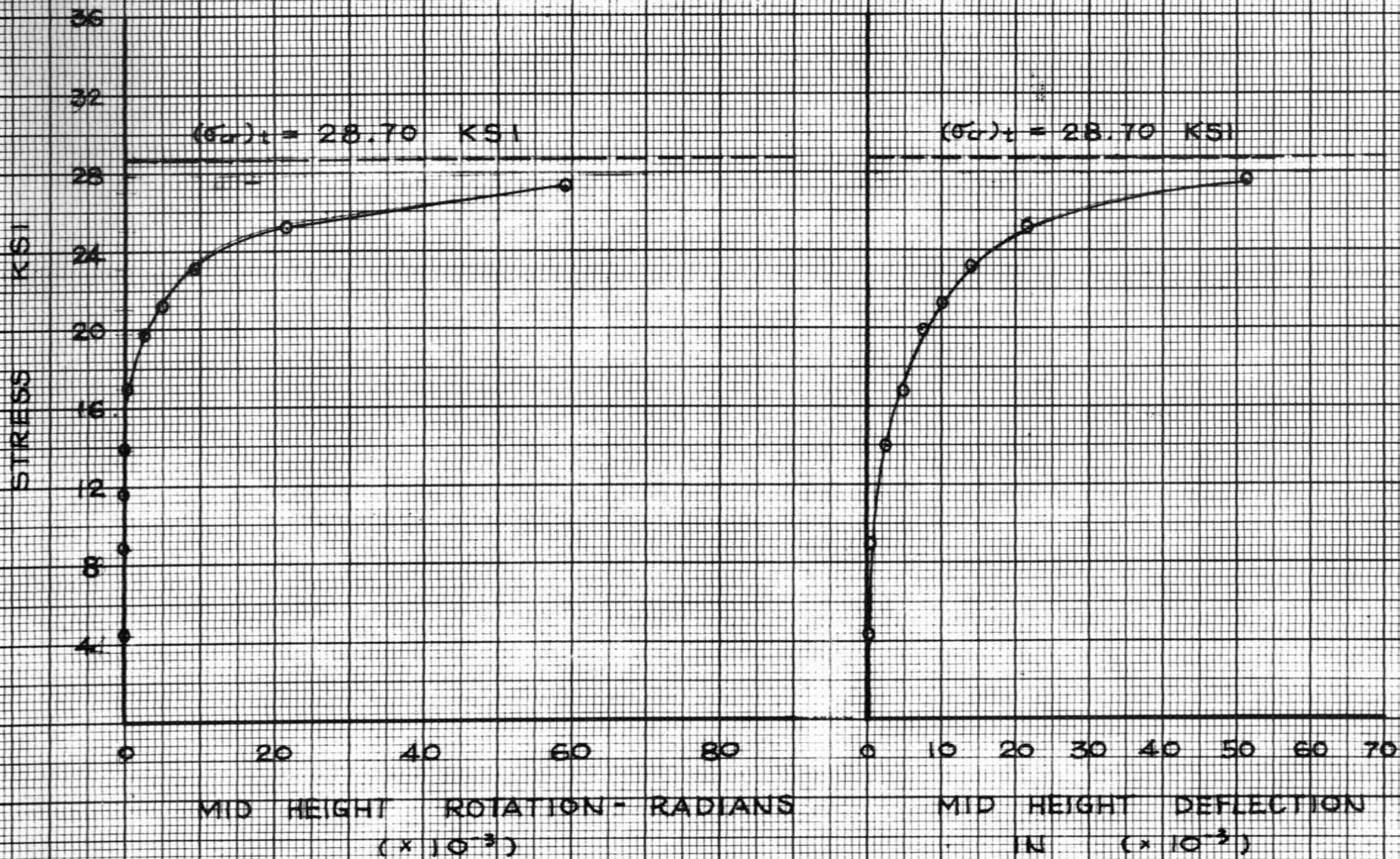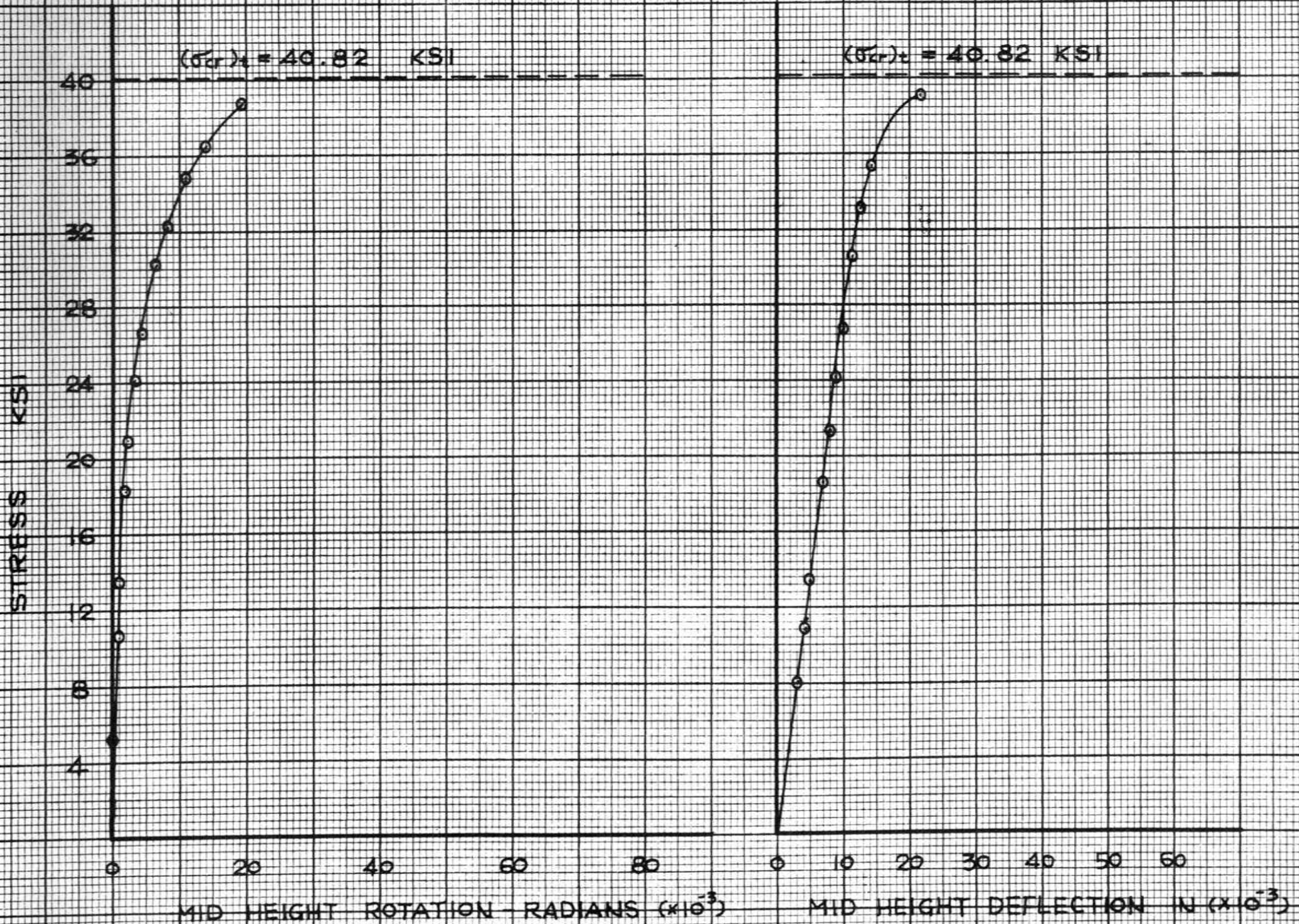
MID HEIGHT ROTATION - RADIANS ($\times 10^{-3}$)   MID HEIGHT DEFLECTION IN ($\times 10^{-3}$)
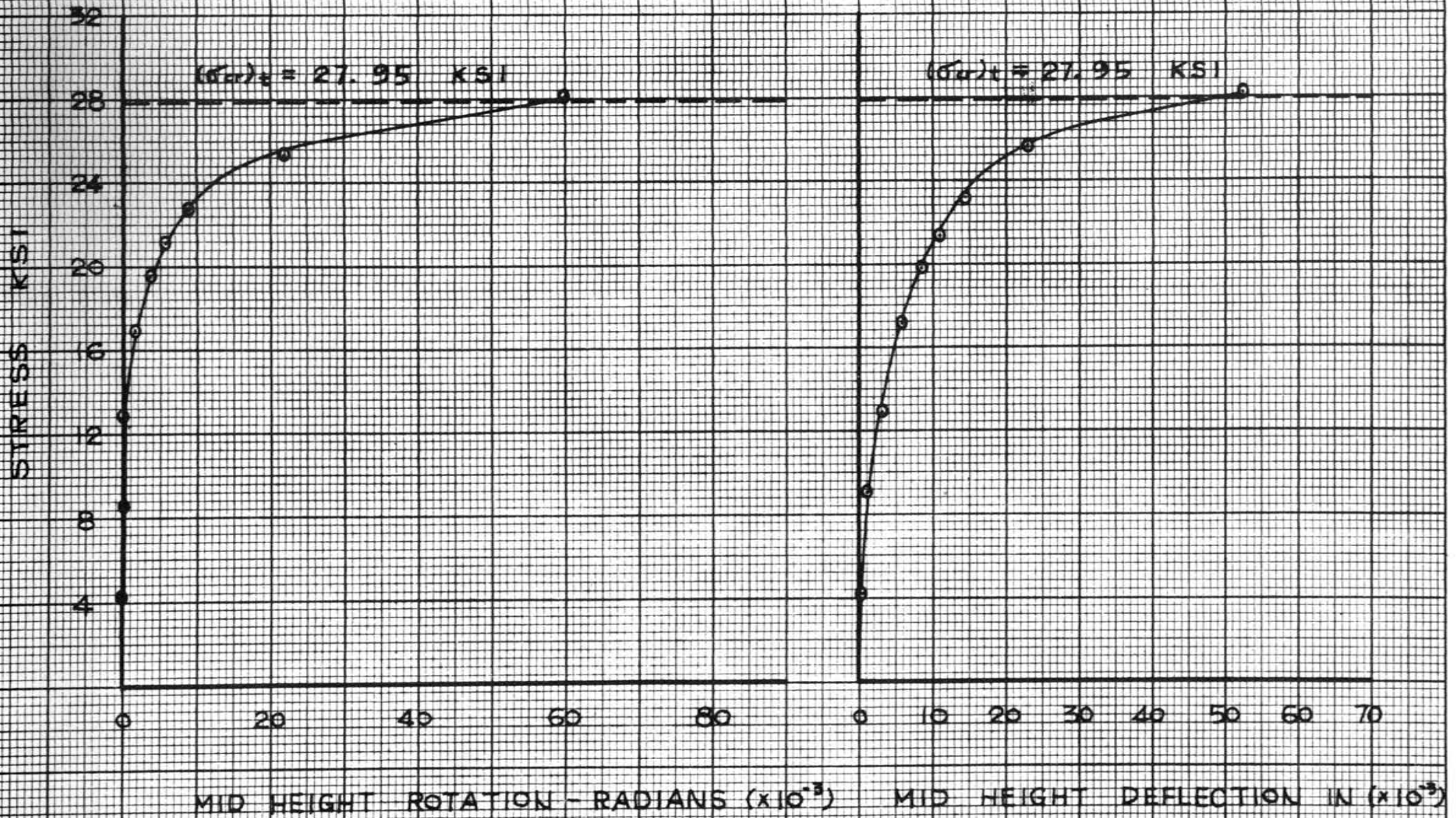
FIG - BCH3   STRESS - DEFORMATION CURVE

TEST — CH4

$(\sigma_{cr})_t = 25.98$ KSI

$(\sigma_{cr})_t = 25.98$ KSI

STRESS KSI

MID HEIGHT ROTATION — RADIANS $(\times 10^{-3})$

MID HEIGHT DEFLECTION IN $(\times 10^{-3})$
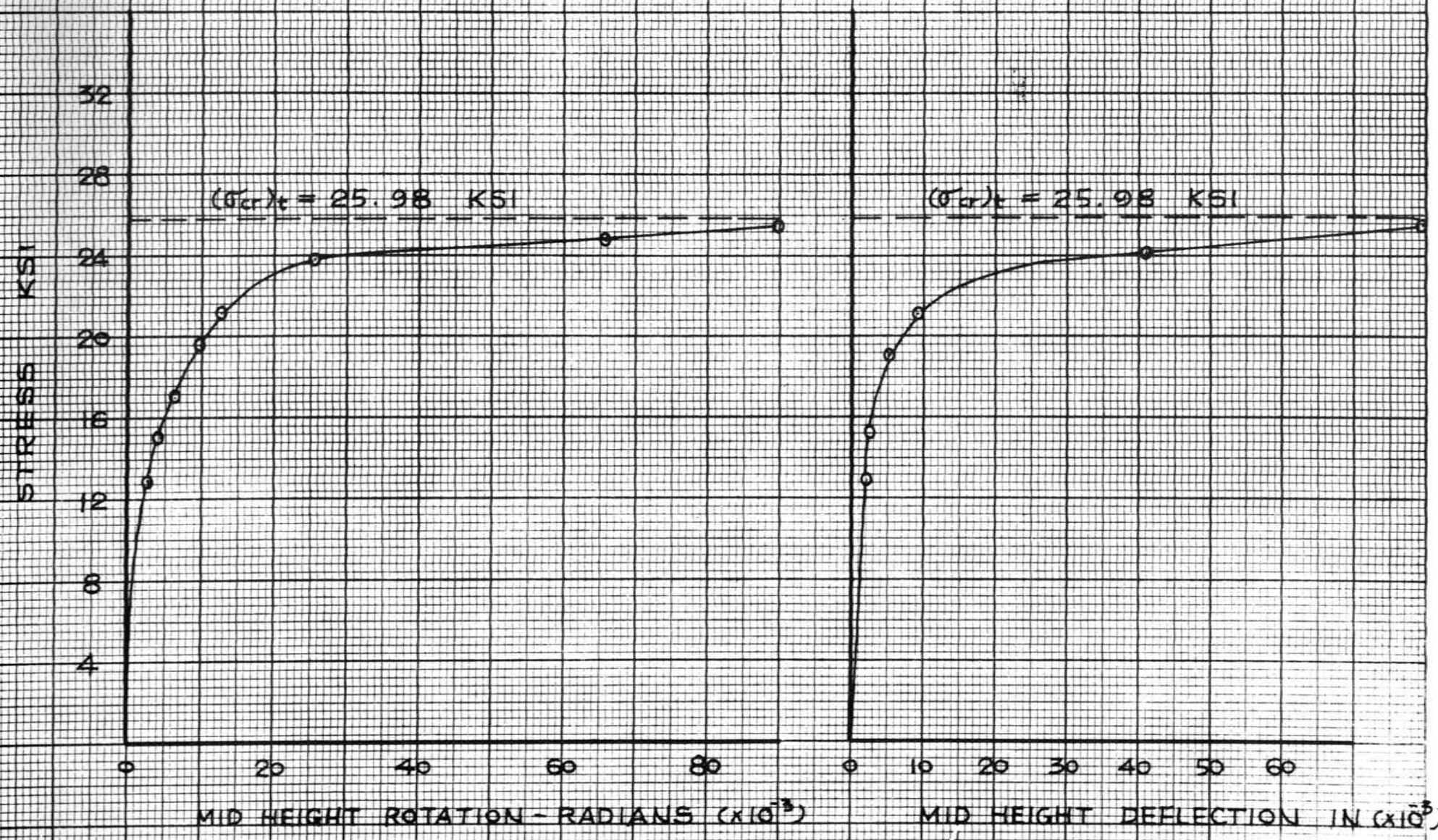
FIG — BCH4   STRESS — DEFORMATION CURVE

TEST CH-5

$(\sigma_{ys})_t = 26.27$ KSI

$(\sigma_{ys})_t = 26.27$ KSI

STRESS KSI

MID HEIGHT ROTATION - RADIANS $(\times 10^{-3})$ MID HEIGHT DEFLECTION IN $(\times 10^{-3})$
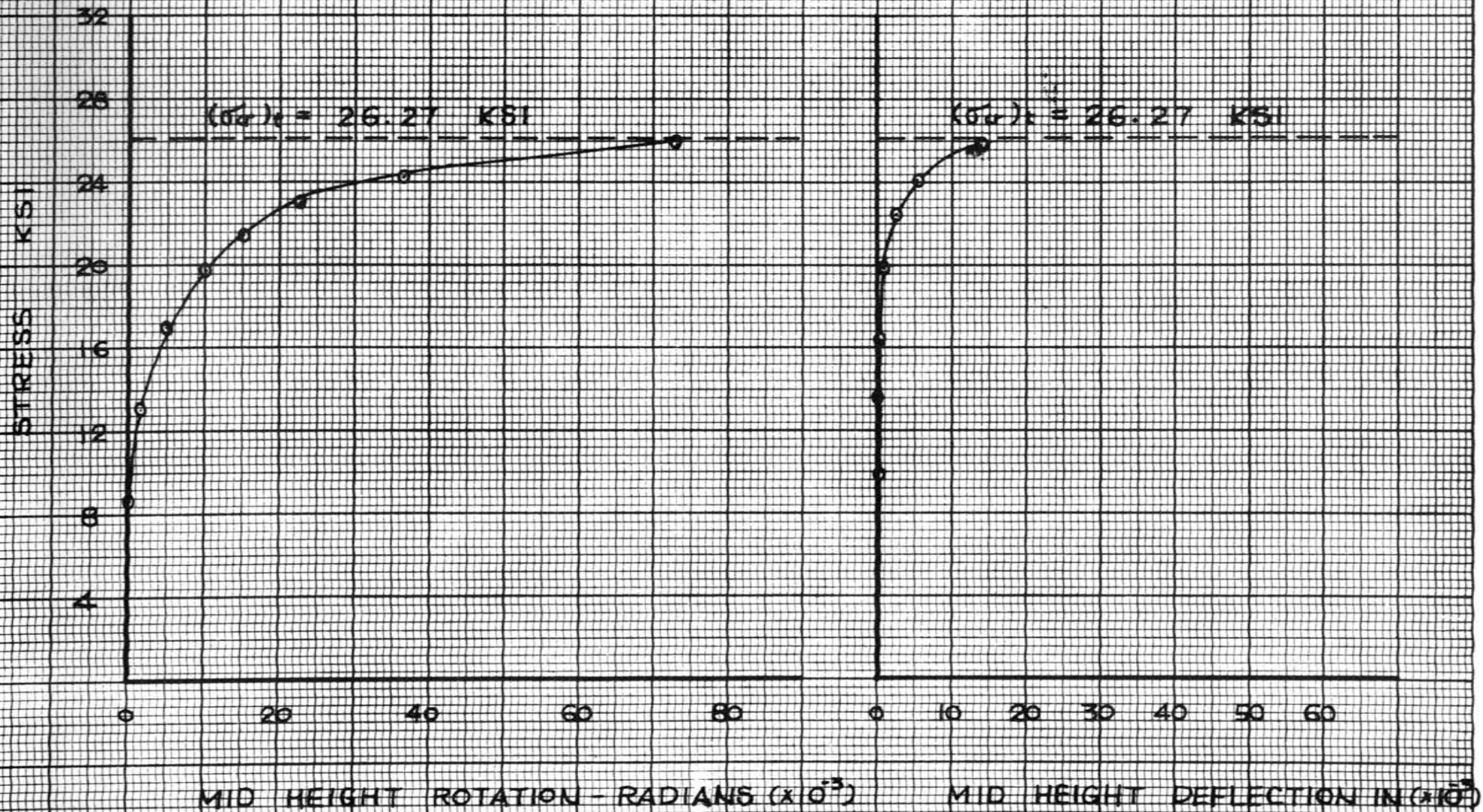
FIG - BCH5   STRESS - DEFORMATION CURVE
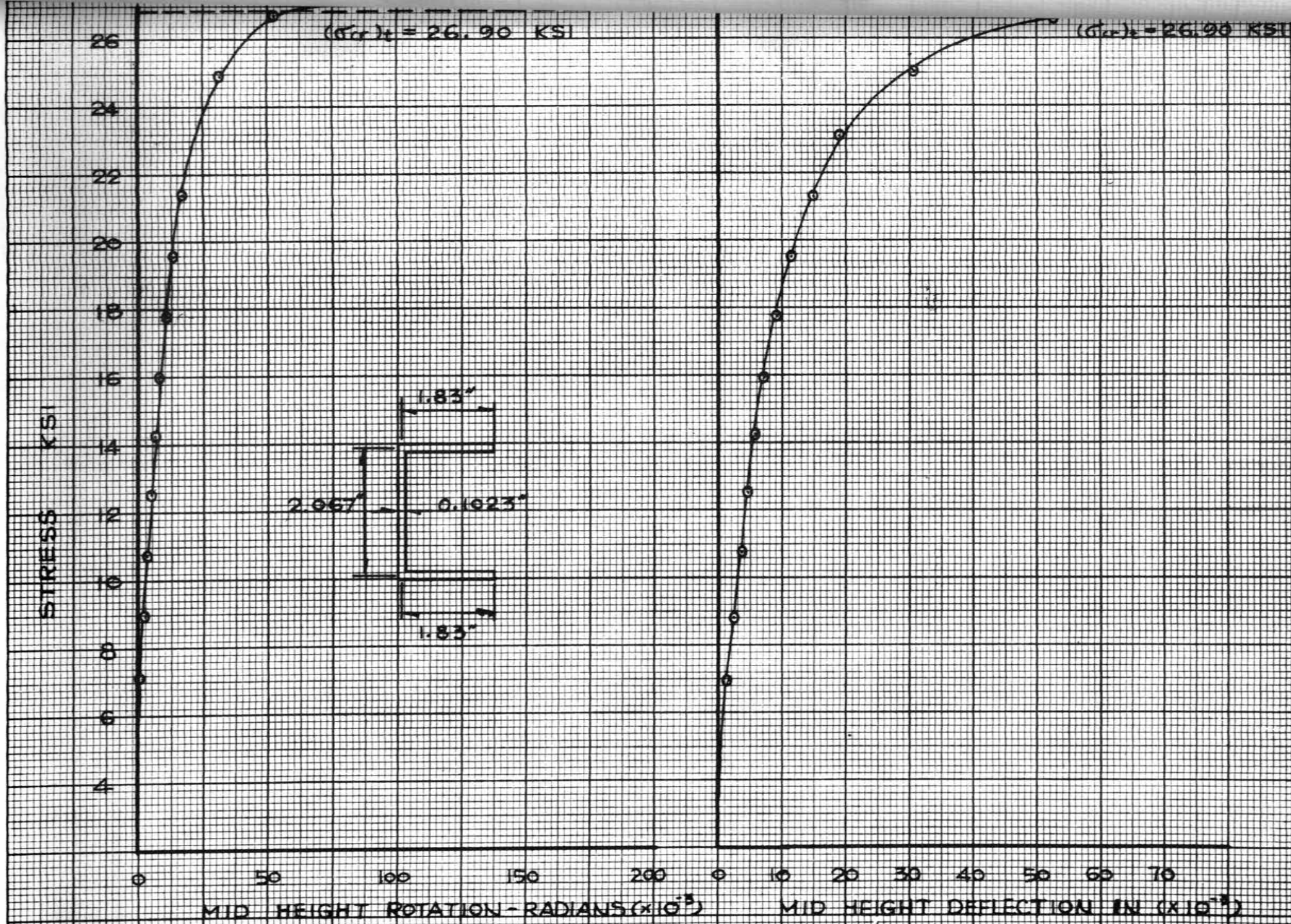
FIG - BCH6 STRESS DEFORMATION CURVE

TEST   CH - 7

$(\sigma_{cr})_t = 26.94$ KSI

$(\sigma_{cr})_t = 26.94$ KSI
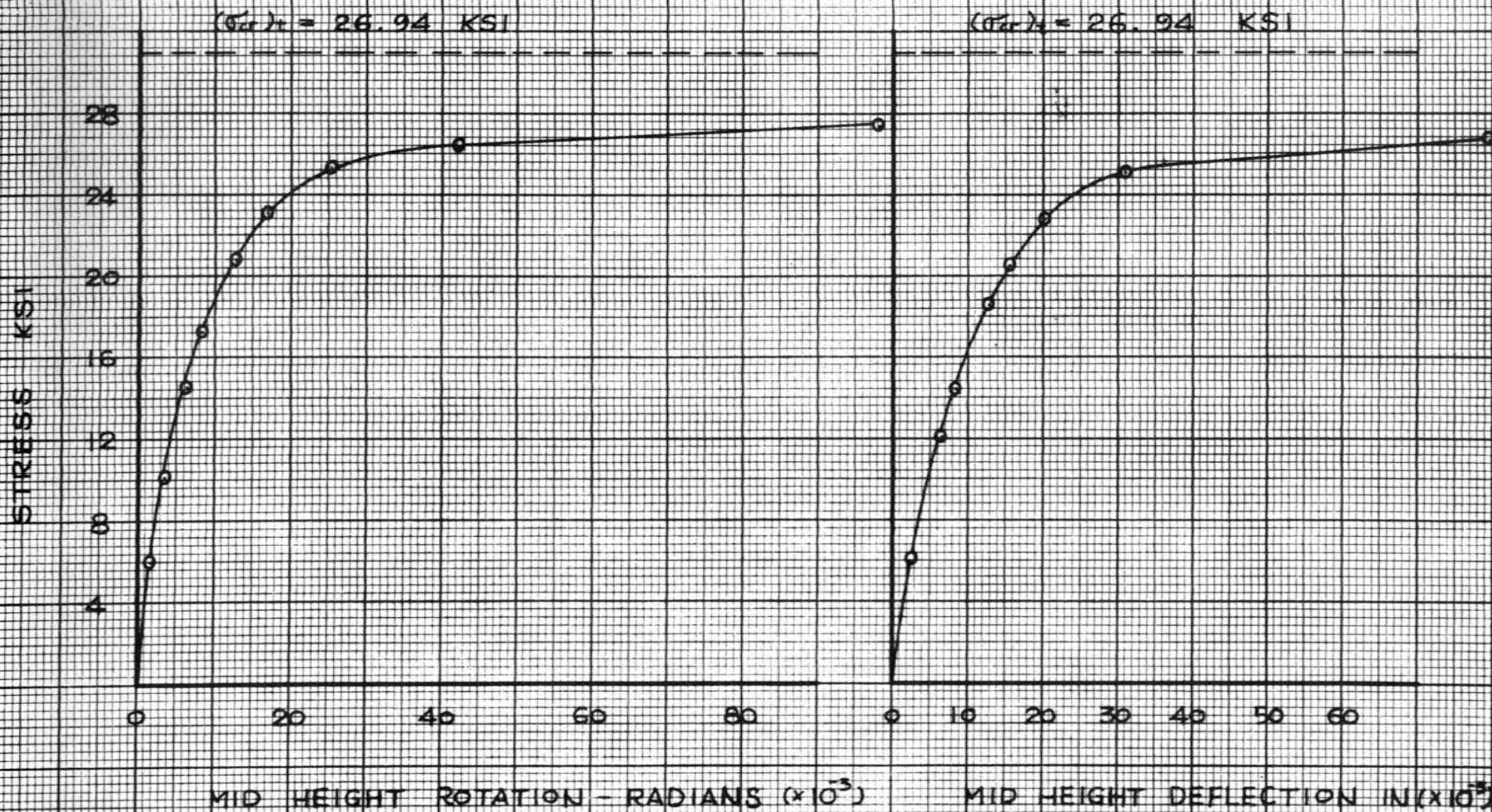
FIG - BCH7   STRESS - DEFORMATION   CURVE

MID HEIGHT ROTATION - RADIANS $(\times 10^{-3})$ MID HEIGHT DEFLECTION IN $(\times 10^{-3})$

STRESS KSI

CORNELL CO-OPERATIVE SOCIETY, ITHACA, N.Y.

TEST   CH - 8

$(\sigma_{cr})_t = 26.96$ KSI

$(\sigma_{cr})_t = 26.96$ KSI

STRESS   KSI

32
28
24
20
16
12
8
4
0

0   20   40   60   80

0   10   20   30   40   50   60

MID HEIGHT   ROTATION - RADIANS $(\times 10^{-3})$ MID HEIGHT DEFLECTION IN $(\times 10^{-3})$
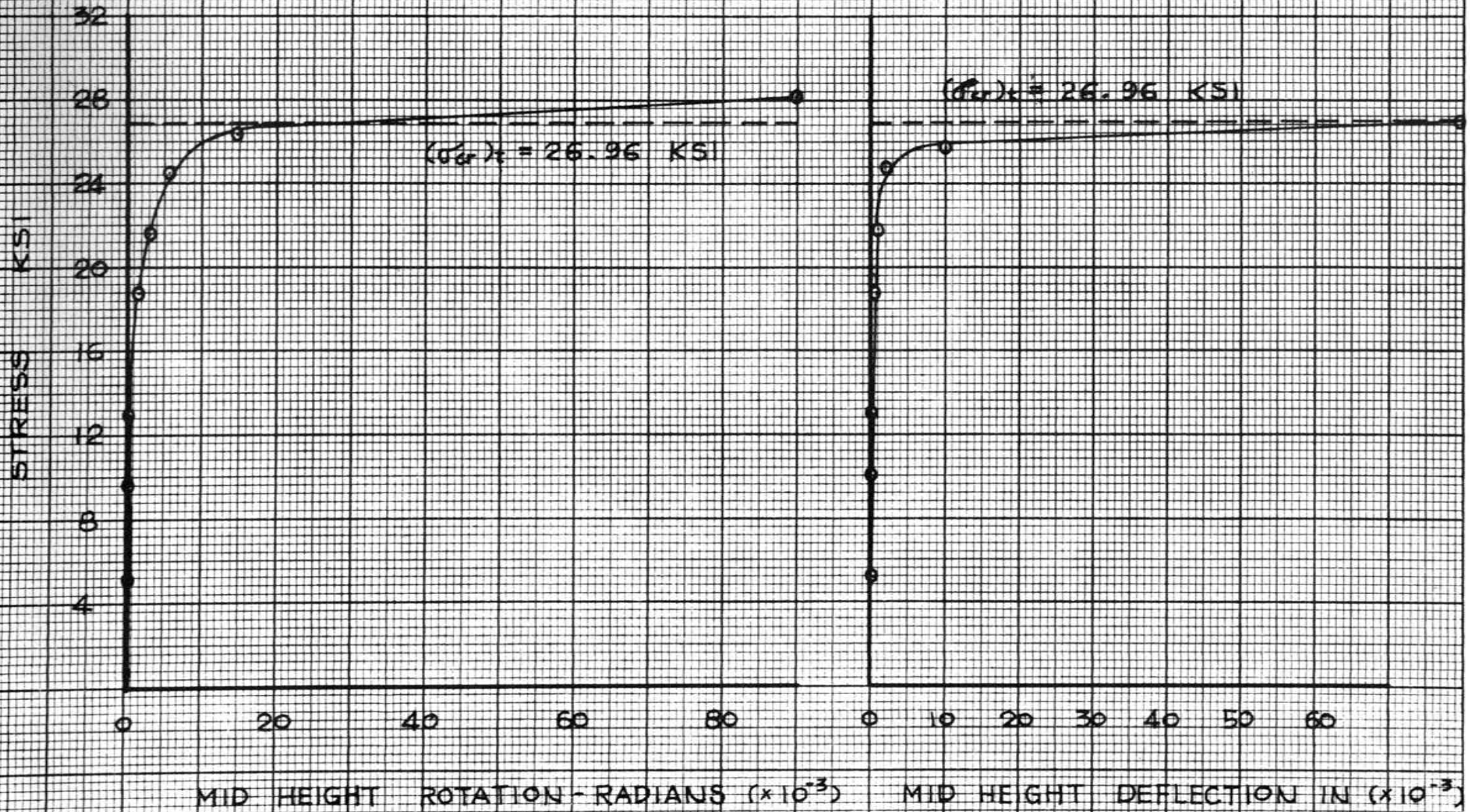
FIG - BCHB   STRESS - DEFORMATION   CURVE

TEST   CH - 9

$(\sigma_{cr})_t = 27.13$ KSI

$(\sigma_{cr})_t = 27.13$ KSI

STRESS   KSI

MID HEIGHT ROTATION - RADIANS $(\times 10^{-3})$ MID HEIGHT DEFLECTION IN $(\times 10^{-3})$
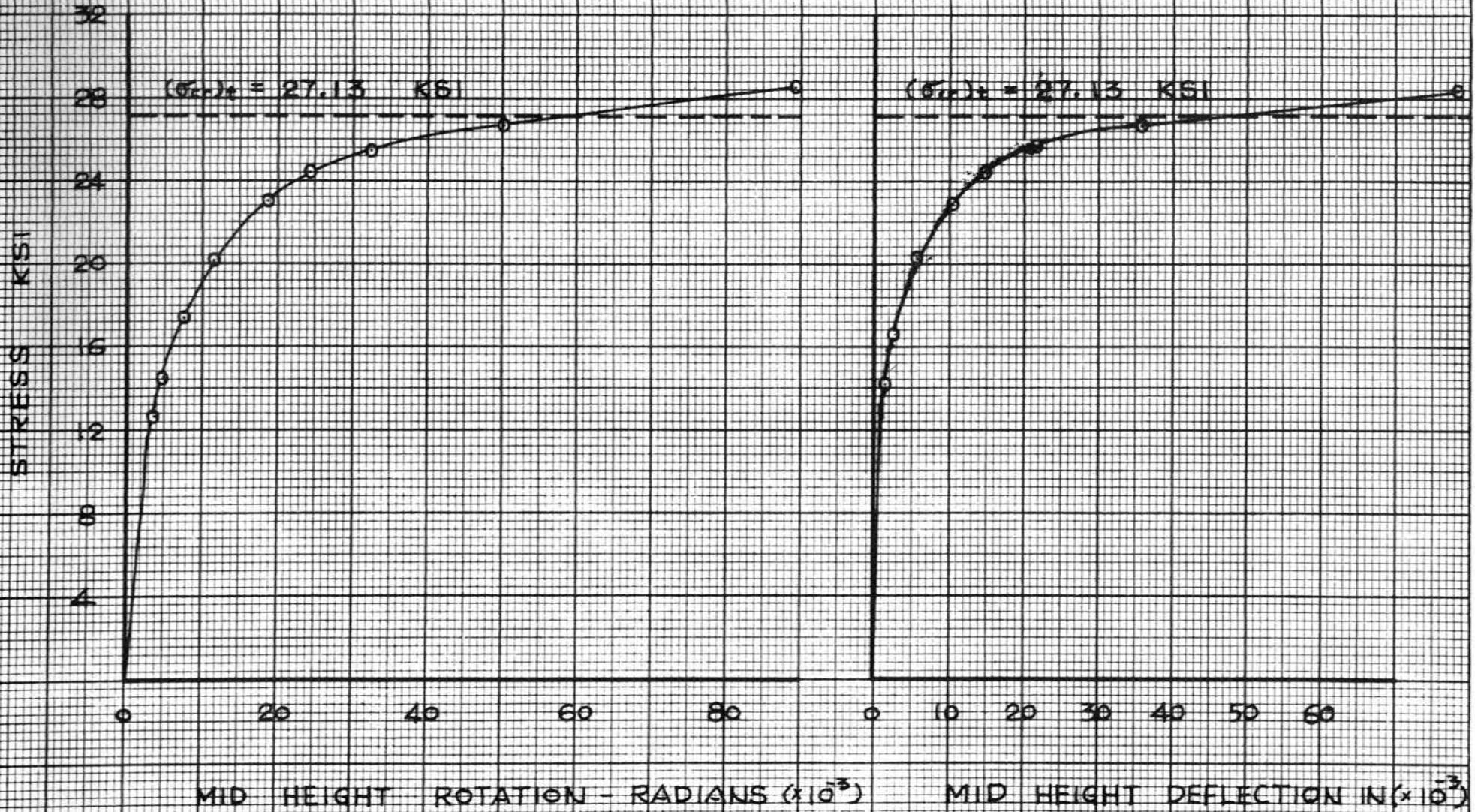
FIG - BCH 9   STRESS - DEFORMATION CURVE

TEST   HA-1

$(\sigma_{cr})_t = 39.58$ KSI

$(\sigma_{cr})_t = 39.58$ KSI

STRESS   KSI

44
40
36
32
28
24
20
16
12
8
4

0   20   40   60   80

0   10   20   30   40   50   60

MID HEIGHT ROTATION - RADIANS $(\times 10^{-3})$

MID HEIGHT DEFLECTION W$(\times 10^{-3})$
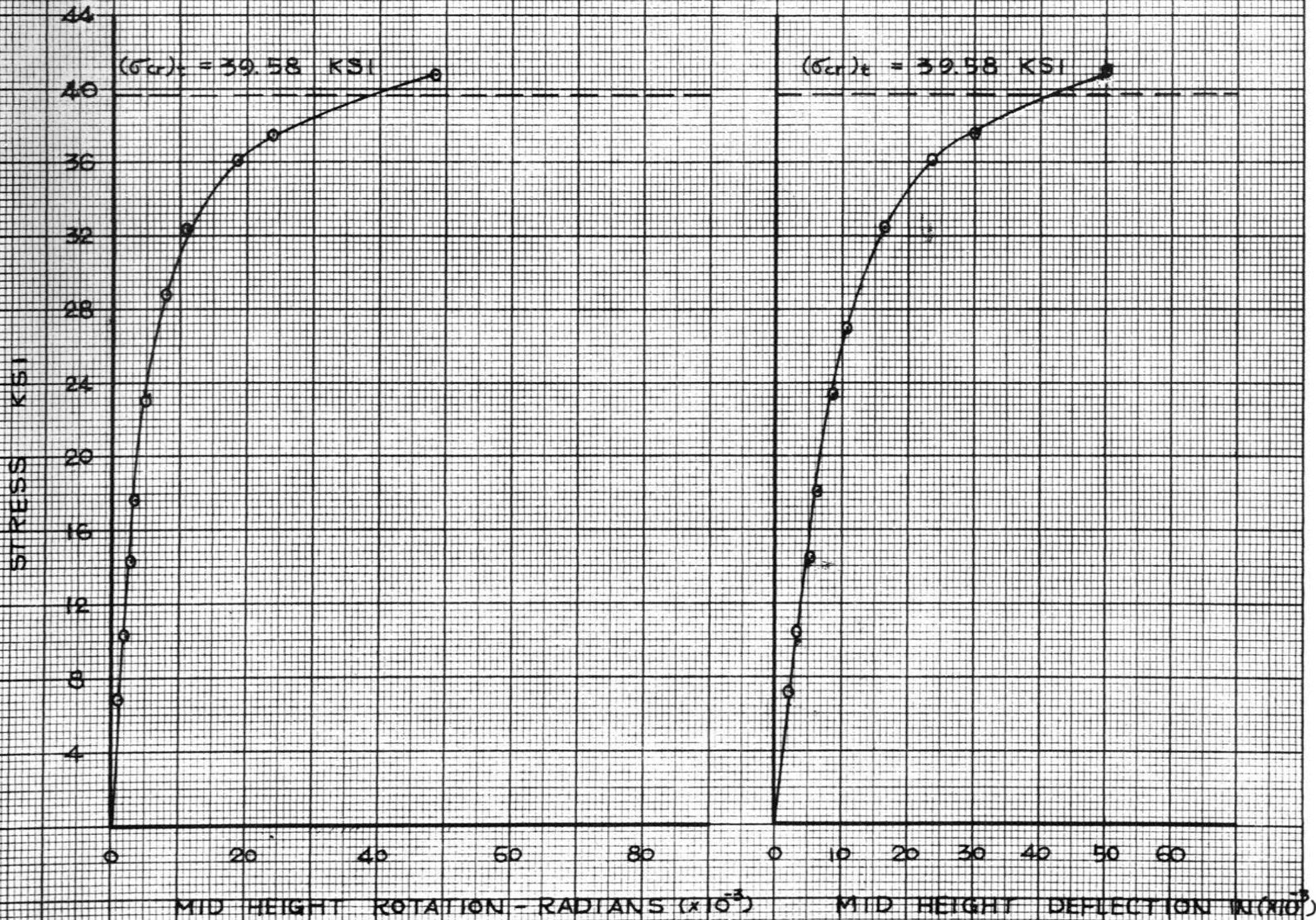
FIG - BHA1   STRESS - DEFORMATION   CURVE

CORNELL CO-OPERATIVE SOCIETY, ITHACA, N.Y.

TEST — HA-2

$(\sigma_{cr})_t = 38.19$ KSI $(\sigma_{cr})_t = 38.19$ KSI

STRESS KSI

MID HEIGHT ROTATION — RADIANS ($\times 10^3$) MID HEIGHT DEFLECTION IN ($\times 10^{-4}$)
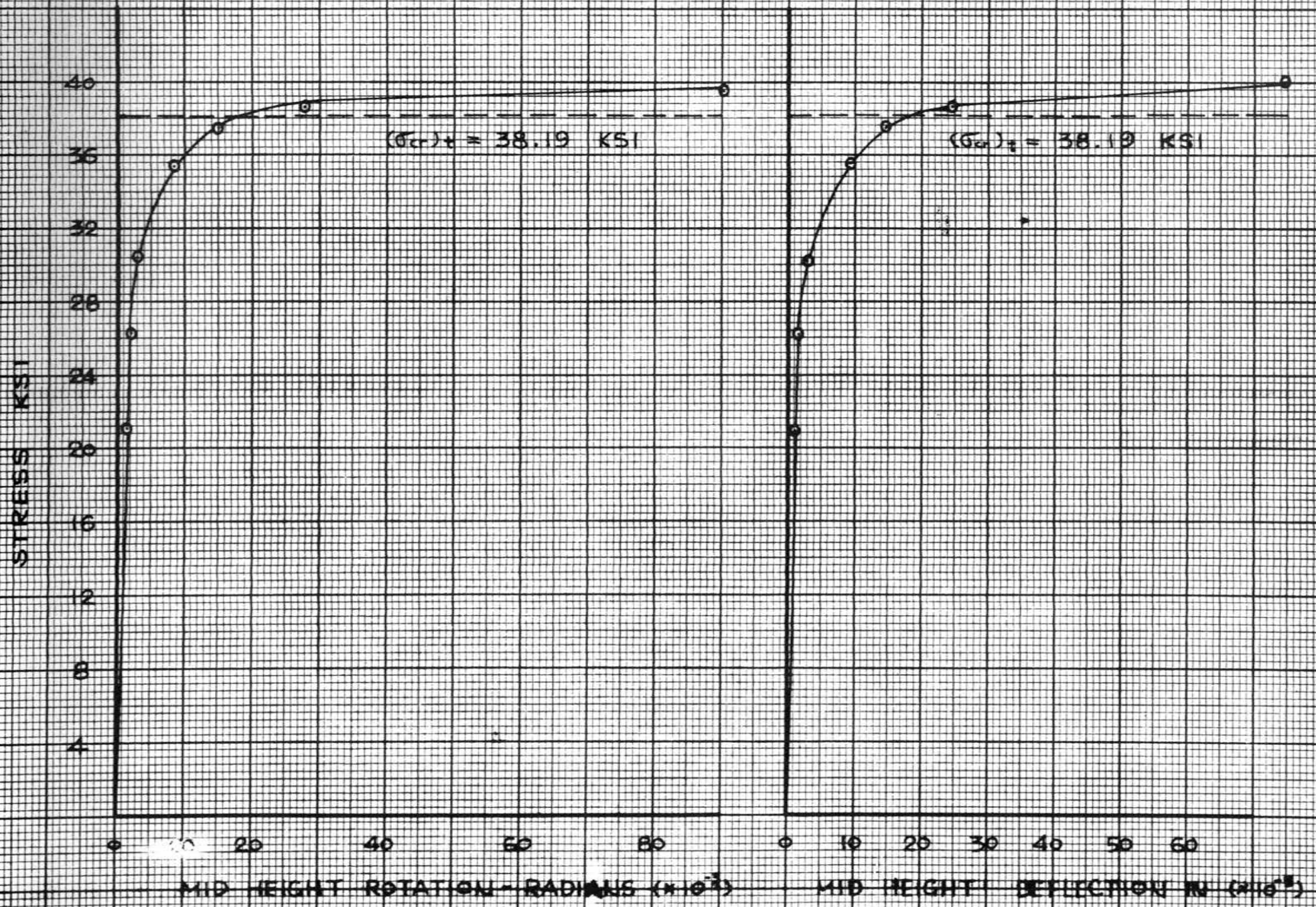
FIG — BHA2 STRESS - DEFORMATION CURVE

TEST HA-4

$(\sigma_{cr})_t = 28.0$ KSI

$(\sigma_{cr})_t = 28.0$ KSI

STRESS KSI

32
28
24
20
16
12
8
4

0 · 20 · 40 · 60 · 80

0 · 10 · 20 · 30 · 40 · 50 · 60 · 70
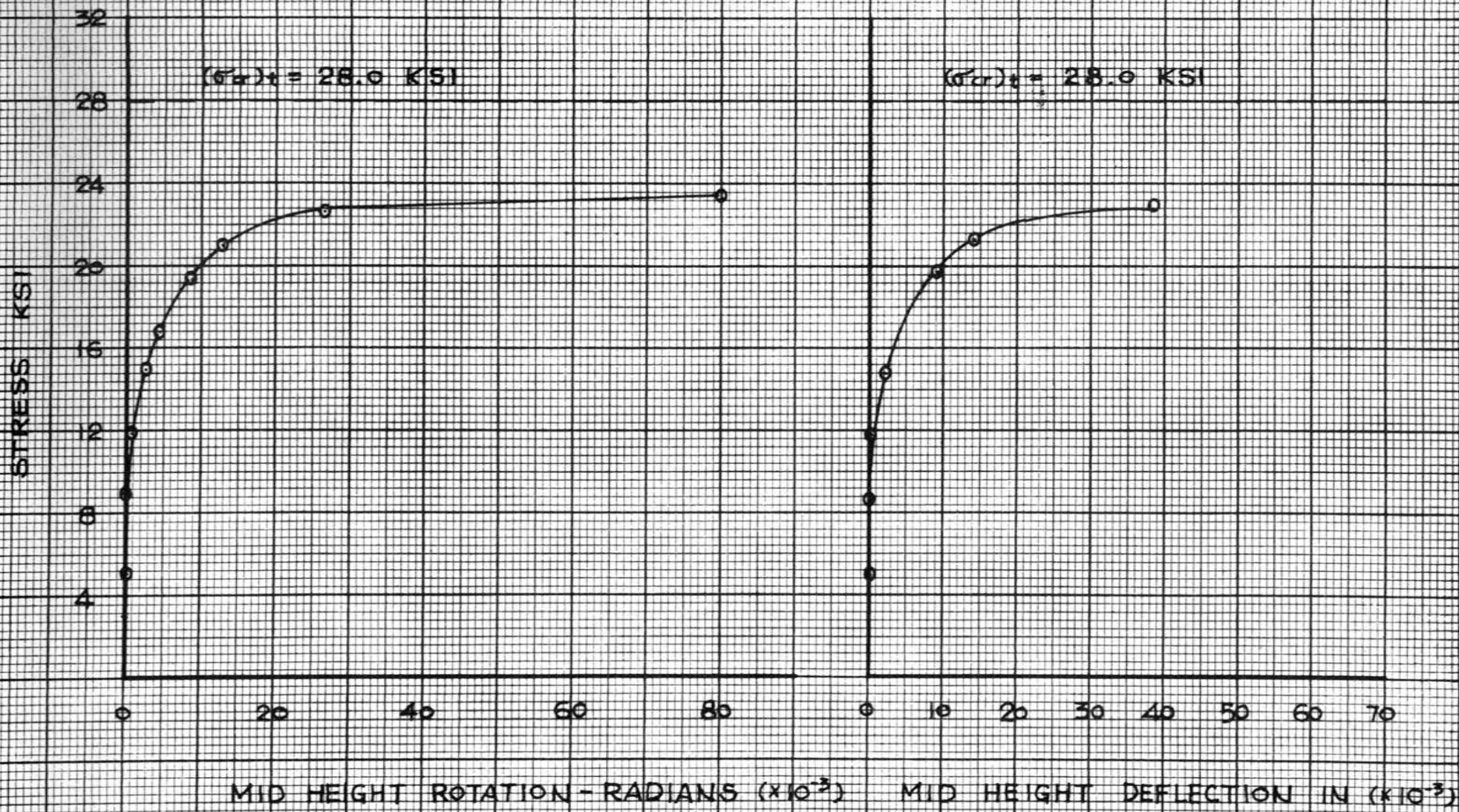
MID HEIGHT ROTATION - RADIANS ($\times 10^{-3}$)   MID HEIGHT DEFLECTION IN ($\times 10^{-3}$)

FIG - BHA4   STRESS - DEFORMATION CURVE
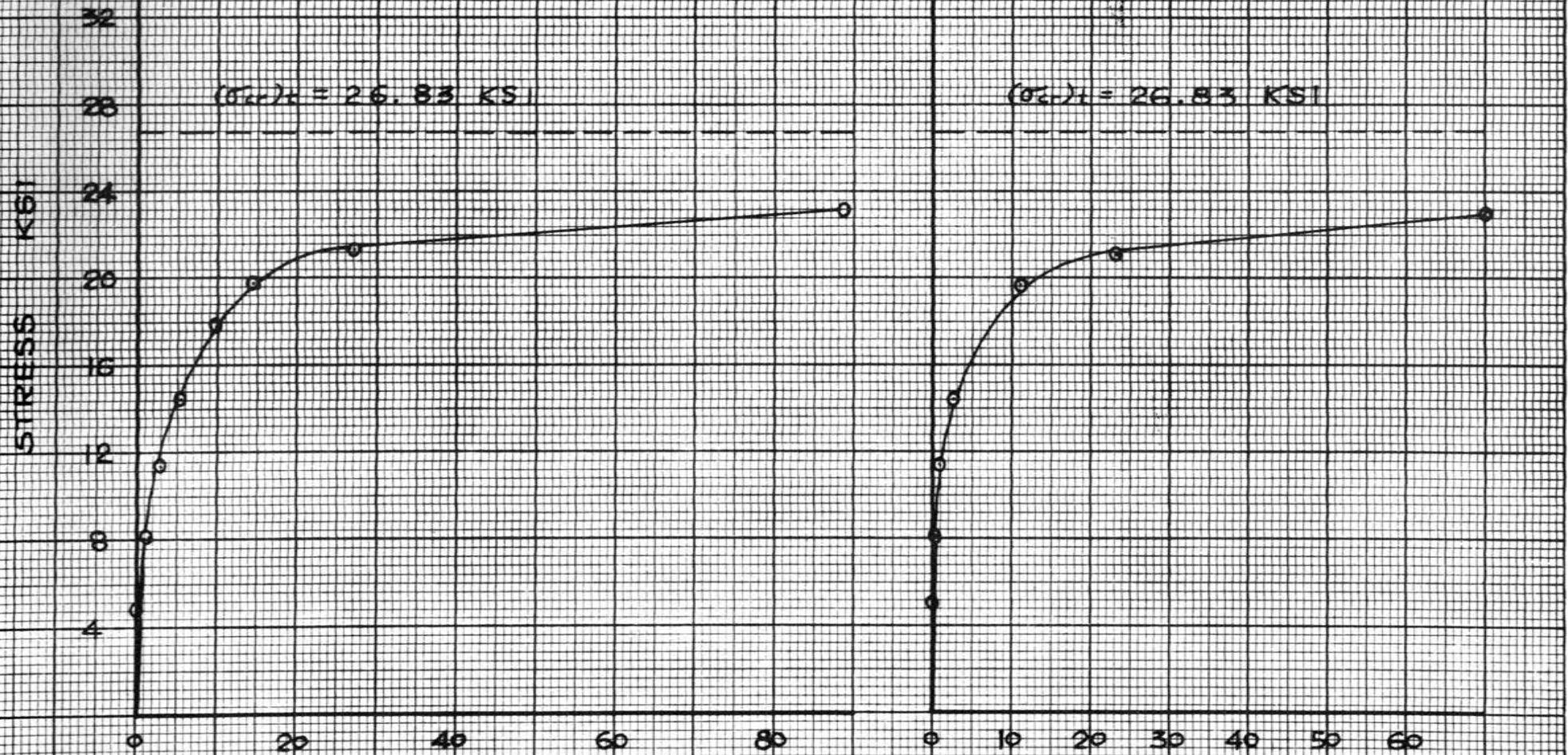
FIG - BHA5 STRESS DEFLECTION CURVE

APPENDIX C

Suggested Code Formulation

SUGGESTED CODE FORMULATION

It is suggested that the following may be substituted for the existing Sections 3.6 in the Manual to cover axially loaded compression members including torsional-flexural buckling.

3.6 AXIALLY LOADED COMPRESSION MEMBERS

3.6.1.1 The average axial stress, P/A, in compression members shall not exceed the values of F_a, as follows:

L/r less than $\dfrac{24,200}{\sqrt{fyQ}}$:

$$F_a = 0.515 \ Qfy - (\frac{QfyL/r}{47,500})^2$$

L/r equal to or greater than $\dfrac{24,200}{\sqrt{fyQ}}$:

$$F_a = \frac{149,000,000}{(L/r)^2}$$

For steel having minimum yielding point of 33,000 psi

L/r less than $132/\sqrt{Q}$:

$$F_a = 17,000Q - 0.485Q^2 \ (L/r)^2$$

L/r equal to or greater than $132/\sqrt{Q}$:

$$F_a = \frac{149,000,000}{(L/r)^2}$$

3.6.1.2 To prevent torsional-flexural buckling of axially compressed members with singly symmetrical cross-section, the average axial stress, P/A, shall not exceed the values of F_a' given below:

f_{TF} greater than $\frac{2}{3} \ fyQ$:

$$F_a' = 0.515Qf_y - \frac{Q^2 fy^2}{8.8 \ f_{TF}}$$

f_{TF} equal to or less than $\frac{2}{3}$ fyQ:

$$F'_a = \frac{f_{TF}}{F.S.} = \frac{f_{TF}}{1.95}$$

In the above formulas:

P = total load, lb.;

A = f_{ull}, unreduced cross-sectional area of the member, in.^{2};

F_a = maximum allowable average axial stress in compression, psi;

F'_a = maximum allowable torsional-flexural buckling stress, psi;

L = unbraced length of member, in.[*];

r = radius of gyration of full, unreduced cross-section, in.;

f_y = yield point of steel, psi;

Q = a factor determined as follows:

(a) For members composed entirely of stiffened elements, "Q" is the ratio between the effective design area, as determined from the effective design widths of such elements, and the full or gross area of the cross-section. The effective design area used in determining Q is to be based on the basic design stress f_b as defined in Section 3.1.

(b) For members composed entirely of unstiffened elements, "Q" is the ratio between the allowable compression stress f_c for the weaker element of the cross-section (the element having the largest flat-width ratio) and the basic design stress f_b; where f_c is as defined in Section 3.2 and f_b is as defined in 3.1

---

[*] L = in frames which depend upon their own bending stiffness, the effective length L in the plane of the frame shall be determined by a rational method and shall not be less than the actual unbraced length.

(c) For members composed of both stiffened and unstiffened elements, the factor "Q" is the product of a stress factor Q_s computed as outlined in paragraph (b) above and an area factor Q_a computed as outlined in paragraph (a) above, except that the stress upon which Q_a is to be based shall be that value of the unit stress f_c which is used in computing Q_s; and the effective area to be used in computing Q_a shall include full area of all unstiffened elements.

f_{TF} = elastic torsional-flexutral buckling stress which shall be determined as follows:

For members whose cross-sections have one axis of symmetry (x-axis), f_{TF} is less than both f_x and f_t and its value shall be such that

$$f_{TF} = \frac{1}{2K} [(f_x + f_t) - \sqrt{(f_x + f_t)^2 - 4kf_x f_t}]$$

where

$$f_x = \frac{\pi^2 E}{(L/r_x)^2} \text{ , psi;}$$

$$f_t = \frac{1}{I_p} [GJ + \frac{\pi^2 E C_w}{L^2}] \text{, psi;}$$

$$r_x = \sqrt{\frac{I_x}{A}} \text{ , in.;}$$

$I_p = Ar_o^2$ = polar moment of inertia about shear center
$= I_x + I_y + Ax_o^2 = Ay_o^2$, in.^{4};

$k = 1 - (x_o/r_o)^2$;

E = modulus of elasticity = 29,500,000 psi;

G = shear modulus = 11,300,000 psi;

L = length of compression member, in.;

I_x, I_y = moments of inertia of cross-section about centroidal principal axes, in.^{4};

x_0, y_0 = distance from shear center to centroid along the principal directions, in. (x_0 and y_0 formulas for commonly used sections may be tabulated);

r_0 = polar radius of gyration of cross-section about the shear center, in. (may be tabulated for common sections);

J = St. Venant torsion constant of the cross-section, in.[4] For sections composed of straight line elements, $J = (1/3)lt^3$;

t = thickness of the member wall, in.;

l = over-all length of cross-section middle line, in.;

C_w = warping constant of torsion of the cross-section in.[6]. (C_w formulas for commonly used sections will be tabulated.)

3.6.1.3 Point symmetrical sections do not buckle in the torsional-flexural mode; they buckle either purely flexurally or purely torsionally. For the former mode, the average axial stress shall not exceed F_a defined in Section 3.6.1.1. For the latter, the average axial stress shall not exceed F_a'' given below:

f_t greater than $\frac{2}{3}$ fyQ

$$F_a'' = 0.515Qfy - \frac{Q^2 fy^2}{8.8 f_t}$$

f_t equal to or less than $\frac{2fyQ}{3}$

$$F_a'' = \frac{f_t}{S.F.} = \frac{f_t}{1.95}$$

where

F_a'' = maximum allowable torsional buckling stress, psi

f_t = elastic torsional buckling stress, defined in Sec. 3.6.1.2.

3.6.1.4. For members whose cross-sections do not have any symmetry, either about an axis or about a point, f_{TF} is less than the smallest of f_x, f_y and f_t and its value is such that

$$\left(\frac{f_{TF}^3}{f_x f_y f_t}\right)h - \left(\frac{f_{TF}^2}{f_y f_t}\right)j - \left(\frac{f_{TF}^2}{f_x f_t}\right)k - \left(\frac{f_{TF}^2}{f_x f_y}\right) + \frac{f_{TF}}{f_x} + \frac{f_{TF}}{f_y} + \frac{f_{TF}}{f_t} = 1$$

f_{TF} may be found from the above relation by trial and error, in which case the following gives a first approximation.

$$f_{TF} = \frac{(f_x f_y + f_x f_t + f_y f_t) - \sqrt{(f_x f_y + f_x f_t + f_y f_t)^2 - 4(f_x f_y f_t)(f_x j + f_y k + f_t)}}{2(f_x j + f_y k + f_t)}$$

in which

$$f_x = \left(\frac{\pi^2 E}{(L/r_x)}\right)^2, \text{ psi}$$

$$f_y = \left(\frac{\pi^2 E}{(L/r_y)}\right)^2, \text{ psi}$$

$$f_t = \frac{1}{I_p}\left[GJ + \frac{EC_w}{L^2}\right], \text{ psi}$$

$$h = 1 - \left(\frac{x_o}{r_o}\right)^2 - \left(\frac{y_o}{r_o}\right)^2$$

$$j = 1 - \left(\frac{y_o}{r_o}\right)^2$$

$$k = 1 - \left(\frac{x_o}{r_o}\right)^2$$

C_w = (No simple expressions can be given in contrast to the case of singly symmetrical sections. If specific unsymmetrical sections were agreed upon, specific expressions could be calculated and tabulated.)

Alternatives:

1. In Section 3.6.1.2, the equation for F_a' is based on C = 4.5, which is the most accurate value developed in the body of this report. Alternatively, one may, for simplicity, employ the CRC column curve based on C = 4.0 which gives computed torsional-flexural buckling stress in the inelastic range which is slightly more conservative. In that case, Section 3.6.1.2 and Section 3.6.1.3 become as follows:

With C = 4.0:

Section 3.6.1.2

f_{TF} greater than $(1/2)Qf_y$:

$$F_a' = 0.515Qf_y - \frac{f_y^2 Q^2}{7.8 f_{TF}}$$

f_{TF} equal to or less than $(1/2)Qf_y$:

$$F_a' = \frac{f_{TF}}{1.95}$$

Section 3.6.1.3

f_t greater than $(1/2)Qf_y$:

$$F_a'' = 0.515Qf_y - \frac{f_y^2 A^2}{7.8 f_t}$$

f_t equal to or less than $(1/2)Qf_y$:

$$F_a'' = \frac{f_t}{1.95}$$

2. Effective Slenderness Method

The effective slenderness method may be used as an alternative approach to Section 3.6.1.2, and it is presented here for ready reference.

For C = 4.5:

$(L/r)_{eff}$ less than $\frac{20,900}{\sqrt{f_y Q}}$:

$$F_a' = 0.515Qf_y - [\frac{Qf_y(L/r)_{eff}}{50,500}]^2$$

$(L/r)_{eff}$ equal to or greater than $\frac{20,900}{\sqrt{f_yQ}}$

$$F_a' = \frac{149,000,000}{(L/r)^2_{eff}}$$

where

$(L/r)_{eff}$ = an effective slenderness ratio given by

$$(L/r)_{eff} = \sqrt{\frac{291,000,000}{f_{TF}}}$$

For $\underline{C = 4.0}$:

$(L/r)_{eff}$ less than $\frac{24,200}{\sqrt{f_yQ}}$:

$$F_a' = 0.515Qf_y - [\frac{Qf_y(L/r)_{eff}}{47,500}]^2$$

$(L/r)_{eff}$ equal to or greater than $\frac{24,200}{\sqrt{f_yQ}}$:

$$F_a' = \frac{149,000,000}{(L/r)^2_{eff}}$$

All notations are as defined in the foregoing.

3. The explicit expression for the torsional-flexural buckling stress, f_{TF}, has been chosen in Section 3.6.1.2 instead of the less explicit interaction formula

$$\frac{f_{TF}}{f_x} + \frac{f_{TF}}{f_t} - k(\frac{f_{TF}}{f_xf_t})^2 = 1$$

It is suggested that this interaction formula and its use be shown in the Commentary.

5. Section 3.6.1.3 concerning point symmetrical sections is somewhat tentative because no shapes of this type have been tested.

6. The provision against torsional-flexural buckling of

unsymmetrical sections is shown on a separate page. It is up to the Sub=committee to decide whether and where it should be included.

<u>Derivations and Explanations:</u>

1. The proportional limit corresponding to a particular value of the parameter C is determined as follows:

In the body of the report the following relation was used:

$$\frac{E_t}{E} = C[\frac{\sigma}{\sigma_y} - (\frac{\sigma}{\sigma_y})^2]\tag{9}$$

Since at the proportional limit, σ_p, E_t/E is unity,

$$1 = C[\frac{\sigma_p}{\sigma_y} - (\frac{\sigma_p}{\sigma_y})^2]$$

Therefore, solving for $\frac{\sigma_p}{\sigma_y}$, one gets

$$\frac{\sigma_p}{\sigma_y} = \frac{C + \sqrt{C^2 - 4C}}{2C}$$

When <u>C = 4.5</u>:

$$\frac{\sigma_p}{\sigma_y} = \frac{2}{3}$$

hence

$$\sigma_p = \frac{2}{3}\sigma_y$$

When <u>C = 4.0</u>:

$$\sigma_p = (1/2)\sigma_y$$

2. The equation for F_a' when f_{TF} is greater than $(2/3)Qf_y$ is derived from Equation (15),(see the Basic Theory) as follows:

<u>C = 4.5</u>

$$F_a' = \frac{(\sigma_{cr})_t}{F.S.}$$

$$= \frac{1}{1.95}\sigma_y [1 - \frac{\sigma_y}{4.5(\sigma_{cr})_E}]$$

$$= 0.515 Q f_y - \frac{Q^2 f_y^2}{8.8 \ f_{TF}}$$

F_a'' expression in Section 3.6.1.3 is derived in the similar way

3. The criterion for the elastic-inelastic boundary by the effective slenderness ratio method is derived as follows:

When $\underline{C = 4.5}$, we know that the proportional limit is 2/3 of the yield strength, f_y, so that when the torsional-flexural buckling stress just coincides with the proportional limit,

$$(L/r)_{eff}^2 = \frac{\pi^2 E}{f_{TF}} = \frac{\pi^2 E}{\frac{2}{3} Q f_y}$$

Whence

$$(L/r)_{eff} = \sqrt{\frac{3 \pi^2 E}{2 \ f_y Q}} = \sqrt{\frac{436 \times 10^6}{f_y Q}}$$

$$= \frac{20,900}{\sqrt{f_y Q}}$$

The expression for F_a' is then

$$F_a' = \frac{1}{1.95} \ \sigma_y \ [1 - \frac{\sigma_y}{4.5 \frac{\pi^2 E}{(\frac{\lambda}{r})_{eff}^2}} \ ]$$

$$= 0.515 Q f_y - \frac{(f_y Q)^2 (L/r)_{eff}^2}{2,555 \times 10^6}$$

$$= 0.515 Q f_y - [\frac{Q f_y (L/r)_{eff}}{50,500}]^2$$

The derivations of other formulas are similar to those in the foregoing and therefore need no more explanations.

4. A table of formulas for the distances between the shear center and the centroid, principal moments of inertia, and the warping constants is attached.

5. The computer programs in FORTRAN language are also attached for computing warping constants.

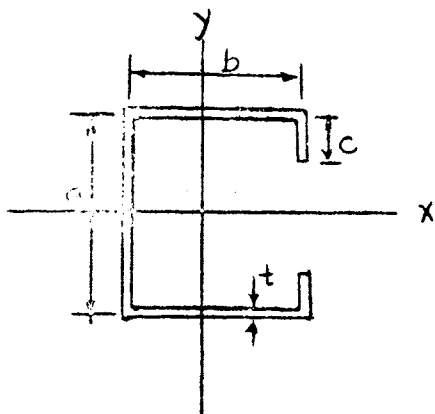FORMULAS FOR WARPING CONSTANTS.
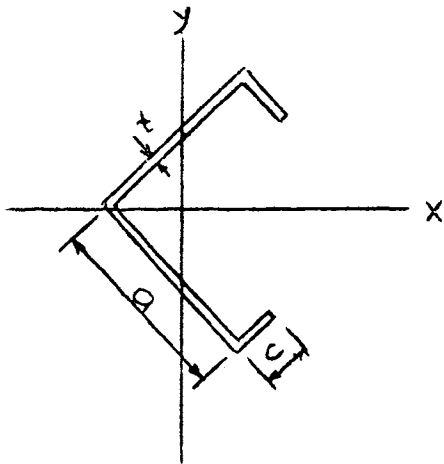
Angle Section

    (1) Plain angle

$$C_w = 0$$

$$I_x = \frac{a^3 t}{3}$$

    (2) Lipped Angle

$$C_w = \frac{t^2 a^4 c^3}{18 \, I_x} \, (4a + 3c)$$

$$I_x = \frac{t}{3}(a^3 + c^3 + 3a^2 c + 3ac^2)$$

Channel Section

    (1) Plain channel

$$C_w = \frac{t a^2 b^3}{12} \, (\frac{3b + 2a}{6b + a})$$

$$I_x = \frac{a^2 t}{12} \, (a + 6b)$$

(2) Lipped Channel

$$C_w = \frac{t^2}{A} \left\{ \left\{ \frac{\bar{x} A a^2}{t} \, [\frac{b^2}{3} + m^2 - mb] + \frac{A}{3t} \, [m^2 a^3 + b^2 c^2 (2c + 3a)] \right. \right.$$

$$- \frac{I_x m^2}{t} \, [2a + 4c] + \frac{mc^2}{3} \left\{ 8b^2 c + 2m[2c(c-a) + b(2c - 3a)] \right\}$$

$$\left. \left. + \frac{b^2 a^2}{6} \, [(3c + 6)(4c + a) - 6c^2] - \frac{m^2 a^4}{4} \right\} \right\}$$

$$A = (a + 2b + 2c)t$$

$$\bar{x} = \frac{bt(b+2c)}{A}$$

$$m = \frac{abt}{12I_x} \left[ab + 2c \left(a - \frac{4}{3}\frac{c^2}{a} \right) \right]$$

$$I_x = \frac{ta^3}{12} + \frac{2bta^2}{4} + \frac{2tc^3}{12} + 2ct \left(\frac{a}{2} - \frac{c}{2} \right)^2$$
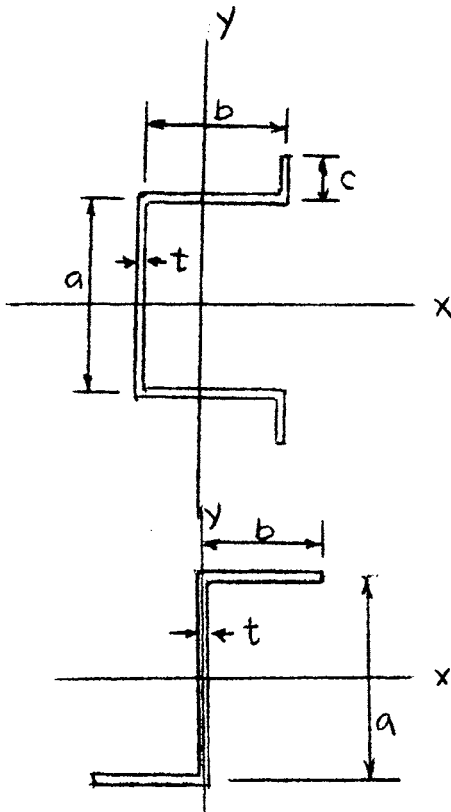

Hat Section

$$C_w = \frac{a^2}{4} \left[I_y + \bar{x}^2 A \left(1 - \frac{a^2 A}{4I_x} \right) \right]$$

$$+ \frac{2b^2 tc^3}{3} - ab^2 c^2 t$$

$$+ \frac{a^2 btc^3 \bar{x} A}{3I_x} - \frac{4b^2 t^2 c^6}{9I_x}$$

$$\bar{x} = \frac{bt(2c+b)}{A}$$

$$I_x = \frac{t}{12} [a^3 + 6ba^2 + 6ca^2 + 12ac^2 + 8c^3]$$

$$I_y = \frac{tb^2}{3(a+2b+2c)} [2ab + b^2 + 4bc + 6ca]$$

Z-Section

$$C_w = \frac{tb^3 a^2}{12} \frac{b+2a}{2b+a}$$

Hat Section (Computer Program for Evaluating Warping Constants)

C Program for Hat Section Warping Constant

C x = (Flange Width/Web width)

C Y = (Lip/Web Width)

C A = Factor of Area

C B = Component Factor of C

C C = Xbar factor

C D = I(x) Factor

C E = Component Factor of F

```
C   F = I(Y) Factor

C   N = Component Factor of C(W)

C   P = Component Factor of C(w)

C   R = Component Factor of C(w)

C   S = C(W) Constant

C   T = Thickness of Wall

C   H = Web Width

C   Z = Warping Constant


    X = .5

    DO   1   IX = 1,9

    X = X + 0.1

    Y = -0.1

    DO   1   IY = 1,11

    Y = Y + 0.1

    A = 1. + 2.* x + 2. * Y

    B =      (2.   Y + x)

    C = B/A

    D = 1. + 6. * x + 6. * Y + 4. * Y * Y (3.+2.*y)

    E = (2. * x ** 2 + 2. * x + 4. * x * y + 6.* y)

        * x **2

    F = E/A

    N = F + 3.* (1-3.* A/D) * A * C ** 2

    P = 4.* (2.* y - 3.) * (x * y)** 2

    Q = x * Y ** 3

    R = (48. * B * Q - 64. * Q ** 2)/D

    S = N + P + R

    T = .015
```

```
        DO 1  IT = 1.4

        T = T + .03

        Dφ 1  IH = 2, 8

        H = IH

        Z = (T*S*H**5)/12.

1       PRINT 2, X, Y, T, Z

2       FORMAT (4E 15.8)
```

APPENDIX D

Torsional-Flexural Buckling Stress in the Inelastic Range on
the Basis of "$G_t/G = \sqrt{E_t/E}$" Theory and Bijlaard's Effective
Inelastic Shear Modulus Theory

TORSIONAL-FLEXURAL BUCKLING STRESS IN THE INELASTIC RANGE ON

THE BASES OF "$G_u\ G_t = \sqrt{E_t/E}$" THEORY AND BIJLAARD'S THEORY

COMPUTED BY ITERATION METHOD

In order to compare the results based on the assumption stated in Eq. (7) of the main body of this report, computations are also made based on the more complicated expressions of G_t, i.e.,

$$\frac{G_t}{G} = \sqrt{\frac{E_t}{E}} \qquad (D-1)$$

$$G_t = E/[2 + 2\nu + 3(E/E_s - 1)] \qquad (D-2)$$

where E_s = the secant modulus,
the latter expression, (D-2), being Bijlaard's theory.

We shall start with Eq. (D-1). Assuming that the parabolic equation of E_t/E

$$\frac{E_t}{E} = 4.5\ \frac{\sigma}{\sigma_y}\ (1 - \frac{\sigma}{\sigma_y}) \qquad (D-3)$$

holds, the relationship is substituted into Eq. (D-1),, thus

$$G_t = G\sqrt{\frac{E_t}{E}}$$

$$= \frac{1.06E}{(1 + \nu)} \sqrt{\frac{\sigma}{\sigma_y}\ (1 - \frac{\sigma}{\sigma_y})} \qquad (D-4)$$

Then Eqs. (2) and (3) of the main body of this report become, respectively,

$$(\sigma_x)_t = \frac{4.5\pi^2 E}{(L/r_x)^2}\ \frac{\sigma}{\sigma_y}\ [1 - \frac{\sigma}{\sigma_y}] \qquad (D-5)$$

$$(\sigma_\phi)_t = \frac{1}{I_p}\ [\frac{1.06EJ}{(1+\nu)}\sqrt{\frac{\sigma}{\sigma_y}\ (1 - \frac{\sigma}{\sigma_y})} + \frac{E_t C_w \pi^2}{L^2}] \qquad (D-6)$$

One sees that, upon substituting Eqs. (D-5) and (D-6) into

$$(\sigma_{cr})_t = \frac{1}{2K} [(\sigma_x)_t + (\sigma_\phi)_t -$$

$$\sqrt{\{(\sigma_x) + (\sigma_\phi)_t\}^2 - 4K(\sigma_x)_t (\sigma_\phi)_t}] , \qquad (D-7)$$

$(\sigma_{cr})_t$ is expressed implicitly as

$$(\sigma_{cr})_t = f[(\sigma_{cr})_t, E, \sigma_y, J, C_w] \qquad (D-8)$$

noting that at the incipient buckling, $\sigma = (\sigma_{cr})_t$ in Eqs. (D-5) and (D-6).

The explicit expression of $(\sigma_{cr})_t$ would be in the form

$$(\sigma_{cr})_t^3 + f_2(\sigma_{cr})_t^2 + f_1(\sigma_{cr})_t + f_o = 0 \qquad (D-9)$$

where

$$f_1 = f_1 (E, \sigma_y, \text{dimensions of column})$$

The solution of Eq. (D-9) is very laborious. Fortunately, with the aid of an electronic computer, one can utilize an iteration technique to get a good approximate solution.

The procedure can be written in a form of flow chart for an electronic computer program as in Fig. (D-1). The variable, x, in the flow chart corresponds to $(\sigma_{cr})_t$ of the torsional-flexural buckling problem.

As to Bijlaard's theory, (D-2), the secant modulus, E_s, can be expressed by the use of Eq. (11) (see the Basic Theory) as follows:

$$E_s = \frac{(\sigma_{cr})_t}{\epsilon} = \frac{4.5E(\sigma_{cr})_t}{\sigma_y[2.306 + \ell n|\frac{(\sigma_{cr})_t/\sigma_y}{1 - (\sigma_{cr})_t/\sigma_y}|]} \qquad (D-13)$$

This expression is then substituted into (D-2) for G_t. The resulting equation for $(\sigma_{cr})_t$ by substitution of these moduli expressions into Eq. (4)(see the Basic Theory), is very complicated. However, the iteration method can also be applied to this case.

The computer results are listed in Table (D-1) together with the values computed by Eq. (15) for ready comparison.

It can be seen that the values computed from Eq. (15) are slightly lower than those from the other, presumably somewhat more rational theories. The differences, however, are small and of no practical consequence. Since Eq. (15) provides much the simplest analytical tool, and since it leads to results satisfactorily confirmed by tests, its use rather than that of one of the two other, more involved expressions appears justified.
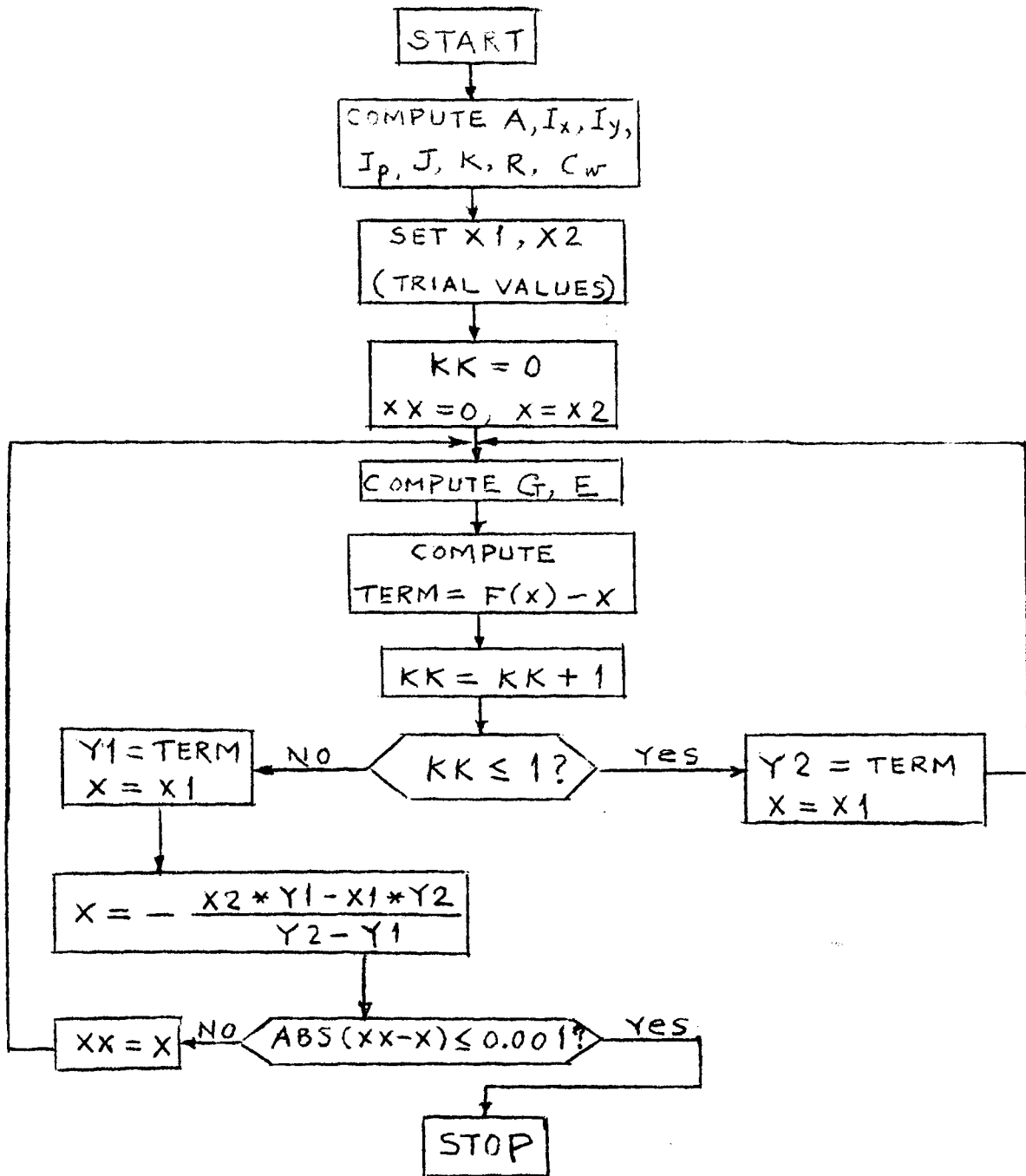
Fig. D-1   Flow Chart for the Iteration Method.

TABLE D - 1

Section	Specimen	$(\sigma_{cr})_t$ ksi		
		Eq. 15	Based on $G_t/G = \sqrt{E_t/E}$	Bijlaard
Plain Angle	A-1	35.87	37.08	39.43
	A-2	37.06	38.74	41.40
	A-3	30.80	31.07	33.18
	A-4	30.47	30.59	32.58
	A-5	28.85	28.27	29.61
Lipped Angle	LA-1	36.85	37.78	38.36
	LA-2	35.05	35.56	35.79
	LA-3	32.52	32.79	31.96
	LA-4	31.59	31.76	31.32
Channel	CH-1	37.48	38.33	38.53
	CH-2	27.91	28.31	28.68
	CH-3	27.06	27.53	27.93
	CH-4	24.05	24.49	24.70
	CH-5	24.89	25.19	25.38
	CH-6	25.79	26.16	26.44
	CH-7	25.45	25.97	26.34
	CH-8	25.74	26.12	26.40
	CH-9	25.80	26.19	26.46
Hat	HA-1	39.34	39.73	39.99
	HA-2	39.86	40.20	40.46